National Library
of Canada

Acquisitions and
Bibliographic Services Branch

395 Wellington Street
Ottawa, Ontario
K1A 0N4

Bibliothèque nationale
du Canada

Direction des acquisitions et
des services bibliographiques

395, rue Wellington
Ottawa (Ontario)
K1A 0N4

Your file Votre référence

Our file Notre référence

NOTICE

The quality of this microform is heavily dependent upon the quality of the original thesis submitted for microfilming. Every effort has been made to ensure the highest quality of reproduction possible.

If pages are missing, contact the university which granted the degree.

Some pages may have indistinct print especially if the original pages were typed with a poor typewriter ribbon or if the university sent us an inferior photocopy.

AVIS

La qualité de cette microforme dépend grandement de la qualité de la thèse soumise au microfilmage. Nous avons tout fait pour assurer une qualité supérieure de reproduction.

S'il manque des pages, veuillez communiquer avec l'université qui a conféré le grade.

La qualité d'impression de certaines pages peut laisser à désirer, surtout si les pages originales ont été dactylographiées à l'aide d'un ruban usé ou si l'université nous a fait parvenir une photocopie de qualité inférieure.

Canada

Red blood cell spacing in capillaries of rat heart

A Thesis Submitted to the School of Graduate Studies and Research of the University of Ottawa in Partial Fulfilment of the Requirements for the Degree of

Master of Science in Physiology

Candidate: David A. Silverman

Supervisor: Dr. Karel Rakusan

ISBN 0-612-11603-4

UNIVERSITÉ D'OTTAWA
UNIVERSITY OF OTTAWA

DEDICATION

To my parents, for their never-ending love and guidance. To Heather, for always being there for me.

ACKNOWLEDGEMENTS

I would like to thank Dr. K. Rakusan for his guidance, support and accessability throughout this project. Just knowing that his deep reservoir of knowledge was at my disposal was a reassurance. I also thank the members of my advisory committee: my co-supervisor, Dr. J.-M. Renaud, for his *significant* contributions throughout the course of this project, and Dr. W. Ross, for his helpful insights and clarifications.

I thank the other members of the lab: Ching, Barb, and Marcia, whose presence defined an environment which was a pleasure to work in. In particular, to Ching, for her technical expertise and optimistic outlook. To Barb, who made things run more smoothly. I extend a special thank you to Marcia, whose unselfish willingness to help was of immeasurable significance to me. I very much value her friendship.

TABLE OF CONTENTS

LIST OF TABLES

LIST OF FIGURES

LIST OF COLOUR PLATES

ABSTRACT

Theoretical studies have demonstrated a pronounced effect of red blood cell (RBC) spacing on tissue oxygen supply. In spite of this, realistic values for RBC spacing and related capillary hematocrit (Hct) are not known in the heart. One of the possible reasons is the lack of proper methodology. Thus, the goal of this research study was twofold: (i) to develop a method to rapidly freeze rat heart *in situ*, following which RBCs and capillary walls could be simultaneously visualized, and (ii) to apply this methodology in rat hearts to establish whether differences exist in capillary Hct and RBC spacing in two distinct locations within the capillary bed, in the subendo- and midmyocardium, during diastole or systole.

The development of the novel freezing procedure and staining methods are discussed in Chapter 2. Briefly, rat hearts were frozen *in situ* by use of precooled copper clamps (heat sink), specifically designed to match the shape of the hearts. The entire heart was encased, exposing it to equal transmural freezing gradients. Freezing the heart *in situ* with these clamps was more rapid than excising the heart and subsequently submerging it in liquid nitrogen. Whereas left ventricular cavity temperature reached 0°C in less than 3.75sec with clamping, it took approximately 10.75sec with submersion.

The staining procedure developed in the present study is an adaptation of a method for dual staining of capillary walls (Lojda, 1979). This method, first employed in cardiac tissue in our laboratory (Batra et al., 1989), distinguishes proximal and distal portions of the capillary bed (i.e. portions located close to and far from their feeding arterioles, respectively) based on a differential localization of enzymes in the capillary walls. Briefly, proximal regions of the capillary bed stain positive for Alkaline Phosphatase, while distal regions stain positive for Dipeptidyl Peptidase IV. The procedure was altered to accommodate a third staining reagent, Papanicolaou OG-6, which stained RBCs. Thus, a novel triple staining procedure was developed ("triple stain") which sequentially stained RBCs within capillaries orange, distal portions of the capillary bed red, and proximal portions blue.

The application of these techniques is detailed in Chapters 3, 4, and 5. Specifically, Chapter 3 deals with the experimental methods, including surgical procedures, definitions of morphometric parameters and data collection protocols. Cardiac arrest in systole and diastole was induced by injection of $CaCl_2$ and KCl, respectively, and confirmed by measuring sarcomere lengths. Representative tracings of capillaries and RBCs in the midmyocardium and subendocardium (both regions in longitudinal fiber orientation) of diastolic- and systolic-arrested hearts were made from triple-stained tissue. In summary, capillary Hct and related RBC spacing were measured at two distinct locations within the capillary bed in two regions of hearts arrested in systole and diastole. **Capillary hematocrit** was defined as the aggregate RBC length divided by the total capillary length measured, from all capillaries traced in each heart. **Red blood cell spacing** was defined as the edge-to-edge distance between two RBCs within an individual capillary.

The major findings of this study, detailed in Chapter 4, can be summarized as follows. There was a significant increase in capillary hematocrit and decrease in the average distance between RBCs in distal portions of the capillary bed, compared to proximal portions. Depending on the region of the heart and phase of the cardiac cycle, average capillary hematocrit ranged from 9.8 to 11.4% in proximal portions of the capillary bed, and from 13.2 to 14.3% in distal portions. The normalized capillary Hct (ratio of capillary Hct to large vessel Hct) was calculated to account for any variability in large vessel Hct between animals which might affect Hct at the capillary level. The findings were similar to those for capillary Hct - normalized capillary Hct was greater in distal portions of the capillary bed compared to proximal portions. The average distance between RBCs ranged from 11.2 to 14.0μm in proximal portions of the capillary bed and from 8.9 to 12.2μm in distal portions. For all three of the above parameters, only the main effect of capillary type was significant. Regional differences, cardiac phase differences, and interactions were not statistically significant.

In order to better characterize the RBC spacing data, individual and mean cumulative frequency distributions were plotted. It was apparent from these distributions that there was a greater frequency of shorter inter-RBC distances in distal portions of the capillary bed compared to proximal portions. This difference seemed to be most evident in the midmyocardium during diastole. In addition, a number of capillary segments (defined as a capillary portion between two successive branch points) were used to determine the red cell content (# of RBCs) in capillaries. Red cell content was obtained by counting capillary segments containing zero, one, or greater than one RBC, and expressing the data as frequencies. Red cell content was greater in distal portions of the capillary bed compared to proximal portions. In other words, there was a greater proportion of capillaries unperfused (no RBCs) in proximal portions of the capillary bed compared to distal portions, in both systolic- and diastolic-arrested hearts. Presumably, in distal portions of the capillary bed where PO_2 is lower, the increased frequency of shorter distances between red cells, as well as the increased number of capillaries perfused with more than one RBC, improve geometrical conditions for oxygen transport.

Finally, the frequency of red blood cell spacing values, arbitrarily categorized as equal to 0μm, ≥20μm and ≥40μm, was determined. It has been suggested that the capillary barrier, representative of the resistance to O_2 transfer out of a capillary, increases as the distance between red cells increases. The frequency of spacing values ≥20μm and ≥40μm was greater in proximal portions of the capillary bed compared to distal portions. This results in a higher capillary barrier in proximal portions of the capillary bed, conserving the O_2 content in this portion, which can then be supplied in distal regions of the capillary bed. There was a significant main effect of cardiac phase on the frequency of spacing values equal to 0μm, with a greater frequency of touching RBCs in systole (12.4%) compared to diastole (10.6%). Since blood flow is reduced in coronary capillaries during systole, due to contraction of the heart and subsequent compression of vessels, it is intuitively appealing that the frequency of touching cells increases, presumably in an attempt to reduce the capillary barrier.

In conclusion, the results of this study suggest that different geometrical conditions (e.g. RBC spacing and capillary Hct) exist at the two distinct locations of the capillary bed studied. Presumably, the oxygen supply conditions in distal portions of the capillary bed are improved by these geometrical adjustments, preventing hypoxic or anoxic conditions in the tissue, which would be detrimental to cardiac function.

CHAPTER 1 INTRODUCTION

1.1 Oxygen supply to tissue

Energy production in mammals relies primarily on oxidation. Thus, without a continuous supply of oxygen, organ function may be lost within minutes. Oxygen is taken up from the air by blood in the pulmonary capillaries and supplied to the tissue by the circulatory system. Even though O_2 diffusion may occur from arterioles, capillaries have been viewed as the major sites of oxygen diffusion to the tissue. The large surface area-to-volume ratio, close proximity to cells, and low velocity of red blood cells passing through capillaries makes them an effective route for diffusion of oxygen.

Our understanding of oxygen transport to tissue is primarily due to the pioneering theoretical work of August Krogh (1919). Krogh's model consists of a tissue cylinder (Krogh cylinder) supplied by diffusion of oxygen from a centrally located capillary (Fig. 1). The principal determinants of tissue oxygenation were identified in this model, and an equation devised, the Krogh-Erlang equation:

$$\Delta P = P_c - P_x = \frac{M}{K}\left(\frac{R^2}{2}\ln\frac{x}{r} - \frac{x^2 - r^2}{4}\right)$$

where ΔP is the gradient in PO_2 from the centre of the capillary to a point x in the tissue (mm Hg), P_x is the tissue PO_2 at a distance x from the centre of the capillary,

Figure 1. Krogh's tissue cylinder model for diffusion of O_2, representing a tissue cylinder being supplied with oxygen from a central capillary. R = tissue cylinder radius; r = capillary radius; L = capillary length; x = distance from centre of capillary to a point in the tissue; P_c = partial pressure of oxygen in the capillary; P_x = partial pressure of oxygen at any point x. Modified from Rakusan, 1971a.

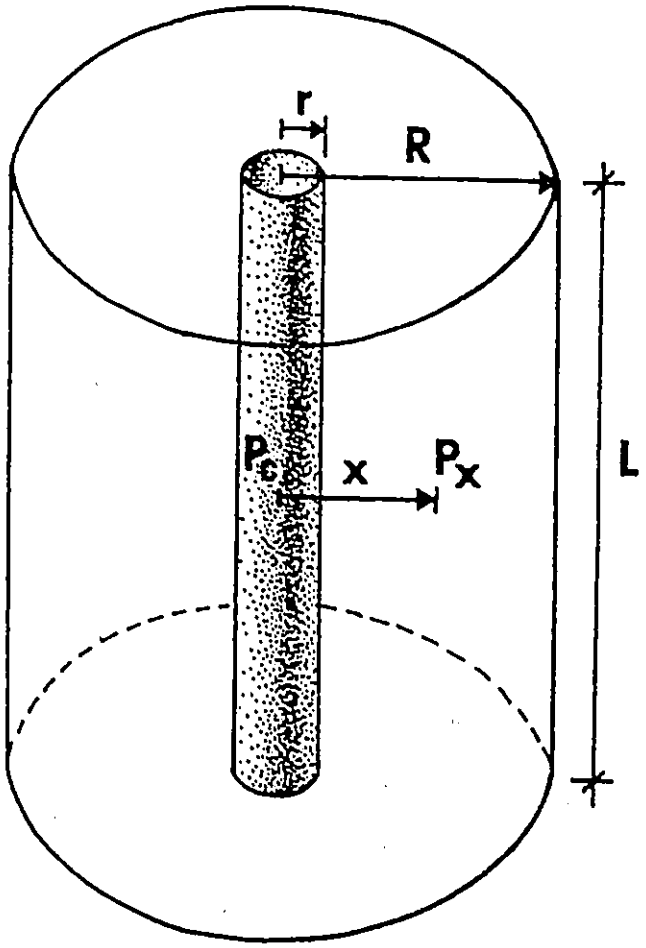
r
R
P_c
x
P_x
L

at the level of the point x (mm Hg), P_c is the PO_2 at the centre of this capillary (mm Hg), M is the tissue O_2 consumption (mL O_2 / mL tissue / min), K is the Krogh diffusion coefficient (mL O_2 / cm min mm Hg), R is the radius of the Krogh tissue cylinder (cm), r is the capillary radius (cm), and x is the distance from the centre of the capillary to the tissue (cm). The solution to this equation represents the partial pressure of oxygen in the tissue as a function of radial distance from the centre of the capillary.

Although the Krogh model has served as the theoretical backbone for studying O_2 supply to tissue since 1919, the model is based on many simplifications and assumptions, reviewed thoroughly by Kreuzer (1982) and Popel (1989). Some of these are the following:

(i) capillaries are straight, run parallel to each other, have unidirectional blood flow and are uniformly distributed,

(ii) capillary blood flow is constant,

(iii) facilitated diffusion doesn't occur (e.g. by hemoglobin and myoglobin),

(iv) tissue O_2 consumption is uniform throughout the tissue and is independent of local tissue PO_2 (zero-order reaction),

(v) capillary length and radius are constant (implying a constant transit time with constant blood flow),

(vi) the capillary wall does not present any resistance to oxygen diffusion,

(vii) only radial diffusion into the tissue occurs (i.e. no axial or longitudinal diffusion),

(viii) O_2 exchange occurs only in the capillary (i.e. not in the arterioles and venules),

(ix) O_2 does not diffuse out of the tissue cylinder,

(x) the diffusion coefficient is the same throughout the tissue,

(xi) intracapillary chemical reactions in the blood are neglected. This assumes that the O_2 concentration is the same over the capillary cross section, and that O_2 and hemoglobin are in chemical equilibrium.

In spite of these assumptions, the Krogh model remains a valuable approach to assessing the general properties of O_2 transport. With advancements in experimental techniques and theoretical analyses, many investigators have modified or expanded Krogh's model. Using the Krogh-Erlang equation and realistic entry data, Rakusan (1971a) examined the individual effects of the O_2 determinants on myocardial PO_2, when the remaining determinants were kept constant. Figure 2 illustrates the changes in myocardial PO_2 as the various O_2 determinants are increased or decreased relative to the normal situation. For example, the most important determinant of PO_2 is the myocardial O_2 consumption (M), followed by flow (F) and O_2 content (C). In addition, the radius of the Krogh tissue cylinder, R, has a significant influence on

Figure 2. Changes in myocardial PO_2 as a result of changes in blood flow (F), blood O_2 content (C), oxygen consumption (M), radius of tissue cylinder (R), capillary radius (r) and diffusion coefficient (K). Modified from Rakusan, 1971a.

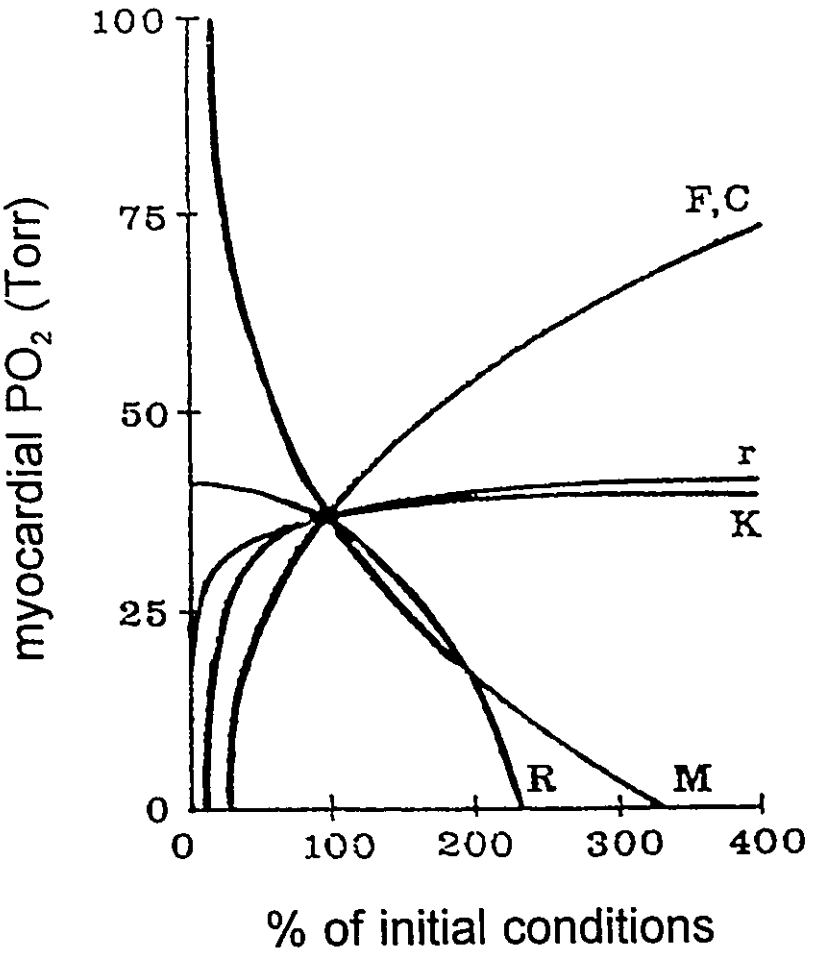
100
75
50
25
0
myocardial PO_2 (Torr)
F,C
r
K
R
M
0
100
200
300
400
% of initial conditions

myocardial PO_2 when R is greater than normal, that is, when the diffusion distance is increasing. The Krogh radius can be determined from the capillary density, which refers to the number of capillaries per unit area of tissue cross section. However, this determination implies that capillaries are evenly spaced throughout the tissue. Herein lies one of the limitations to the Krogh model: the reliance on mean entry data, neglecting heterogeneity of capillary spacing. Other heterogeneities neglected in the model include blood flow in space and time, capillary hematocrit, terminal vascular bed structure, distribution of O_2 sinks (mitochondria) and diffusion paths.

Heterogeneity of capillary spacing exists in tissue and can affect average tissue PO_2 as well as the percentage of anoxic tissue (Turek and Rakusan, 1981). While there are several ways to determine heterogeneity of capillary spacing, the method of capillary domains has been favoured (Turek et al., 1986). Briefly, with the aid of a digitizer, the centre of a capillary in a photomicrograph is converted to (x,y) coordinates. Equidistant border lines are calculated between each capillary and all of its immediate neighbours. The resulting polygonal area of tissue is referred to as the capillary domain, and represents the region of tissue supplied by an individual capillary. This polygon is converted to a circle of equivalent surface area, whose radius represents R, the radius of the tissue cylinder. The distribution of radii determined in such a fashion is log-normal, and the standard deviation of this logarithmic distribution (SD_{log}) characterizes the heterogeneity of capillary spacing. There are two factors affecting this heterogeneity: (i) the uneven distribution of

capillaries in space with all capillaries running parallel to each other along a preferred axis, and (ii) the deviation from this preferential alignment. Figure 3 illustrates a digitized output of capillary domains, as well as the two factors which may lead to heterogeneity of capillary spacing. Thus, the concept of capillary domains is valuable in that it enables evaluation of the local capillary supply to tissue and subsequently the heterogeneity in this supply.

The occurrence of heterogeneity in capillary spacing was first determined by Turek and Rakusan (1981). In 1985, Rakusan and coworkers used modelling to determine the effects of this heterogeneity on tissue PO_2 histograms in cardiac muscle. When all other determinants were held constant, an increase in heterogeneity of spacing resulted in a shift of tissue PO_2 histograms to lower PO_2 values and an increased percentage of anoxic tissue. The percentage of anoxic tissue accounts for heterogeneity in spacing and thus was found to be a better index of tissue oxygenation than mean PO_2.

Heterogeneity of blood flow was also incorporated into the above model (Rakusan et al., 1985). Two flow conditions were considered. The first condition assumed a constant blood flow per volume of tissue ("homogeneous flow"). Thus, large tissue cylinders (large Krogh radius) had higher flow values than small cylinders. In the second situation, capillary blood flow was equally distributed, irrespective of the size of the tissue supply region ("heterogeneous flow"). The first type of blood flow is considered optimal, with the real situation existing somewhere in between.

Figure 3. Digitized output of capillary domains as well as two sources of heterogeneity. Capillary domains are calculated by drawing equidistant border lines between each capillary (dots in left picture) and all of its immediate neighbours. Heterogeneity is affected by an uneven distribution of capillaries in space with all capillaries running parallel to each other along a preferred axis and derivation of capillaries from this preferential alignment. Modified from Rakusan et al., 1993.

capillary domains

sources of heterogeneity

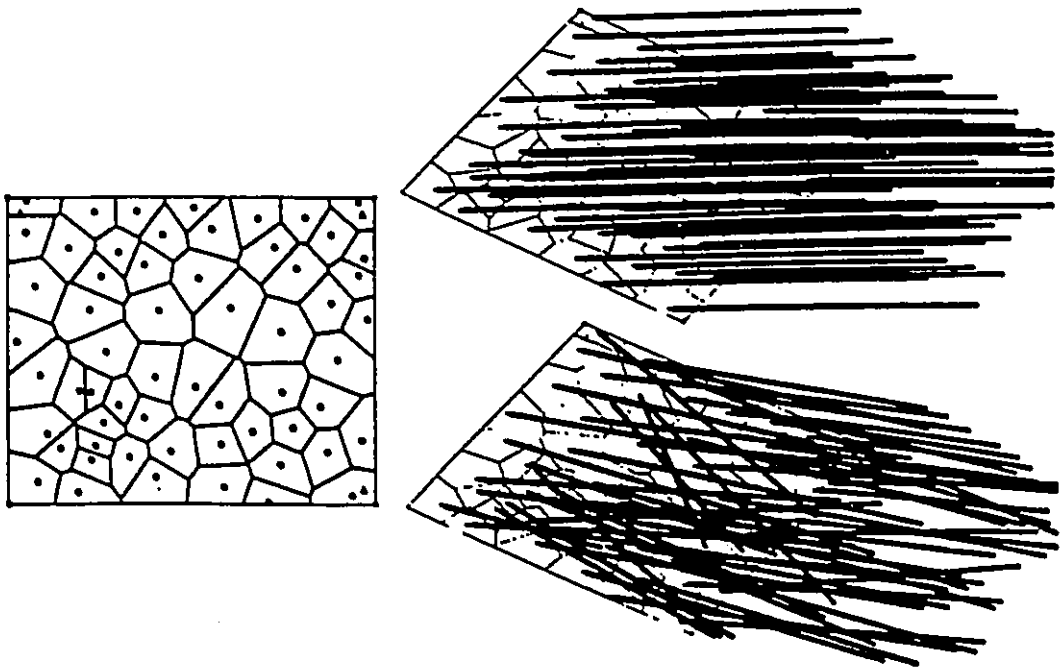

Indeed, changes in capillary spacing were more pronounced in the second flow situation.

Rakusan and Turek (1985) subsequently utilized this model to account for changes in mean tissue cylinder radius. The percentage of anoxic tissue was greatest when Krogh's radius (R) and heterogeneity of spacing (SD_{log}) were greatest. In addition, heterogeneous blood flow exacerbated these results. In fact, when a large tissue cylinder was considered, the percentage of anoxic tissue could range from 0 - 45% depending on the heterogeneity of spacing and blood flow.

Many of the other assumptions of the Krogh model have also been examined and are briefly discussed below. For instance, it has been calculated that axial diffusion of O_2, which is neglected in the model, improves O_2 supply to tissue in the lethal corner (venous end of capillary network at periphery of tissue cylinder) by increasing venous PO_2 in the capillary (e.g. decreased PO_2 at the arterial end of the capillary network and increased PO_2 at the venular end) (Kreuzer, 1982). However, Hoofd and coworkers (1990) determined that axial diffusion would account for less than 5% of the total O_2 flux. Although O_2 exchange has been reported to occur prior to capillaries in skeletal muscle, precapillary O_2 shunting is thought to be negligible in the heart and the Krogh assumption that O_2 exchange only occurs in capillaries may be valid in the heart (Honig and Gayeski, 1989).

Oxygen consumption in tissue is confined to discrete organelles, mitochondria, which are not always uniformly distributed (Hoppeler et al., 1981). In fact, in the

heart, mitochondria are not randomly distributed, but clustered around capillaries (Rakusan and Tomanek, 1986). From theoretical analyses, Mainwood and Rakusan (1982) determined that mitochondrial clustering near capillaries increases the efficiency of O_2 transfer from capillaries to cells and that energy generated at the cell periphery can be effectively transported over larger intracellular distances. Thus, this type of non-uniform distribution may actually improve conditions for O_2 transfer. Fletcher (1978) determined that modelling with Michaelis-Menten kinetics for O_2 consumption (local PO_2-dependent consumption) resulted in higher tissue PO_2 values than zero-order kinetics. It has been suggested that facilitated diffusion (e.g. Hb, Mb) may play a role in O_2 supply by augmenting the diffusional transport of O_2. This may increase tissue PO_2, particularly at the lethal corner. Fletcher (1980) found that in skeletal muscle, Mb-facilitation does raise tissue PO_2, particularly at the venous end. Perhaps Mb-facilitation acts as a safety mechanism against hypoxia.

More recent models have accounted for flow and capillary spacing heterogeneities described earlier, and have also accounted for myoglobin (Mb)-facilitation, Michaelis-Menten PO_2-dependent O_2 consumption and resistance to O_2 transport operating at the capillary level in skeletal (Turek et al., 1989) and cardiac (Turek et al., 1991) muscle. The term "capillary barrier" refers to the resistance to O_2 transport at the level of the capillary, and accounts for all possible mechanisms which may lead to a PO_2 drop across the capillary wall. Figure 4 illustrates the effects of heterogeneity of capillary spacing and blood flow on myocardial PO_2 without the

Figure 4. The effect of heterogeneity in capillary spacing and blood flow on myocardial PO_2 histograms. **No capillary barrier considered.** Flow type A = identical specific flow ("homogeneous flow"); Flow type B = identical absolute flow in all capillaries ("heterogeneous flow"). Log SD = index of heterogeneity in capillary spacing, increasing from front to back of figure. Hatched bars represent anoxic tissue. An increase in either heterogeneity in capillary spacing or blood flow results in an increase in the percentage of anoxic tissue. Modified from Turek et al., 1991.

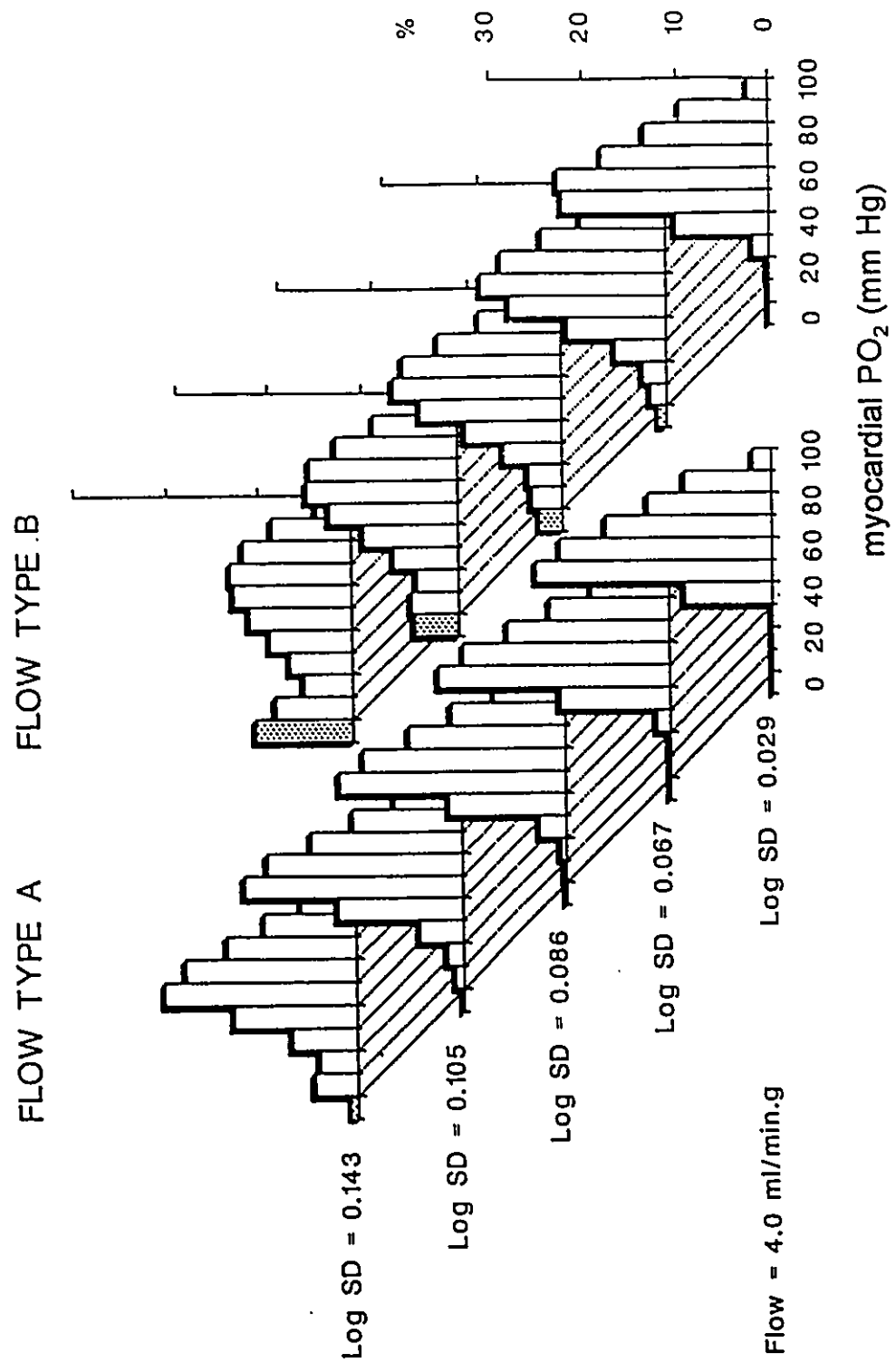
FLOW TYPE A
FLOW TYPE B
%
30
20
10
0
0 20 40 60 80 100
0 20 40 60 80 100
myocardial PO_2 (mm Hg)
Log SD = 0.143
Log SD = 0.105
Log SD = 0.086
Log SD = 0.067
Log SD = 0.029
Flow = 4.0 ml/min.g

capillary barrier. Figure 5 illustrates the same, with the incorporation of the capillary barrier. If a capillary barrier is considered with zero-order O_2 consumption, a larger percentage of anoxic tissue occurs, which remains dependent upon the heterogeneity of capillary spacing and blood flow. It should be noted that the authors in this study stressed the dependence of tissue PO_2 histograms on input data. Although the relationship between tissue PO_2 and several O_2 determinants was elucidated, the models were still oversimplifications of reality. Furthermore, these models still neglect the variation of tissue PO_2 due solely to the particulate nature of blood.

In the last 6 years, a method for dual staining of capillary walls has been employed in our laboratory which distinguishes capillaries located within proximal or distal portions of the capillary bed (i.e. close to or far from their feeding arterioles) (Batra et al., 1989). Studies from our lab on the coronary capillary bed reveal geometrical differences between these capillary regions, which contradict the Krogh model assumptions of a constant tissue cylinder radius from feeding arteriole to collecting venule. In fact, compared to proximal capillary regions, distal portions have a greater capillary diameter (Batra et al., 1992), are shorter (Batra and Rakusan, 1990), have smaller regions of tissue supplied by an individual capillary (capillary domain) and thus decreased intercapillary distances (Batra et al., 1991), and have a trend for lower heterogeneity of capillary spacing (Batra et al., 1992). These modifications in microvascular design provide improved geometrical conditions for O_2 supply on the venous side of the capillary network, where PO_2 values are lower.

Figure 5. The effect of heterogeneity in capillary spacing and blood flow on myocardial PO_2 histograms. Similar to Figure 4, but **capillary barrier considered**. Flow type A = identical specific flow ("homogeneous flow"); Flow type B = identical absolute flow in all capillaries ("heterogeneous flow"). Log SD = index of heterogeneity in capillary spacing, increasing from front to back of figure. Hatched bars represent anoxic tissue. The percentage of anoxic tissue is increased due to the capillary barrier. Modified from Turek et al., 1991.

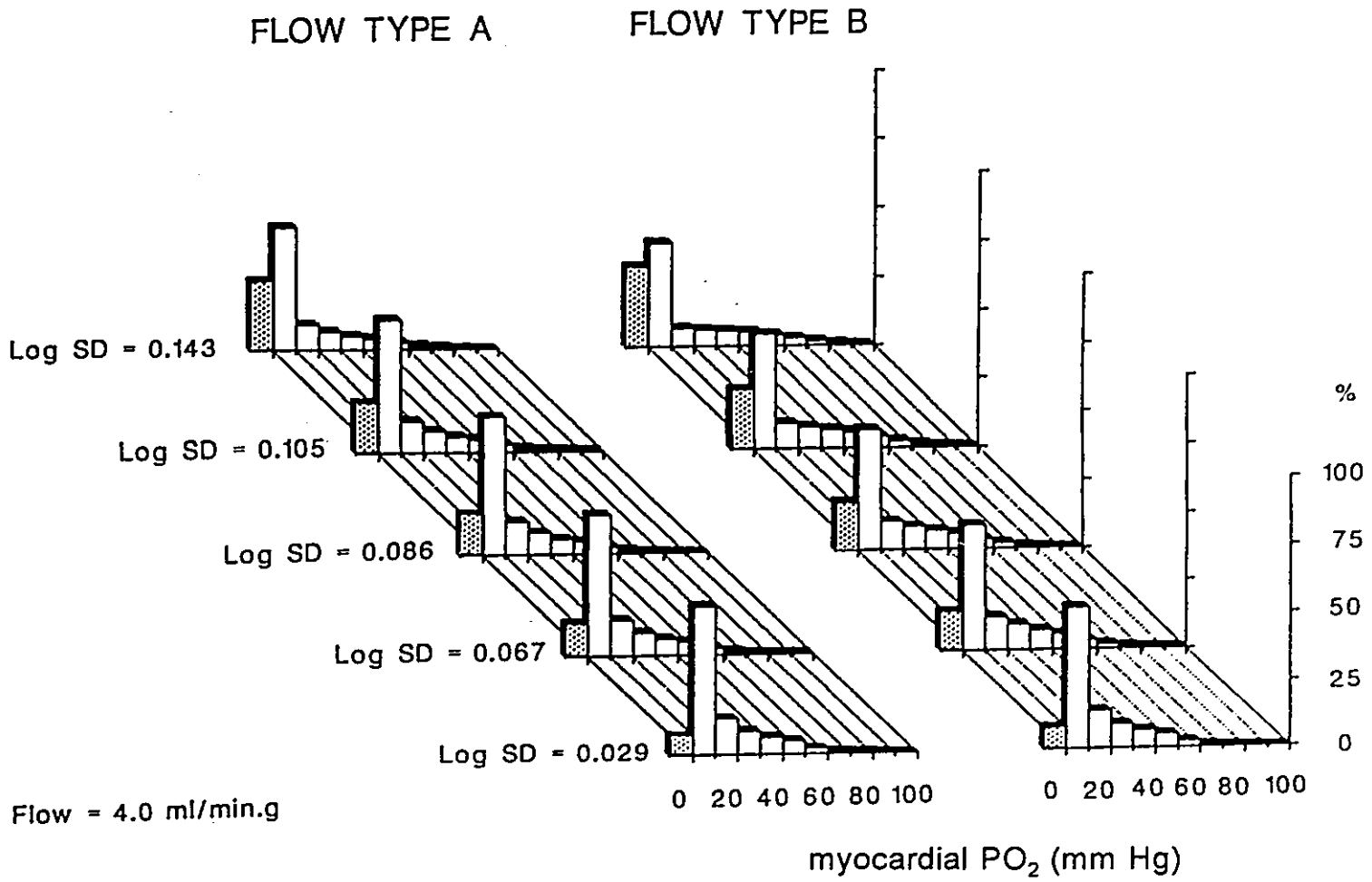
FLOW TYPE A
FLOW TYPE B
Log SD = 0.143
Log SD = 0.105
Log SD = 0.086
Log SD = 0.067
Log SD = 0.029
%
100
75
50
25
0
0 20 40 60 80 100
0 20 40 60 80 100
Flow = 4.0 ml/min.g
myocardial PO_2 (mm Hg)

Given these findings, it has been proposed that the Krogh cylinder model should be transformed to a truncated cone, which would better characterize the coronary microvascular bed (Batra et al., 1992). The truncated cone model, based on shorter intercapillary distances and smaller heterogeneities of capillary spacing at distal portions of the capillary network leads to a more homogeneous tissue PO_2 distribution, thus decreasing the occurrence of anoxia. This occurs despite identical average entry data of the O_2 determinants. These results are consistent with the view that the local architecture of the capillary network adjusts to the lower capillary PO_2 conditions at the distal portions of the capillary bed.

Of particular importance to this thesis is the Krogh model assumption that capillary blood is homogeneous with respect to its O_2 supply. However, it is the erythrocytes within the capillaries which are the actual sources of O_2. In fact, O_2 dissolved in the plasma accounts for less than 2% of the total O_2 in the blood with the remainder bound to Hb. Thus, the O_2 capacity of the blood is classically determined by the blood volume occupied by the red blood cells and ultimately by their hemoglobin content. In capillaries, RBCs usually travel in single file, separated by plasma gaps of variable lengths. Due to the relatively uniform size of RBCs, capillary hematocrit (Hct) and the distance between red cells (RBC spacing) are very closely related, as Hct is a reflection of the number of cells per unit length. These are two related determinants of O_2 supply.

1.2 Oxygen transport resistance

Many diffusion-related mechanisms are involved in the process of oxygen uptake at the lungs and oxygen delivery to the tissue. Along this path, many "resistances" are encountered, which result in a PO_2 drop, decreasing the driving force or PO_2 gradient between source and sink. Considering only O_2 delivery from the red blood cell to tissue, there are four major components to O_2 transport resistance (Clark and Clark, 1986): (i) *red cell* PO_2 drop from red cell interior to red cell membrane, (ii) *transcapillary drop* from RBC surface to capillary wall, (iii) *tissue drop* from capillary wall to tissue interior and (iv) *mitochondrial drop* from tissue to mitochondrial interior. The term "intracapillary resistance" usually refers to the first two components, whereas "extracapillary resistance" or tissue resistance, usually refers to the latter two.

Experimental and theoretical studies have assumed that intracapillary resistance is secondary to extracapillary resistance. In fact, most studies using the Krogh model deal only with resistance in the tissue. Estimates of the tissue PO_2 drop from capillary wall to tissue interior have been variable, as low as 5-10 mm Hg (Gayeski and Honig, 1986). However, it is extremely difficult to compare modelling studies, due to differences in input data and limitations imposed in the model (i.e. boundary conditions). The contribution of mitochondrial resistance to the total O_2 transport resistance has been found to be negligible (Clark and Clark, 1986).

If intracapillary resistance to O_2 transport is in fact significant, any variable influencing intracapillary O_2 transport resistance will influence PO_2 and O_2 distribution in the tissue. Transport resistance in the red cell, one of the two intracapillary resistances to O_2 transport, has been studied. Hellums (1977) emphasized the importance of the internal resistance of the RBC to O_2 diffusion. While Hb and O_2 are essentially in chemical equilibrium in the interior of the RBC, a boundary layer exists within the RBC near the RBC membrane, where chemical equilibrium may not exist. This boundary layer comprises a major part of the total internal resistance of the RBC. Clark and Clark (1986) determined that in maximally working skeletal muscle with maximum O_2 flux, RBC resistance contributes approximately 10-15% of the total O_2 transport resistance. This value, however, depends on the total ΔPO_2 from the cell interior to mitochondria, as well as the original and final O_2 saturations of the RBC.

While the unloading time of a RBC depends on both this internal resistance and the external environment to which it is exposed (e.g. plasma PO_2), the internal resistance alone determines the minimum possible unloading time for a RBC. Clark and coworkers (1985) calculated RBC desaturation with time, with the RBC exposed to a plasma PO_2 of zero mm Hg. For example, a RBC that is 100% saturated with O_2 will take approximately 0.1sec for 90% of its available O_2 to be removed. The values in their study are based on the steepest possible PO_2 gradient between RBC interior and plasma. Thus, *in vivo* unloading times would be longer than those

calculated, since plasma PO_2 is usually greater than 0 mm Hg. In any event, the transit time of the erythrocyte must be longer than the time needed to unload O_2.

Red blood cell transit time can be estimated from erythrocyte velocity (v_{rbc}) and capillary length (time = distance / velocity). Honig et al. (1977) estimated a mean transit time of 4.29sec in skeletal muscle, using mean capillary length measured in rat gracilis muscle, and previously published data on erythrocyte velocity in cat sartorius muscle. Tyml et al. (1981) used capillary segment lengths and v_{rbc} to estimate the spatial distribution of transit times in frog sartorius. The mean transit time was 7.2sec (range 0.7-24.3sec). Sarelius (1986) determined that the mean flow path of RBCs is approximately double the anatomical capillary length, and that actual transit times are longer than expected from anatomic determinations. In her study, transit time in golden hamster cremaster muscle was 3.2sec and 4.2sec in juveniles and adults, respectively. *In vivo* observations in skeletal muscle show tremendous variation of transit times in both space and time. In summary, transit times seem to be an order of magnitude greater than the time required for unloading of O_2 from RBCs.

1.3 The particulate nature of blood - effects on intracapillary resistance

The previous section outlined the four major contributors to O_2 transport resistance. Of these four, the PO_2 drop due to mitochondrial, tissue and RBC resistances were discussed. The effect of the particulate nature of blood on intracapillary resistance, and more specifically transcapillary PO_2 drop, will be

discussed below. The transcapillary PO_2 drop (from RBC surface to capillary wall) may be large, but it is difficult to estimate. Studies which have considered resistance within the capillary originally only treated capillary blood as a continuous Hb solution, ignoring the particulate nature of blood. In treating blood as particulate, the individual contributions of plasma and RBCs, and hence RBC spacing, to O_2 supply need to be addressed.

Aroesty and Gross (1970) examined the effect of plasma motion on transport of materials between the RBC and capillary endothelium. Their theoretical study concluded that convection of physiologically important gases (e.g. O_2) in the plasma was negligible. Accordingly, they suggested that diffusion is the primary transport mechanism of O_2, and plasma acts as a medium to transport cells within the microcirculation to regions where such diffusion could occur. A more recent rat heart model by Bos and coworkers (1994), with different boundary conditions, determined that plasma mixing due to convection may play a role in tissue oxygenation, especially at high flow and low hematocrit (20%). In this case, O_2 flux from the plasma to the tissue increased by approximately 20%. Plasma mixing may enhance O_2 transport, but the physiological importance cannot be predicted until more detailed modelling exists, accounting for more parameters.

The mean PO_2 in the plasma decreases with increasing distance from the RBC (Aroesty and Gross, 1970; Homer et al., 1981). Aroesty and Gross (1970) determined that if RBC separation is greater than 2 capillary diameters, regions devoid of O_2

should occur in the plasma. However, Homer and coworkers (1981) suggest that the PO_2 differences in the plasma are probably small at normal Hct, whereas large differences may exist at large separation distances (e.g. during anemia). Since the O_2 flux from the capillary to tissue is greatest when the PO_2 gradient is largest (i.e. adjacent to the erythrocyte), overall O_2 flux should depend on red cell separation.

In 1977, Hellums estimated the effect of the particulate nature of blood on the resistance to O_2 transport in the capillaries. In his theoretical study, RBCs of equal length were separated by plasma gaps of equal length. This discrete cell model allowed for O_2 diffusion from only the RBCs. Thus, the plasma was assumed to have an infinite resistance to O_2 transport, and only 50% of the capillary length was involved in O_2 exchange. This model was compared to the continuum model, which assumed that the same amount of hemoglobin from the discrete cells was evenly distributed in the capillary. Hellums' (1977) estimation of the intracapillary resistance to O_2 diffusion was approximately 20% of the total resistance in the continuum model and 50% in the discrete model. Therefore, the impact of the particulate nature of blood on capillary resistance to O_2 transport is significant, suggesting that resistance in the capillary may be at least as important as, if not more than, that in the tissue.

The values of resistance in Hellums' model (1977) were only approximations, since plasma convection and diffusion of O_2, and diffusion of O_2 from the ends of the RBCs into the plasma, as well as Hb-facilitation were ignored. Federspiel and Sarelius (1984) also studied the effect of the particulate nature of blood and

specifically addressed the question of whether capillary blood can actually be treated as homogeneous with respect to its O_2 supply. That is, can capillary blood supply a constant flux of O_2 at the capillary wall? Equations in their model allowed for the description of O_2 transport in the plasma gaps between two cells. Their model utilized skeletal muscle experimental data to predict a critical cell separation (S_c) distance. If two cells were separated by a distance greater than S_c, capillary blood could not be considered homogeneous in its O_2 supply since uniform O_2 flux could not be maintained at the capillary wall between the two RBCs. Consequently, once S_c is reached, an area of anoxia will occur midway between the two RBCs.

Results of their model suggest that, in skeletal muscle, increases in spacing of RBCs decrease the ability of the RBCs to maintain constant O_2 flux at the capillary wall (Federspiel and Sarelius, 1984). The critical separation distance was calculated to be approximately 4 cell lengths (24-28μm) at rest and 1 cell length (6-7μm) during maximal O_2 consumption. Therefore, RBC spacing must decrease during exercise to maintain the level of flux provided at rest. Indeed, *in vivo* observations in skeletal muscle have shown cell separation to be approximately 1 cell length during exercise (Federspiel and Sarelius, 1984). Although RBC spacing significantly affects the ability of RBCs to provide a uniform flux of O_2 at the capillary wall, the assumption of a homogeneous solution may be correct at normal Hct values observed in the microcirculation of skeletal muscle.

In 1986, Federspiel and Popel presented a skeletal muscle model to examine the intracapillary resistance due to RBC spacing, which accounted for the particulate nature of blood, O_2 diffusion in the plasma gaps, Hb-facilitation of O_2 diffusion and Hb-O_2 kinetics. They calculated a mass transfer coefficient (k*) which represented a conductance for O_2 release from the capillary. The effect of two relevant parameters were examined: (i) RBC spacing, representing the axial distance between cells, and (ii) RBC clearance, representing the radial distance between red cell and capillary wall. The mass transfer coefficient was found to be greatest with nearly touching RBCs with small clearances. Indeed, the particulate nature of blood had a major effect on k*. First, k* decreased 2-3 times due to the discreteness of blood, when compared to a continuous Hb solution. Second, k* rapidly decreased as the space between cells increased. In other words, the "zone of influence" of O_2 released from the RBC does not extend far beyond the RBC. Red blood cell clearance also affected k*, but to a lesser extent than cell spacing. Thus, RBC spacing, in addition to its role as an important source of O_2 (e.g. O_2 flux), also affects O_2 transport by affecting intracapillary O_2 transport resistance.

Previously described models, however, did not account for the movement of RBCs. Groebe and Thews (1989) incorporated the effects of both RBC spacing and RBC movement into their skeletal muscle model. In agreement with Federspiel and Popel (1986), they found O_2 conductance to decrease with increased spacing. However, RBC movement enhanced O_2 conductance at a given red cell separation.

Essentially, the movement of erythrocytes maintained an oxygen level at the capillary wall, so that tissue can receive O_2 during the passage of plasma gaps (i.e. storage and release of O_2 at the capillary wall during the passage of RBCs or plasma gaps, respectively).

While overall O_2 conductance out of the capillary decreased with increased red cell spacing in both models, individual RBC O_2 conductance increased. Due to improved diffusion geometry, O_2 flux out of a single RBC is enhanced with increasing RBC spacing within a certain range. If red cells are stationary, flux from individual cells is enhanced as cell spacing increases from 0 to 1 cell length, or approximately 6-7μm (Federspiel and Popel, 1986; Groebe and Thews, 1989). If red cells are moving, the range increases to four cell lengths (Groebe and Thews, 1989). It should be noted that the decreased overall conductance with increased RBC spacing is in part compensated for by these increases in individual RBC O_2 conductances (Groebe and Thews, 1989).

Although RBC movement enhances O_2 conductance at a given red cell separation distance, an increase in RBC velocity (v_{rbc}) does not fully compensate for the negative effects of increased RBC spacing, or decreased Hct (Tsai and Intaglietta, 1989). In a more recent modification to the model, the effects of uneven RBC spacing patterns on tissue oxygenation were considered (Tsai and Intaglietta, 1992). Three indices were used: (i) average tissue PO_2, (ii) the axial distance to which O_2 was delivered along the capillary, and (iii) the volume of oxygenated tissue. Using a three

RBC model, evenly spaced red cells resulted in a constant release of O_2 to the tissue by each cell. On the contrary, uneven spacing patterns reduced the average O_2 release by each cell, decreasing the overall transfer of O_2 to tissue. In fact, uneven spacing patterns resulted in a decrease in average tissue PO_2 of up to 40%, despite an equivalent time-averaged flux of RBCs.

Statistically distributed RBC spacing patterns were also generated (15 spacing values) for the normal (mean spacing of 4.2 cell lengths, 18.2% Hct) and hemodiluted (mean spacing of 9.4 cell lengths, 9.6% Hct) cases. Variable RBC spacing patterns did not affect any of the oxygenation indices under normal conditions. However, at reduced Hct (hemodilution), the average tissue PO_2 and volume of tissue oxygenated were reduced by 23% and 28% respectively due to variable spacing, compared to even spacing. These reductions could be due to the fluctuation in the radial penetration of oxygen due to the passage of variably spaced RBCs (Tsai and Intaglietta, 1992). Nonuniformity in RBC spacing affects the gradients for O_2 release to which the red cells are exposed (e.g. large gradients with large spacing), whereas uniformly spaced cells minimize the deviations in the O_2 gradients between cells and tissue. Thus, although RBC flux is maintained constant between evenly spaced and unevenly spaced cells, the tissue does not effectively use the O_2 delivered by unevenly spaced RBCs, when exposed to low Hct conditions.

Two recent models (Hoofd et al., 1994; Bos et al., 1995) modelled erythrocytes as point-like O_2 sources in a Krogh cylinder model, using input data from rat heart.

Evenly distributed O_2 sources with identical spacing were assumed, moving along the axis of the cylinder. In order to account for the particulate nature of blood, an extraction pressure (EP) was used to quantify the ΔPO_2 due to the capillary barrier mentioned earlier. Essentially, EP was a pressure drop used in the model to account for the difference between homogeneous and heterogeneous blood (with respect to O_2). Therefore, EP specifically accounts for the particulate nature of blood and represents the difference in PO_2 seen in the tissue versus PO_2 in the RBC. In their studies, there was a strong dependence of EP on capillary Hct. As RBC separation distance increased with decreasing Hct, EP increased, and tissue PO_2 significantly decreased.

The above models did not account for RBC velocity in the calculation of extraction pressure. The effect of RBC velocity on EP was incorporated into a subsequent model in the heart (Bos et al., in press). As in earlier models, increased red cell spacing resulted in decreased tissue PO_2, due to an increase in the capillary barrier, quantified by extraction pressure. However, at RBC spacing values greater than 10μm, the increase in EP could be compensated for by an increase in v_{rbc}. At lower spacing values, increased v_{rbc} actually increased extraction pressure, possibly due to a decrease in the time available for O_2 unloading. Thus, RBC spacing may be more important than velocity, as EP always increased with increased spacing (Bos et al., in press). The relationship between RBC spacing and EP, as well as between velocity and EP, are illustrated in Figure 6.

Figure 6. Extraction pressure (EP) plotted against red blood cell spacing at different RBC velocities. EP increases with increasing red cell spacing, regardless of RBC velocity. At large cell separation distances, an increase in RBC velocity decreases EP. However, at small separation distances, an increase in RBC velocity will actually increase the EP. Modified from Bos et al., in press.

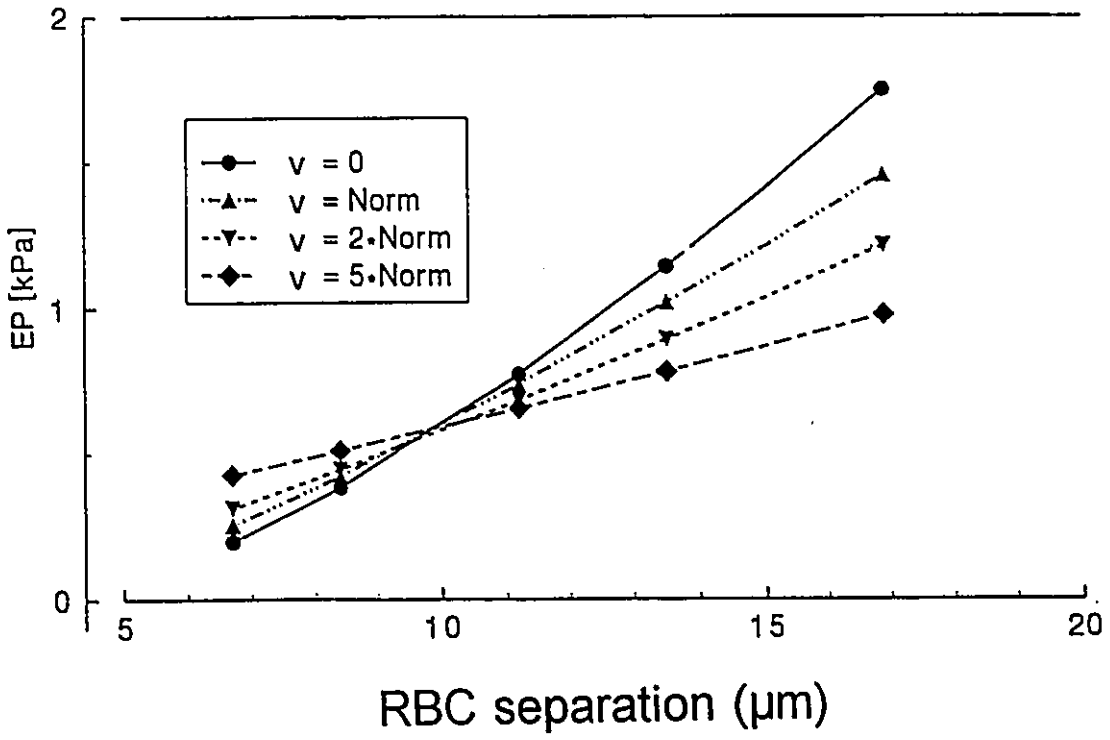
2
1
0
EP [kPa]
v = 0
v = Norm
v = 2•Norm
v = 5•Norm
5
10
15
20
RBC separation (μm)

Taken together, modelling studies suggest that RBC spacing and heterogeneity in RBC spacing are important factors affecting tissue PO_2 both in skeletal and cardiac muscle. Although some investigators suggest that these parameters may not be critical at rest under normal Hct conditions in skeletal muscle, the physiological importance of RBC spacing may be more pronounced in cardiac muscle, where there is a higher O_2 consumption and possibly less O_2 reserve.

1.4 Red blood cell spacing in coronary capillaries - experimental evidence

Despite the importance of RBC spacing for O_2 supply, as indicated by the theoretical studies, our knowledge of realistic values for capillary hematocrit and related RBC spacing in coronary capillaries is lacking. The primary reason for this is the lack of proper methodology for visualization of RBCs within coronary capillaries. While *in vivo* observations are appropriate and useful in skeletal muscle, only superficial layers of the heart may be observed in such a fashion. The movement of a beating heart still poses technical difficulties for such *in vivo* observations.

In an effort to overcome many of the technical difficulties in viewing surface vessels of the beating heart *in vivo*, and to allow examination of deeper layers of the heart, many post-mortem histological techniques are available. We are aware of only two studies which experimentally determined capillary Hct or RBC spacing in coronary capillaries. Vetterlein and coworkers (1989) determined the red cell content of coronary capillaries from the subendo- and subepicardium of the left ventricle of

rat heart. The red cell content was established by determining the fraction of plasma gaps per capillary length. The vascular system was visualized by using FITC-labelled γ-globulin injected prior to freezing the heart. However, no values for individual red cell spacing were presented. Under normoxic conditions, the percentages of measured capillary length without RBCs were 45% and 54% in the subepi- and subendocardium, respectively. However, this difference was not statistically significant. Both of these values were each based on means from 500 capillaries. In their study, however, hearts were frozen by clamping at the base and then transferring the heart to isopentane at -100°C. It is possible that changes in red cell distribution occurred during this process of removal and freezing.

The first observations of RBC spacing in coronary capillaries were made in the subepicardium of the rat by Honig et al. (1989). Based on the earlier work of Federspiel and Popel (1986) who stated that plasma PO_2 is zero a few microns from the RBC, Honig et al. (1989) categorized their RBC spacing data into two populations (≤5μm and >5μm). Mean RBC spacing was 2.1 and 16.5μm in the ≤5μm and >5μm populations, respectively. However, the sample size in their study was small, containing only 15 capillaries from one heart. In addition, RBC-free capillaries were not visualized, so tissue Hct could not be accurately determined from their data.

BASIS FOR THE THESIS

In the theoretical research of the past two decades, the importance of RBC spacing in oxygen transport to tissue has become more apparent. Modelling studies have shown that RBC spacing affects both the oxygen carrying capacity of the blood as well as the resistance to transport of this oxygen from capillaries to tissue. However, the majority of theoretical and experimental studies have focused on skeletal muscle. Recent theoretical models incorporating rat heart data have begun to incorporate the particulate nature of blood, treating red blood cells as discrete oxygen sources. However, erythrocytes were assumed to be evenly distributed with identical spacing and heterogeneity of RBC spacing was not considered. To date, no systematic measurements of red blood cell spacing have been performed in coronary capillaries, and our knowledge of realistic values for this important oxygen determinant is lacking. Thus, despite the recent advances in theoretical modelling of oxygen supply to tissue, an unrealistic geometry is being considered, with respect to red blood cells.

Basic entry data regarding RBC spacing in the microvascular bed in the heart is essential for a better understanding of O_2 transport. Since most mathematical models assume a very simplified geometry (e.g. 2 stationary RBCs), the relevance of computer simulation outputs are limited to very specific situations. Thus, not only are realistic data regarding these important parameters needed, but heterogeneity of the

data is also needed to serve as input parameters in future mathematical models.

It may be important where along the capillary pathway Hct and RBC spacing measurements are taken. No reliable method was available to visualize RBCs and measure RBC spacing in coronary capillaries at different locations in the capillary bed. The advantages of such a method are two-fold: (i) it allows determination of RBC spacing and its heterogeneity in coronary capillaries, but more importantly, (ii) it allows investigators to examine changes in these parameters at two different locations in the capillary network (e.g. proximal and distal portions) which have very different conditions for O_2 transport (e.g. lower PO_2 in capillaries located closer to collecting venules).

The heart is an extremely dynamic organ, exposed to wall pressures and O_2 conditions which vary in time (e.g. diastole vs. systole) as well as space (e.g. subendocardium vs. midmyocardium). It is known that the subendocardial layers of the left ventricle are especially threatened during ischemic episodes. There is a differential transmural distribution of stress in the heart. In fact, greater systolic and diastolic tissue tensions are developed in the subendocardium compared to the midmyocardium and subepicardium (Kirk and Honig, 1964b). So much so, that during systole, tissue tension exceeds cavity pressure and subendocardial blood flow can be stopped. Thus, there exists a perfusion pressure gradient, decreasing from the subepicardial to subendocardial layers, resulting in perfusion of the subendocardium during diastole only. Furthermore, O_2 consumption of the left ventricle is greater in

the subendocardium than in the subepicardium (Winbury et al., 1971). Given that a recent study from our laboratory has shown capillary geometrical alterations during systole compared to diastole (Batra and Rakusan, 1992), as well as the regional differences explained above, we were prompted to investigate RBC spacing and capillary Hct in two regions of the heart during both diastole and systole.

In this thesis, the development of a novel experimental method to determine capillary Hct and red cell spacing in frozen cardiac tissue is reported, including freezing and staining methodologies. Following development of this method, realistic data on red blood cell spacing and capillary hematocrit have been collected in rat hearts arrested in diastole or systole, in the subendo- and midmyocardium, at two distinct locations in the capillary bed.

STATEMENT OF THE PROBLEM

Correct input data for theoretical models cannot be obtained without the ability to reliably collect data on red blood cell spacing in coronary capillaries. With the mounting evidence supporting the importance of red blood cell spacing in tissue oxygenation, the development of such a method is critical. The following questions will be addressed in this thesis:

1. Is it possible to rapidly freeze the heart *in situ* and stain the tissue to discern red blood cells within capillaries which are located within proximal or distal portions of the capillary bed (i.e. close to and far from their feeding arterioles)?

2. Are there differences in capillary hematocrit and red blood cell spacing in capillaries located within proximal and distal portions of the capillary bed?

3. Are there differences in these parameters during different stages of the cardiac cycle (diastole or systole)?

4. Are there regional differences in these parameters between the subendocardium and midmyocardium of the left ventricle?

5. Are there any interactions between phase of the cardiac cycle and region of the left ventricle which affect either of these parameters?

CHAPTER 2 DEVELOPMENT OF TECHNIQUES

2.1 Introduction

This study was divided into two distinct parts. The first part (Chapter 2), details the development of two novel experimental techniques: (i) an efficient method to rapidly freeze rat hearts *in situ*, minimizing changes in RBC distribution, and (ii) a method to simultaneously visualize capillaries located in two distinct locations within the capillary bed (proximal and distal portions) and the RBCs within them. The second part (Chapters 3, 4, and 5) deals with the application of the developed techniques to collect data on capillary hematocrit and related RBC spacing.

2.2 Freezing of rat hearts

2.2.1 Development of freezing technique

Various techniques for rapid freezing of the heart were attempted. The two most favourable approaches are explained, while other possibilities are discussed in the next section (2.2.2). The heart could be: (i) frozen following excision, by direct contact with liquid nitrogen by submersion (e.g. *ex situ*), or (ii) frozen by use of a heat sink, *in situ*. As a heat sink, we specifically designed copper clamps to match the shape of rat hearts, and precooled them in liquid N_2.

In designing the copper clamps, both the shape and the size of the heart were considered. Two copper blocks (20.3mm x 16.3mm x 9.5mm) were used. An

ellipsoid hole was drilled into the blocks, which decreased in diameter and increased in depth gradually. The dimensions of the cavity were 12.7mm x 11.7mm x 5.5mm at the greatest length, width and depth respectively, and were chosen to correspond to the size of hearts used in the second part of this study (see Chapter 3). At one end of each block, a 'tunnel' was drilled 3.9mm in width, 1.3mm deep which accounted for the large vessels exiting at the base of the heart. The upper two corners of each block were cut at 45° to improve the dynamics when the clamps were inserted into the chest cavity. The two copper plates were then soldered onto the arms of a pair of stainless steel crucible tongs, so that when closed, the cavity of the blocks would encase the whole heart, without squeezing it.

In order to determine the most rapid transmural freezing method, a wire connected to a thermocouple digital thermometer (Cole Parmer) was inserted into the left ventricular cavity of an excised heart, via the aorta. The large vessels of the heart were clamped shut, closing any opening to the ventricular cavity and securing the thermistor wire. The heart was warmed in normal saline (37°C) and then either (i) submerged in liquid nitrogen (N_2) or (ii) clamped with precooled clamps; cavity temperature was recorded every 5 seconds.

Transmural freezing of the heart was achieved most rapidly using precooled copper freezing clamps (Fig. 7). Cavity temperature reached 0°C within 3.75sec when precooled clamps were used, but not until 10.75sec when submerged in liquid N_2. The thermistor wire alone reached 0°C in 0.2sec, and its full response time from 37°C

Figure 7. Cavity temperature of rat hearts submerged in liquid nitrogen (n=5) or frozen with precooled freezing clamps (n=5), as a function of time. Hearts were warmed to 37°C and exposed to liquid nitrogen or freezing clamps at time=0sec. Temperature was taken at t=0, 2, 5sec, and every 5sec following.

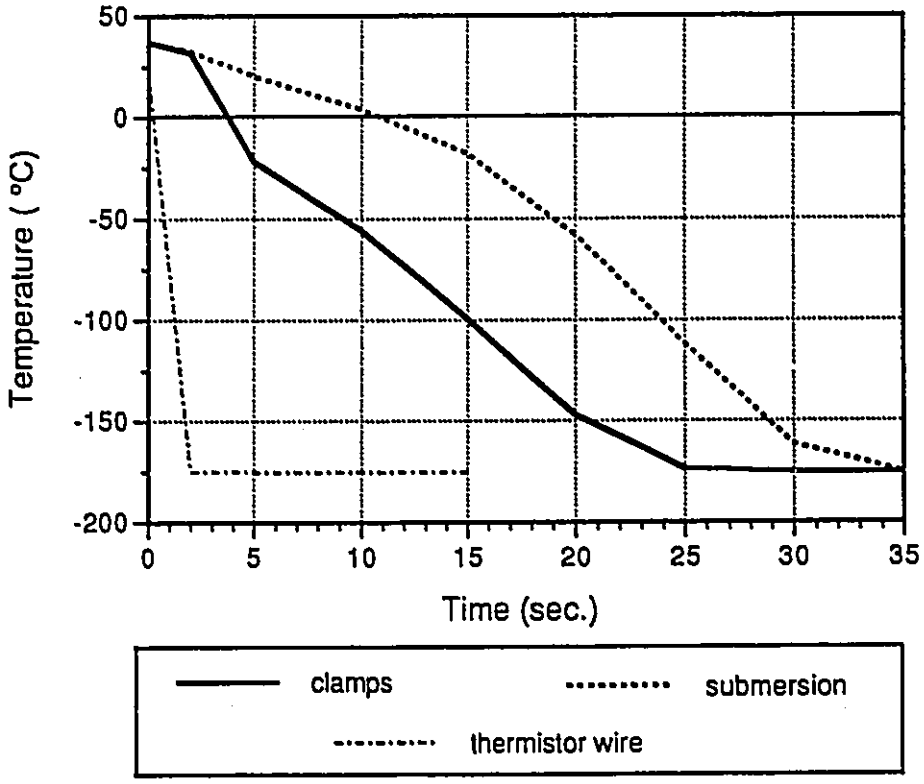
50
0
-50
-100
-150
-200
Temperature (°C)
0
5
10
15
20
25
30
35
Time (sec.)
clamps
submersion
thermistor wire

to -175°C was less than 2sec.

2.2.2 Summary and discussion

In any morphometric study, the characteristics of the objects being measured in tissue sections should reflect those characteristics seen *in vivo*. It was extremely important that the positions of erythrocytes were preserved during the experimental protocol. Thus, freezing of the heart must be as rapid as possible, and the freezing method itself should not affect the position of RBCs.

In order to determine a rapid freezing method, we compared direct submersion of tissue in liquid N_2, with tissue frozen by precooled clamps. The concept of precooled clamps was inspired by Honig et al. (1989), who used a copper heat sink to freeze rat hearts *in situ*, in their study of RBC spacing discussed previously. As can be seen in Figure 7, the freezing point inside the ventricular cavity was reached within 3.75sec following contact with the clamps, less than half the time taken if submerged in liquid N_2. Not only is freezing slower with submersion, but arrest of the heart, excision, and subsequent submersion in liquid N_2 could potentially alter RBC geometry (e.g. due to physical movement of the heart and the time taken to transfer to liquid N_2). Thus, the use of clamps as a heat sink is advantageous for two reasons: (i) manipulation is minimized by *in situ* freezing and (ii) transmural freezing is quickest.

It is important to consider possible alterations in RBC geometry due to the clamps themselves, as maintenance of cardiac structure is important. To minimize any such alterations, the clamps were specifically designed to match the contours of rat hearts. The contoured clamps serve to encase the entire heart and prevent squeezing of the heart which would occur if flat copper "plates" were used. According to Vetterlein and coworkers (1991), who used flat, precooled clamps to freeze hearts, only vessels >100μm appeared flattened. Thus, in the event of minor squeezing by our contoured clamps, presumably only larger vessels in the epicardial layer would be affected.

An alternative to the introduction of clamps into the chest cavity would be direct application of liquid N_2 (e.g. pouring). This technique was abandoned due to several potential complications: (i) freezing with liquid N_2 was determined to be slower, (ii) the heart was often frozen to other tissues in the region (e.g. liver, lungs), (iii) the entire surface of the heart was not exposed to liquid N_2 and (iv) the rate of application could be variable, affecting equal transmural freezing across the heart.

Finally, young animals (i.e. small hearts) were used to minimize transmural freezing distances. Clark and Clark (1983) determined that after 1sec exposure to liquid N_2, the depth of freezing in tissue was at least 1mm. In addition, Judd and Levy (1991) suggest that blood viscosity increases greatly when temperature decreases (from 37°C to 10°C). Taken together, blood redistribution is probably negligible during the freezing process of rat hearts in our study.

We believe that (i) *in situ* freezing, (ii) the use of contoured copper freezing clamps, and (iii) the use of smaller animals, and thus smaller hearts, would result in morphometric observations which accurately reflect the actual situation *in vivo*.

2.3 Staining of capillaries and red blood cells

2.3.1 Development of staining technique

The staining procedure includes a previously developed method, whereby capillaries in frozen tissue can be identified as located in either proximal or distal regions of the capillary bed. This method was first introduced by Lojda (1979) and first applied to cardiac tissue in our laboratory (Batra et al., 1989). Briefly, capillaries which are located in proximal portions of the capillary network can be distinguished from those capillaries located more distal, based on the differential localization of enzymes along the length of capillaries. Alkaline Phosphatase (AP) activity has been demonstrated in the endothelial cells of capillaries located in proximal portions of the capillary bed, and its detection results in capillary walls staining blue. Dipeptidyl Peptidase IV (DPP IV) activity has been demonstrated in the endothelial cells of capillaries located in distal portions of the capillary bed, and its detection results in capillary walls staining red.

The major goal of this development was to add a third colour to the AP/DPP IV stained tissue sections, one which would identify RBCs. In an effort to clearly explain the development of the staining technique, the process has been categorized

into three sections: (i) fixation of RBCs, (ii) staining of RBCs, and (iii) combination of RBC staining with the dual staining of capillary walls. It must be emphasized that a categorical description is for conceptual purposes. The processes are not independent of one another, nor were they developed sequentially. The final staining procedure is the culmination of various combinations of trials from within and between categories. For example, although many methods exist to stain RBCs, they were not all compatible with the capillary wall stains. Finally, within each section, only the major points are discussed; all combinations are not listed.

(i) Fixation of RBCs

During the freezing process of tissue, cellular cytosol is also frozen, resulting in ice crystal formation. In our study, as ice crystals form within RBCs, the erythrocyte membrane may be punctured. This becomes problematic upon thawing, as the cytosol will leak out of the RBC (lysis), leaving membrane fragments behind. This makes it difficult, if not impossible, to perform morphometric analyses of RBC spacing. It was therefore necessary to fix the tissue during the thawing process to preserve RBC shape. Many fixatives were tested, including: ethanol, chloroform, acetone, and chloroform-acetone combined. Fixative temperature and fixation time were varied as well. In addition, various cryostat sectioning methods were attempted: (i) cutting cryostat sections onto slides and incubating them in fixatives, (ii) cutting cryostat sections onto slides precoated with fixatives, (iii) cutting cryostat sections

onto slides precoated and prefrozen with fixatives, and (iv) cutting cryostat sections into a fixative bath and subsequently placing tissue sections onto slides.

Although many of the above combinations of times, temperatures and sectioning were successful to allow subsequent RBC staining, not all were compatible with the capillary wall stains. The most successful combination was as follows. A fixative bath of chloroform-acetone (1:1 vol/vol) was sealed in a rectangular staining dish to prevent evaporation, and precooled in dry ice to approximately -22°C. Cryostat sections were cut directly onto a cool petri dish in the cryostat chamber (-22°C). The precooling of the chloroform-acetone was timed to coincide with completion of cryostat sectioning. Once all sections were cut, they were placed into the fixative bath and left at room temperature (21°C) for 15min. This allows the tissue to warm up gradually from -22°C to room temperature. More importantly, RBCs are being fixed as they thaw, preserving shape.

The best results were obtained when the chloroform-acetone fixative bath was precooled to -22°C. However, it was just as important to ensure that the fixative was the same temperature as the cryostat chamber. For example, a large temperature gradient between cryostat chamber and fixative would have had negative effects on the tissue (e.g. curling up and/or wrinkling). The timing of fixation was also crucial, so that damage to the tissue was prevented.

(ii) Staining of RBCs

Various histological stains and staining methods exist which allow for RBC visualization in paraffin sections (e.g. Sheehan and Hrapchak, 1980; Garvey et al., 1987), as well as in plastic sections (e.g. Dupont, 1979). However, the AP/DPP IV staining technique, as well as the need to preserve RBC geometry, required the use of frozen tissue samples. We tried the aforementioned staining techniques in frozen tissue, as well as other reagents such as Fast Green, EA-65, Eosin, and Papanicolaou OG-6 (OG6). Most of these procedures were incompatible with the AP/DPP IV staining. However, Papanicolaou OG6 was compatible, and efficiently stained RBCs orange, in frozen tissue sections. White (1950) has shown that the globin of erythrocytes and intranuclear histones retain Orange G. Since mammalian RBCs are not nucleated, presumably only globins are being stained. In summary, following removal of tissue sections from the fixative bath, the slides were allowed to dry (chloroform-acetone evaporates) and then placed into OG-6 at room temperature for 40min.

(iii) Combination of RBC stain and enzyme stains

Trials involving various reagent temperatures and concentrations, as well as incubation times and sequences were attempted. Staining for DPP IV was less versatile than AP, and many alterations were needed to optimize all three colours. For example, enhanced RBC staining occurred at the expense of distal capillary staining

(DPP IV). The concentrations of reagents in the incubation media as well as incubation times for DPP IV and AP were modified from the previously developed dual staining (Batra et al., 1989). Finally, a staining procedure which sequentially stains RBCs, distal capillaries, then proximal capillaries was developed, hereafter referred to as the 'triple stain'. Briefly, cryostat sections (16μm) were prefixed by floating the tissue in a solution of cooled chloroform-acetone for 15 minutes. The sections were put onto slides and sequentially incubated for 40 minutes in OG6, 110 minutes in a medium sensitive to DPP IV, and 25 minutes in a medium sensitive to AP. Sections were rinsed with distilled water between incubations. Finally, sections were postfixed for 15 minutes in 4% formalin and coverslipped using glycerol gelatin.

2.3.2 Summary and discussion

The procedure explained briefly in the preceding section is detailed in Appendix 1. The development of the triple staining procedure enables us, for the first time, to quantitatively determine capillary Hct and RBC spacing at two locations in the capillary network (proximal and distal portions). In our opinion, the chosen combination of reagent temperatures and concentrations, as well as incubation times and sequences result in clearly defined staining. Plate 1 contains micrographs of longitudinal sections of the midmyocardium, illustrating proximal capillaries (blue), distal capillaries (red), and RBCs (orange). In these pictures, it is not possible for all RBCs to be in focus simultaneously. The actual process of making measurements

(explained in the next chapter) requires constant re-focusing while viewing under a microscope.

Plate 1. Photomicrographs (A and B) of triple-stained midmyocardial longitudinal tissue sections (mag. 775X). Proximal capillaries stain blue (solid arrows), distal capillaries stain red (open arrows), and red blood cells stain orange (arrowheads). Scale bar represents 25μm in both pictures.

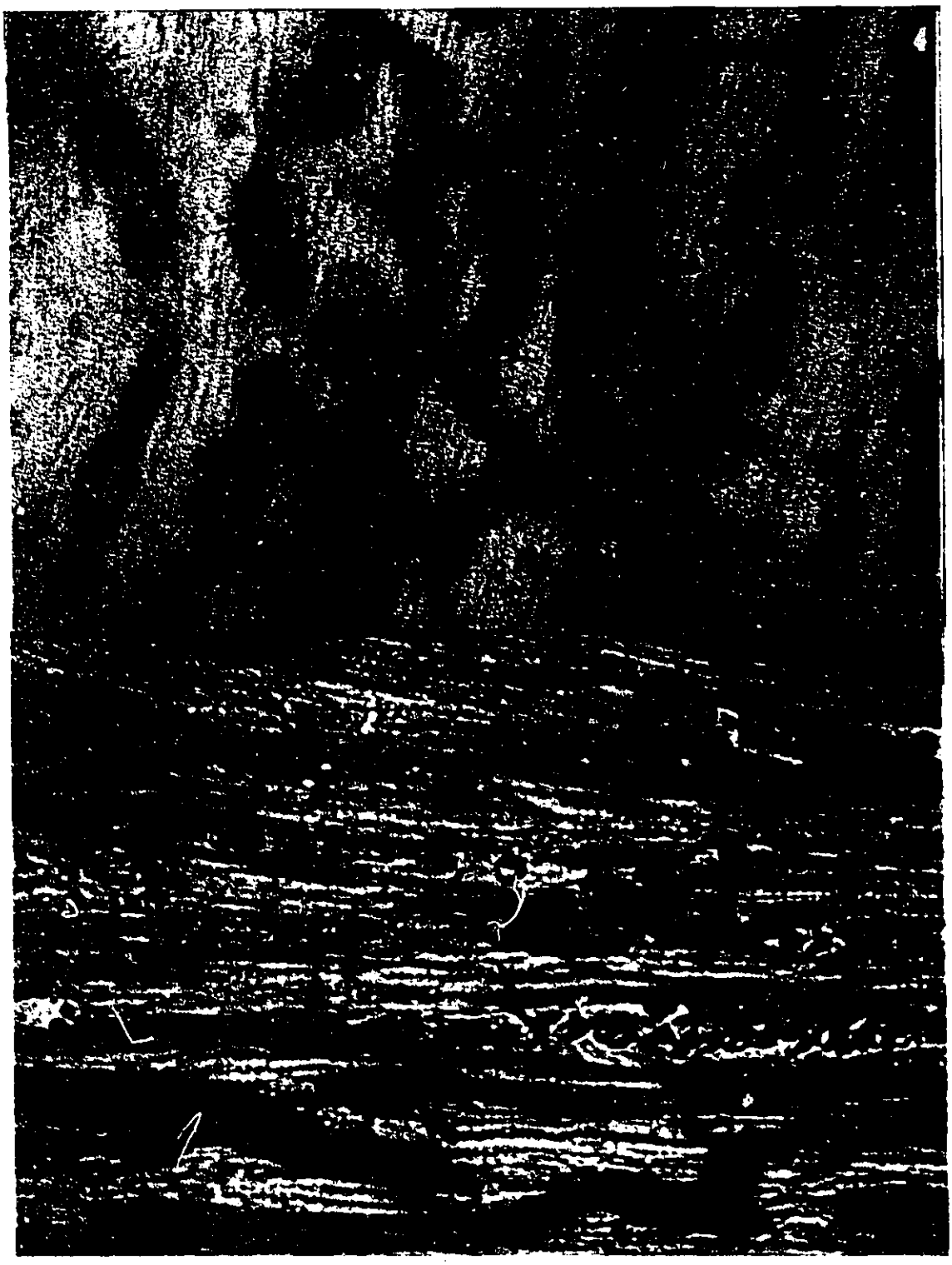

CHAPTER 3 METHODS

This chapter describes in detail the application of the methods developed in the previous chapter. The results and discussion follow in the two subsequent chapters.

3.1 Animals

Young male Sprague-Dawley rats (Charles River) weighing approximately 140g (range 130-155g) were used in this study. Rats were acclimatized 5 days in the animal care facilities prior to use. Food and water were available *ad libitum*. The following protocol was approved by the Animal Care Committee, and all procedures are in accordance with the Canadian Council on Animal Care.

3.2 Surgical procedure

Following anaesthesia (sodium pentobarbitol: 52mg/kg i.p.), a blood sample was taken from the right femoral vein (≈0.3mL) for large vessel Hct determination. A tracheotomy was performed and the animal was artificially ventilated (Harvard Apparatus Rodent Respirator). The diaphragm was exposed and cut. The ribs were cut bilaterally, exposing the heart, and the thorax was held away with clamps. The heart was kept moist with warm saline (37°C). A silk ligature was passed under the heart at the base, around the large vessels exiting the heart (a loose loop was made which would be used during extraction of the heart - see Appendix 2).

The lungs were retracted and bolus injections of KCl or $CaCl_2$, into the apex of the left ventricle, were used to arrest the heart in "diastole" (DIAS) or "systole" (SYS), respectively. Immediately, the heart was frozen with precooled freezing clamps, excised while still in contact with the clamps, and placed in liquid N_2. The loose loop made earlier was used simultaneously with the clamps to lift the heart outward from the cavity to make it more accessible to the clamps. Hearts were stored at -86°C until cryostat sectioning.

The concentrations of KCl and $CaCl_2$ used were determined empirically. The goal was to arrest the heart as quickly as possible, with the least volume of injected substance. The concentrations used were; 4M KCl and 2M $CaCl_2$. The average volumes of KCl and $CaCl_2$ used were approximately 0.75mL and 1.6mL, respectively. On average, a greater volume of $CaCl_2$ was injected, since increasing the concentration of $CaCl_2$ above 2M resulted in a solution which was too viscous to inject.

The average time the heart was exposed (from cutting of the diaphragm until excision of the heart) was 3 min. The average surgical time, in total, was 11.5min.

Large vessel Hct from the femoral vein was determined using micro-capillary tubes (Micro-capillary centrifuge and reader, International Equipment Company, Mass.). For each animal, approximately 5 micro-capillary tubes were used, and an average Hct reading was obtained.

3.3 Cryostat sectioning

For each heart, the subendo- and midmyocardium samples were required in longitudinal orientation. Therefore, hearts were first cut perpendicular to the base-apex axis, resulting in the midmyocardium (MID) fibers being in longitudinal orientation. The middle one third of the heart was used for staining. Approximately 8 tissue sections were cut onto slides for sarcomere length determination (described below). Following sarcomere length determination for each heart, to confirm the phase of the cardiac cycle, approximately 14 tissue sections (16μm) were cut and subjected to the triple staining procedure described in the previous chapter and detailed in Appendix 1. The remainder of the tissue block was cut in half, parallel to the base-apex axis. One of these halves was rotated 90° and mounted for cryostat sectioning. Thus, the subendocardium (ENDO) fibers were in longitudinal orientation. Approximately 16-20 tissue sections (16μm) were cut and subjected to the triple staining procedure. Since the volume of tissue occupied by ENDO is less than MID, more tissue sections were needed for data collection.

3.4 Sarcomere length determination

In order to determine that the injections of KCl and $CaCl_2$ resulted in the desired phase of the cardiac cycle, sarcomere lengths in the midmyocardium were determined for each heart. Tissue sections (5μm) were cut and stained with Periodic acid-Schiff's reagent to allow for visualization of myofiber Z bands.

Sarcomere lengths were determined from well defined longitudinal sections of the midmyocardium by oil immersion light microscopy using a 100X objective. The overall magnification, determined by viewing a micrometer, was 2875X. These measurements were made with the aid of a microscope and a graphic tablet (Bioquant Hipad™ Tablet) connected to an image analysis system (Bioquant IV, R&M Biometrics Inc., TN). Ten successive sarcomeres (distance between 11 successive Z lines) were measured along muscle fibers. Thus, each measurement represents the mean length of 10 sarcomeres. For each heart, approximately 50 such measurements were made. The average of these measurements was divided by 10 to obtain a single average sarcomere length measurement.

3.5 Triple staining

As explained in the previous chapter, and detailed in Appendix 1, a staining procedure was developed which permitted the simultaneous visualization of capillaries proximal and distal to their feeding arterioles and the RBCs within them. The staining process sequentially stains RBCs orange, capillaries located far from their feeding arterioles red and those capillaries close to their feeding arterioles blue.

3.6 Representative tracings

From tissue sections stained with the triple stain, representative tracings of capillaries and RBCs were made from the midmyocardium and subendocardium (both regions in longitudinal orientation) of the left ventricle. Regions were selected randomly using a 40X objective, based on the following criteria: (i) staining in the field of view was regular and consistent, and (ii) the tissue was not damaged. Due to the smaller volume of subendocardium compared to the midmyocardium, it was not always possible to satisfy both of these conditions. In order to do so, a significant amount of suitable regions would be excluded, requiring extra tissue sections. This would increase the variability due to possible base-apex heterogeneities. Following selection of the field, the objective was increased to 63X and tracings were made by the use of a drawing arm (Olympus Drawing Attachment Model BH2-DA, NFK 5X eyepiece) connected to a microscope (Olympus BH-2). The overall magnification of the tracings was 625X.

From these tracings, measurements (described below) could be obtained. Similarly to sarcomere length measurements, these measurements were digitized with the aid of a graphic tablet (Bioquant Hipad™ Tablet) connected to an image analysis system (Bioquant IV, R&M Biometrics Inc., TN).

3.7 Parameter definitions

Various morphometric parameters were defined, described below and illustrated in Figure 8.

3.7.1 Capillary hematocrit

$$= \frac{\text{aggregate RBC length}}{\text{total capillary length}}$$

This parameter represents a one dimensional, ***linear capillary hematocrit***, which can be taken to represent the actual capillary hematocrit. For each capillary type (proximal or distal portions of the capillary bed), the sum of all RBC lengths, measured along the direction of the capillary, was determined (=aggregate RBC length). Total capillary length was determined as the sum of all capillary portions of each capillary type from all tracings. Thus, each region of each heart had one capillary Hct value per capillary type, based on all tracings from that region. Since all capillaries were traced, this parameter included plasma perfused capillaries (no RBCs) as well, which effectively decreased capillary Hct.

3.7.2 Normalized capillary hematocrit

$$= \frac{\text{capillary Hct}}{\text{large vessel Hct}}$$

Capillary Hct was normalized to determine whether variability in large vessel Hct (e.g. between animals) affects Hct at the capillary level. The parameter was

Figure 8. Schematic representation of tracings made from triple stained tissue. See section 3.7 for description of parameters.

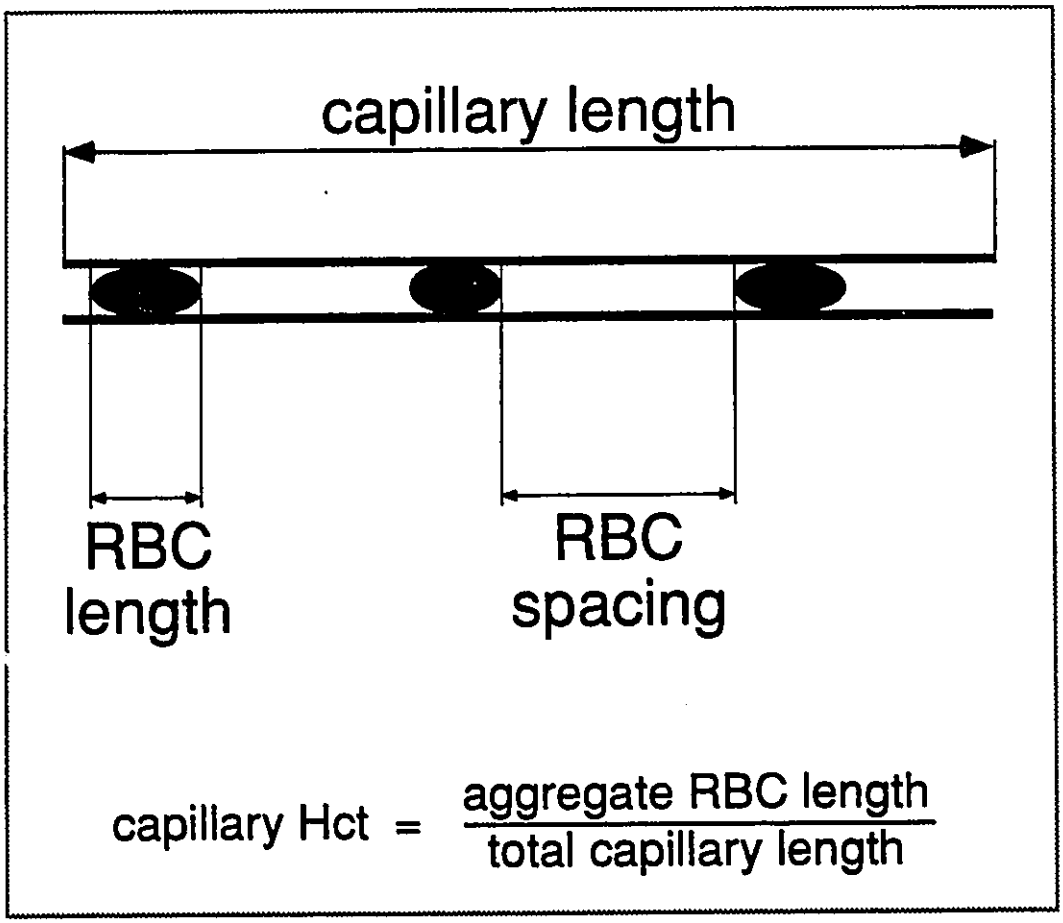
capillary length
RBC
length
RBC
spacing
capillary Hct = aggregate RBC length / total capillary length

calculated from the measured capillary Hct and Hct of blood taken from the femoral vein. The value obtained is not a hematocrit value *per se*, but it represents a ratio of capillary Hct to large vessel Hct. Each heart had one value for normalized capillary Hct per capillary type, per region.

3.7.3 Red blood cell spacing

In capillary portions with two or more RBCs, the edge-to-edge distance betweer two adjacent RBCs was determined for each capillary type. This length measurement was taken along the path of the capillary. From each region of each heart, a mean RBC spacing value was determined for each capillary type, based on at least 100 individual measurements. A spacing value was not included in the data if a capillary branch was present between two RBCs or a RBC was located within a branch point.

3.7.4 Red cell content

In the midmyocardium, where larger amounts of tissue were available for analysis (compared to the subendocardium), the number of RBCs within capillary segments was also determined. A capillary segment is defined as the distance between two consecutive branch points. Capillary segments were categorized as containing zero, one or more than one RBC. Thus, capillaries with no RBCs would be equivalent to capillaries perfused only with plasma. Despite the relatively small

sample size, this parameter is useful as an indication of possible changes in RBC distribution at different times and locations. For example, does the number of unperfused segments change between systole and diastole, or between proximal and distal capillaries?

3.8 Statistical analyses

All results are reported as means ± SEM (standard error of the mean). In some cases, additional descriptive statistics are provided. The coefficient of variation (CV) represents the standard deviation of data normalized to the mean (CV = SD/mean x 100%) and represents an additional measure of variability. Student t-tests (unpaired) were used to determine if there were significant differences in sarcomere lengths between diastolic- and systolic-arrested hearts. Student t-tests (paired) were also used to determine if there were significant differences in the percentage of unperfused (zero RBCs) capillary segments between proximal and distal portions of the capillary bed, in both diastolic- and systolic-arrested hearts.

Analysis of variance (ANOVA) was used to test the significance of cardiac phase, cardiac region and capillary type on capillary Hct, normalized capillary Hct, RBC spacing, and frequency of spacing values equal to 0μm, ≥20μm, and ≥40μm. For these analyses, a split plot design was used because the type of capillary as well as region of the heart were from the same heart, whereas phase differences were from different hearts. The ANOVA calculations were made using the GLM (General Linear

Model) procedures of the SAS statistical software package (SAS Institute, Cary, NC, USA). When a main effect was significant, a Duncan multiple comparison test (MCT) was used to locate the significant differences. In this thesis, the term "main effect" is used to refer to significant differences in one parameter, independent of the others. The word "significant" refers only to a statistical difference ($P \leq 0.05$).

CHAPTER 4 RESULTS

4.1 Sarcomere length

Sarcomere lengths in the midmyocardium were significantly shorter in systolic-arrested hearts compared to diastolic (SYS=1.76 ± 0.06μm, DIAS=2.03 ± 0.04μm; P=0.0039). Mean sarcomere lengths ranged from 1.53 - 1.91μm in systole and 1.96-2.17μm in diastole (Fig. 9). The lowest individual sarcomere length obtained during systole was 1.20μm, while the greatest length obtained in diastole was 2.72μm.

Frequency histograms of all sarcomere lengths in systolic- and diastolic-arrested hearts illustrate a shift toward lower sarcomere length values in systolic-arrested hearts (Fig. 10). Although the mean coefficient of variation (SD/mean) was greater in systole than diastole, indicating greater variability in the data, the difference was not significant

4.2 Capillary hematocrit

Representative tracings of capillaries and the RBCs within them were made from triple-stained tissue of the subendo- and midmyocardium (longitudinal orientation) of hearts arrested in diastole and systole. From these tracings, data were obtained for both capillary Hct and RBC spacing as a function of capillary type. In tissue exposed to the triple stain procedure, there was a prevalence of proximal (blue) capillary portions compared to distal (red). In fact, capillaries located in proximal

Figure 9. Individual (∘) and mean (•) sarcomere lengths in the midmyocardium of rat hearts arrested in diastole (n=6) and systole (n=6). Error bars represent SEMs. Sarcomere lengths in diastole are significantly greater than systole (P=0.0039).

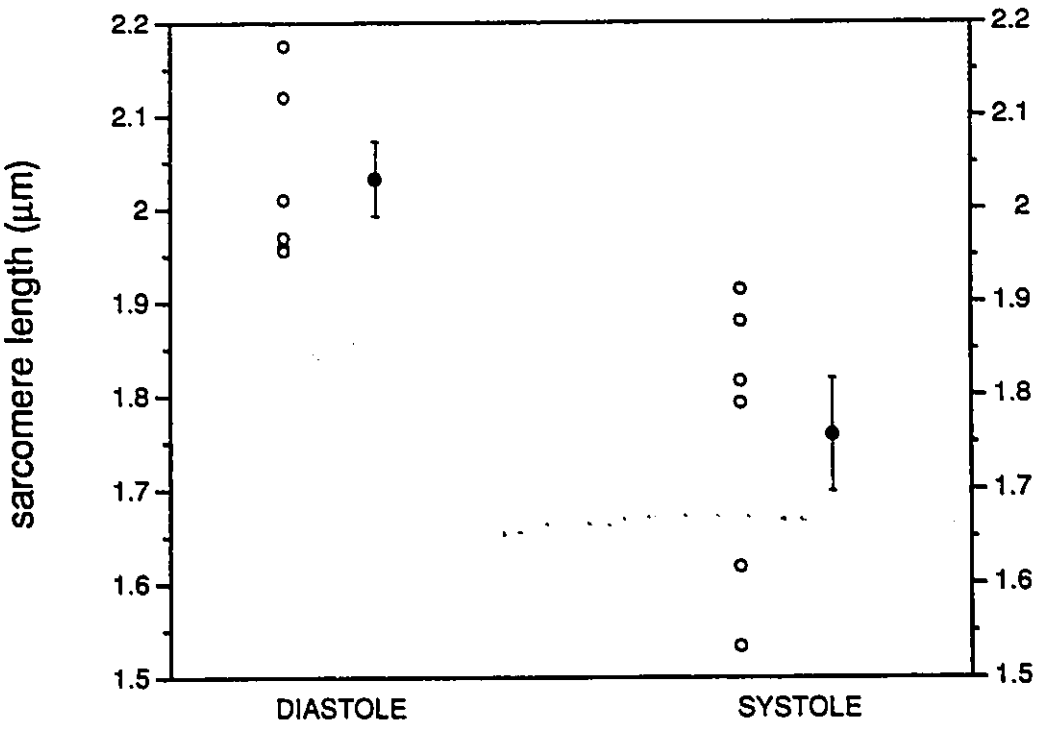
sarcomere length (µm)
2.2
2.1
2
1.9
1.8
1.7
1.6
1.5
DIASTOLE
SYSTOLE

Figure 10. Frequency histograms of sarcomere length data, combined for all hearts in diastole (n=332) and systole (n=420). Mean values are inset in graphs. There is a shift toward lower sarcomere length values in systolic-arrested hearts.

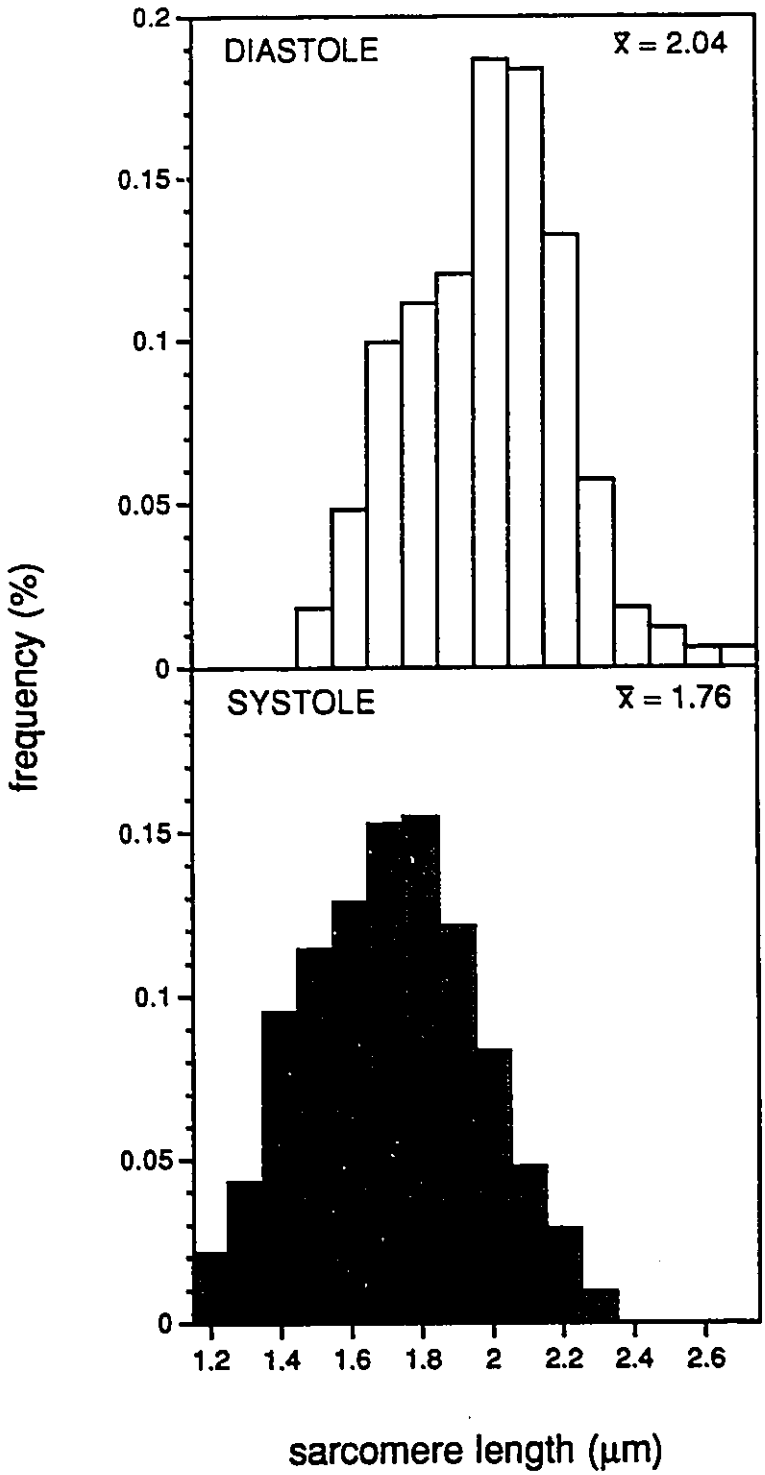
DIASTOLE
x̄ = 2.04
SYSTOLE
x̄ = 1.76
frequency (%)
0.2
0.15
0.1
0.05
0
1.2
1.4
1.6
1.8
2
2.2
2.4
2.6
sarcomere length (µm)

portions of the capillary bed accounted for approximately 60% of the total capillary length drawn. This is illustrated in Table 1, which reports the total capillary length traced for each phase/region/capillary type combination (expressed as a mean of values from individual hearts in each category). This proportion is similar to the blue/red distribution found previously (Batra et al., 1991; Heron and Rakusan, 1994).

Results for capillary Hct and normalized capillary Hct are summarized in Table 2. Mean large vessel Hcts are also presented. There were no significant differences in large vessel Hct from animals whose hearts were arrested in systole and those in diastole. The main effect of capillary type on capillary Hct was significant (P=0.0002). Capillaries located in distal portions of the capillary bed had a significantly greater capillary Hct than those located in proximal portions (Fig. 11). There were no significant main effects of cardiac phase or region on capillary Hct values. Similar patterns existed for normalized capillary Hct (Table 2). Again, the main effect of capillary type was significant (P=0.0014), but no regional or phase differences were significant. Surprisingly, the coefficient of variation of normalized Hct values was either unchanged or increased compared to the CV for capillary Hct values. Therefore, the variability in capillary Hct does not depend on variation in large vessel Hct, within normal limits.

Table 1. Mean values for the total capillary length (mm) traced in each phase/region/capillary type category.

PHASE - REGION	TOTAL CAPILLARY LENGTH (mm)	
	PROXIMAL	DISTAL
DIASTOLE - MID	23.4 ± 3.5	16.1 ± 1.9
DIASTOLE - ENDO	20.5 ± 0.6	15.2 ± 1.3
SYSTOLE - MID	26.0 ± 0.7	13.9 ± 0.7
SYSTOLE - ENDO	22.2 ± 1.4	13.2 ± 0.9

Values represent means ± SEM. ENDO, subendocardium; MID, midmyocardium; PROXIMAL, proximal capillaries; DISTAL, distal capillaries

Table 2. Capillary hematocrit and normalized capillary hematocrit in the rat myocardium.

phase (large vessel Hct, %)	region/ capillary type	capillary Hct		normalized capillary Hct	
		mean (%)	CV (%)	mean	CV (%)
DIASTOLE (32.6 ± 1.3)	M / P	9.8 ± 1.2	29.2	0.27 ± 0.03	24.7
	M / D	13.9 ± 1.5	26.3	0.40 ± 0.04	25.0
	E / P	11.4 ± 1.1	24.1	0.34 ± 0.05	33.0
	E / D	14.3 ± 1.6	26.6	0.43 ± 0.07	35.8
SYSTOLE (36.3 ± 1.4)	M / P	10.3 ± 0.9	20.3	0.29 ± 0.02	20.1
	M / D	13.7 ± 0.2	4.2	0.38 ± 0.02	11.2
	E / P	11.0 ± 1.4	30.3	0.31 ± 0.04	29.9
	E / D	13.2 ± 1.4	26.0	0.36 ± 0.04	24.7

Values represent mean ± SEM (when applicable). E, subendocardium; M, midmyocardium; P, proximal capillaries; D, distal capillaries; CV, coefficient of variation = (SD/mean) x 100%

Figure 11. Capillary hematocrit (%) in the subendo- (ENDO) and midmyocardium (MID) of rat hearts arrested in diastole (n=6) or systole (n=6), as a function of capillary type. Results are presented as mean ± SEM. Mean values are inset at base of bars. The main effect of capillary type is significant, with capillary Hct in distal capillaries being greater than proximal (P=0.0002).

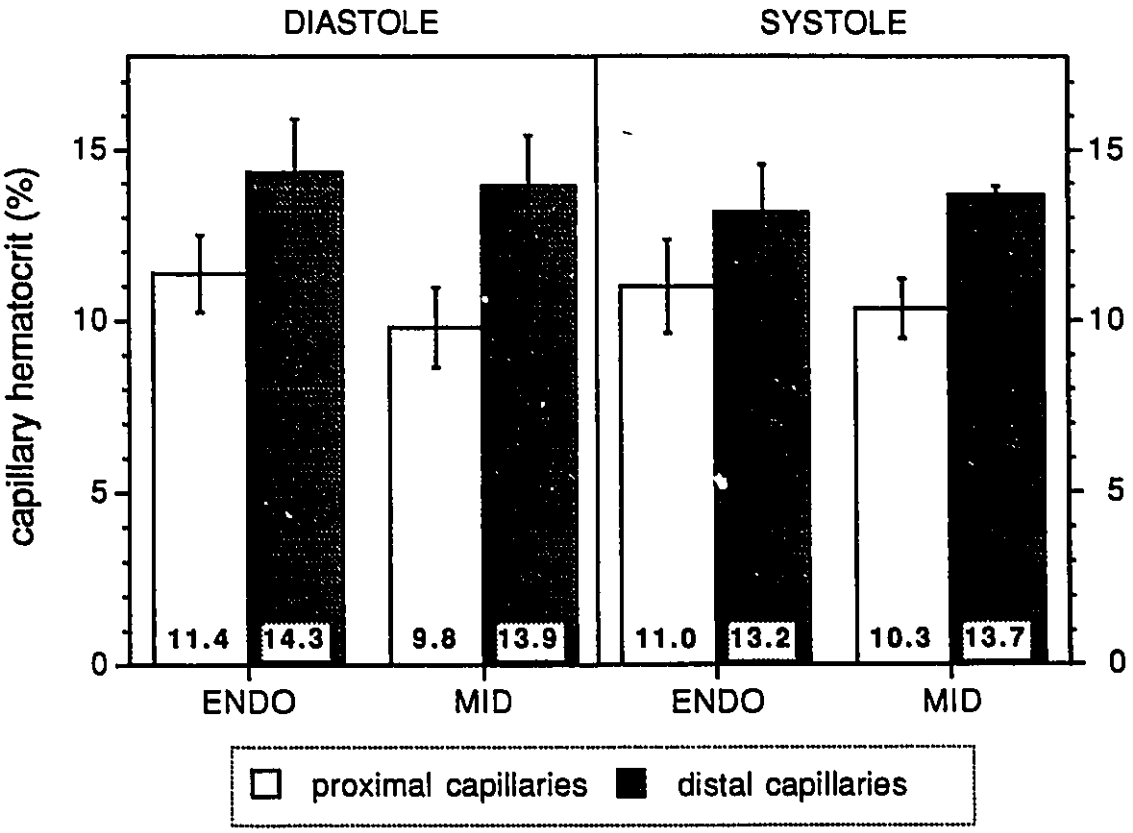
DIASTOLE
SYSTOLE
capillary hematocrit (%)
15
10
5
0
11.4
14.3
9.8
13.9
11.0
13.2
10.3
13.7
ENDO
MID
ENDO
MID
proximal capillaries
distal capillaries

4.3 Red blood cell spacing

The same tracings used for Hct determination were used to calculate values for the distances between RBCs (RBC spacing). Red cell spacing results for diastolic-arrested hearts are summarized in Table 3. Similar results for systolic-arrested hearts are summarized in Table 4. Descriptive parameters are included in these tables as well.

The main effect of capillary type was significant for mean RBC spacing values (P=0.004). Capillaries located in distal portions of the capillary bed had significantly lower mean values for distances between RBCs than those located proximal (Fig. 12). There were no significant differences in mean RBC spacing values between regions of the heart. The main effect of cardiac phase on RBC spacing approached significance with a tendency for decreased spacing in systole (P=0.0725). The reason significance was not reached may be due to a trend reversal in one experimental group, the subendocardium for proximal capillaries, where systolic values are greater than diastolic.

As can be seen from Tables 3 and 4, the coefficients of variation of mean RBC spacing were greater than 100%, indicating that the standard deviations were greater than the mean values for the data. This supports the need to examine the distribution of RBC spacing values. In order to do so, cumulative frequency line graphs were plotted for individual hearts categorized by phase and capillary type in the midmyocardium (Fig. 13) and subendocardium (Fig. 14). In these graphs, each line

Table 3. Descriptive parameters for RBC spacing in the rat myocardium during diastole.

	MID - PROXIMAL	MID - DISTAL	ENDO - PROXIMAL	ENDO - DISTAL
Mean (μm)	14.0 ± 1.3 *	11.0 ± 1.1	12.9 ± 0.6	12.2 ± 0.9
Median (μm)	7.2 ± 1.2	5.7 ± 0.7	6.8 ± 0.7	5.7 ± 0.6
Standard Deviation (μm)	17.9 ± 1.0 *	14.8 ± 1.7	16.6 ± 0.5	17.2 ± 1.4
Coefficient of Variation (%)	131.7 ± 9.3	134.0 ± 3.7	130.6 ± 9.0	141.3 ± 5.8
Freq. of unperfused segments (%)	54.2 ± 3.6 ‡	44.0 ± 3.4	-	-
Freq. of segments with 1 RBC (%)	23.2 ± 2.2	32.4 ± 3.1	-	-
Freq. of segments with >1 RBC (%)	22.6 ± 5.6	23.6 ± 4.6	-	-
Freq. of spacing =0μm (%)	9.8 ± 1.9 †	11.0 ± 2.4	9.8 ± 1.8	11.7 ± 0.9
Freq. of spacing ≥20μm (%)	21.9 ± 2.1 *	14.5 ± 1.7	18.2 ± 0.9	17.0 ± 1.7
Freq. of spacing ≥40μm (%)	7.8 ± 1.5 *	4.3 ± 0.9	6.3 ± 0.6	6.1 ± 0.8

Values represent means (± SEM). n=6. ENDO, subendocardium; MID, midmyocardium; PROXIMAL, proximal capillaries; DISTAL, distal capillaries. Coefficient of Variation = (SD/mean) x 100%. * significant (P≤0.05) main effect of capillary type (independent of cardiac phase or region); † significant (P≤0.05) main effect of cardiac phase (independent of capillary type or region, compare with Table 4); ‡ P≤0.05 vs. DISTAL within same region

Table 4. Descriptive parameters for RBC spacing in the rat myocardium during systole.

	MID - PROXIMAL	MID - DISTAL	ENDO - PROXIMAL	ENDO - DISTAL
Mean (μm)	11.2 ± 0.7 *	8.9 ± 0.6	13.4 ± 1.3	11.0 ± 0.9
Median (μm)	5.2 ± 0.5	4.3 ± 0.7	6.1 ± 0.5	6.3 ± 0.9
Standard Deviation (μm)	16.3 ± 0.8 *	12.3 ± 0.5	20.0 ± 4.0	13.8 ± 0.9
Coefficient of Variation (%)	145.8 ± 3.5	141.2 ± 8.5	143.7 ± 13.6	126.2 ± 5.7
Freq. of unperfused segments (%)	50.4 ± 2.4 ‡	42.1 ± 1.6	-	-
Freq. of segments with 1 RBC (%)	25.1 ± 2.0	25.2 ± 1.8	-	-
Freq. of segments with >1 RBC (%)	24.5 ± 3.3	32.7 ± 3.1	-	-
Freq. of spacing =0μm (%)	13.5 ± 2.0 †	14.9 ± 1.4	10.7 ± 1.4	10.5 ± 1.6
Freq. of spacing ≥20μm (%)	14.9 ± 1.5 *	11.4 ± 1.1	19.6 ± 1.3	14.4 ± 2.1
Freq. of spacing ≥40μm (%)	5.0 ± 0.6 *	2.6 ± 0.4	6.8 ± 1.2	4.3 ± 1.2

Values represent means (± SEM). n=6. ENDO, subendocardium; MID, midmyocardium; PROXIMAL, proximal capillaries; DISTAL, distal capillaries. Coefficient of Variation = (SD/mean) x 100%. * significant (P≤0.05) main effect of capillary type (independent of cardiac phase or region); † significant (P≤0.05) main effect of cardiac phase (independent of capillary type or region, compare with Table 3); ‡ P≤0.05 vs. DISTAL within same region

Figure 12. Red blood cell spacing (μm) in capillaries of the subendo- (ENDO) and midmyocardium (MID) of rat hearts arrested in diastole (n=6) or systole (n=6), as a function of capillary type. Results are presented as mean ± SEM. Mean values are inset at base of bars. The main effect of capillary type is significant, with the distance between RBCs being shorter in distal capillaries compared to proximal (P=0.004).

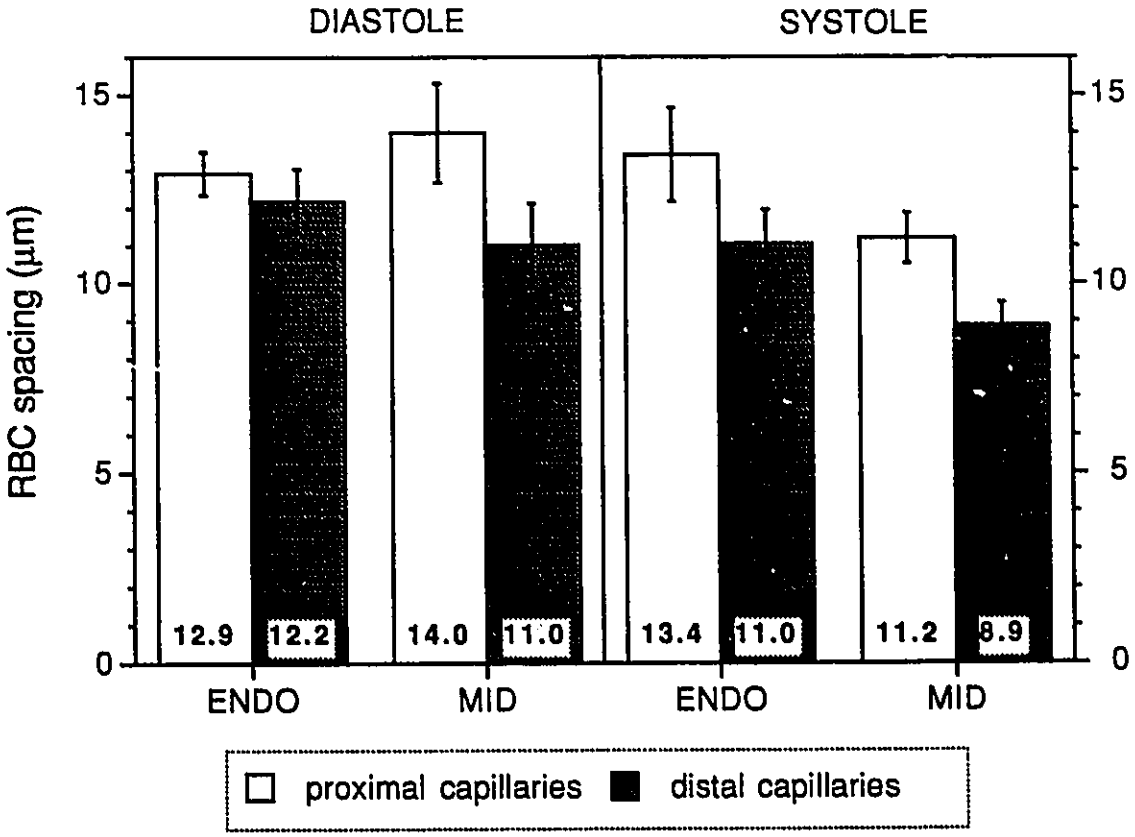
DIASTOLE
SYSTOLE
RBC spacing (µm)
15
10
5
0
12.9
12.2
14.0
11.0
13.4
11.0
11.2
8.9
ENDO
MID
ENDO
MID
proximal capillaries
distal capillaries

Figure 13. Cumulative frequency (%) of RBC spacing values in capillaries of the midmyocardium of rat hearts arrested in diastole (n=6) or systole (n=6), as a function of capillary type (PROXIMAL or DISTAL portions of capillary bed). Each line represents an individual heart.

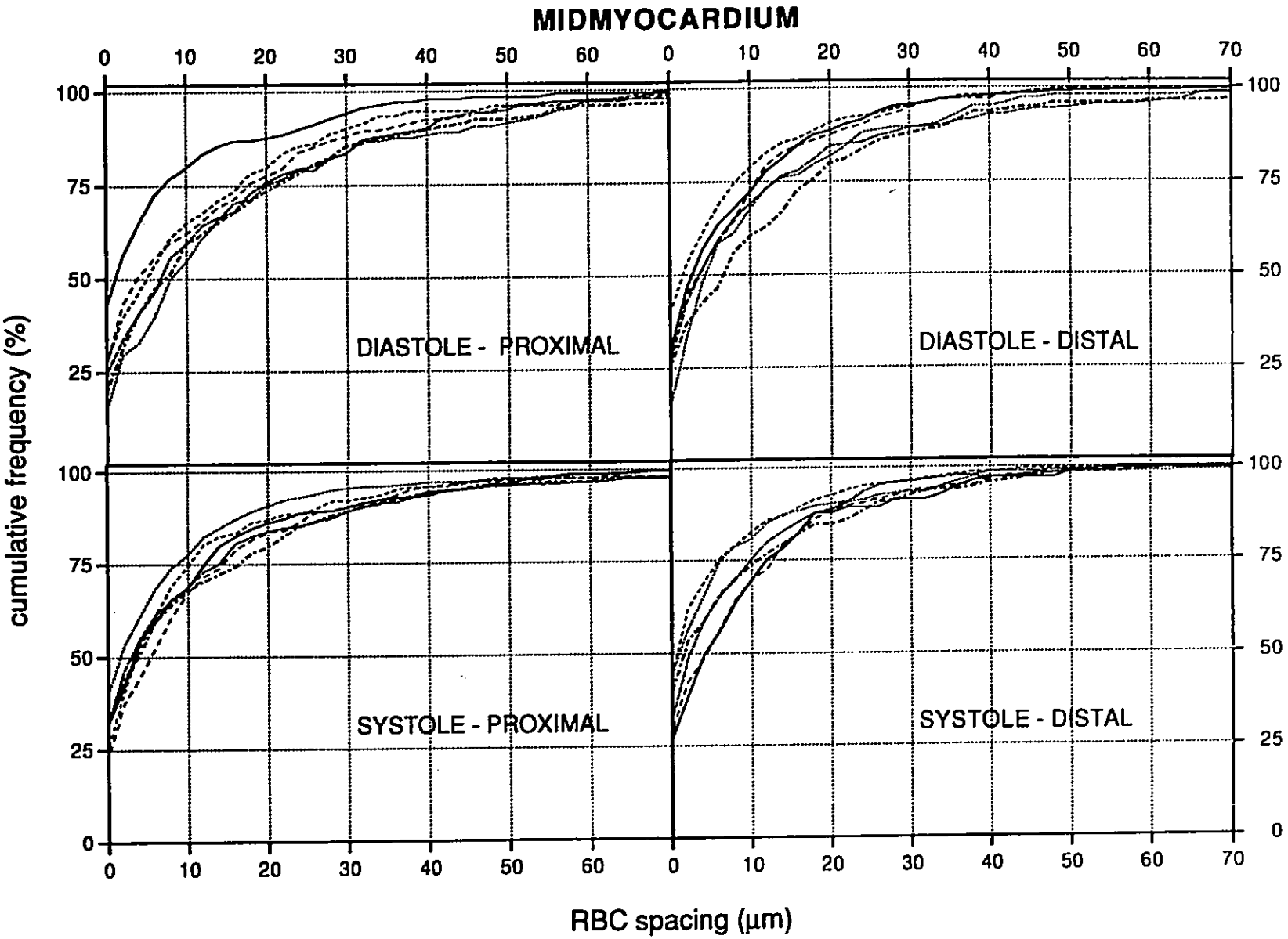
MIDMYOCARDIUM
DIASTOLE - PROXIMAL
DIASTOLE - DISTAL
SYSTOLE - PROXIMAL
SYSTOLE - DISTAL
cumulative frequency (%)
RBC spacing (µm)
0
10
20
30
40
50
60
70
0
25
50
75
100

Figure 14. Cumulative frequency (%) of RBC spacing values in capillaries of the subendocardium of rat hearts arrested in diastole (n=6) or systole (n=6), as a function of capillary type (PROXIMAL or DISTAL portions of capillary bed). Each line represents an individual heart.

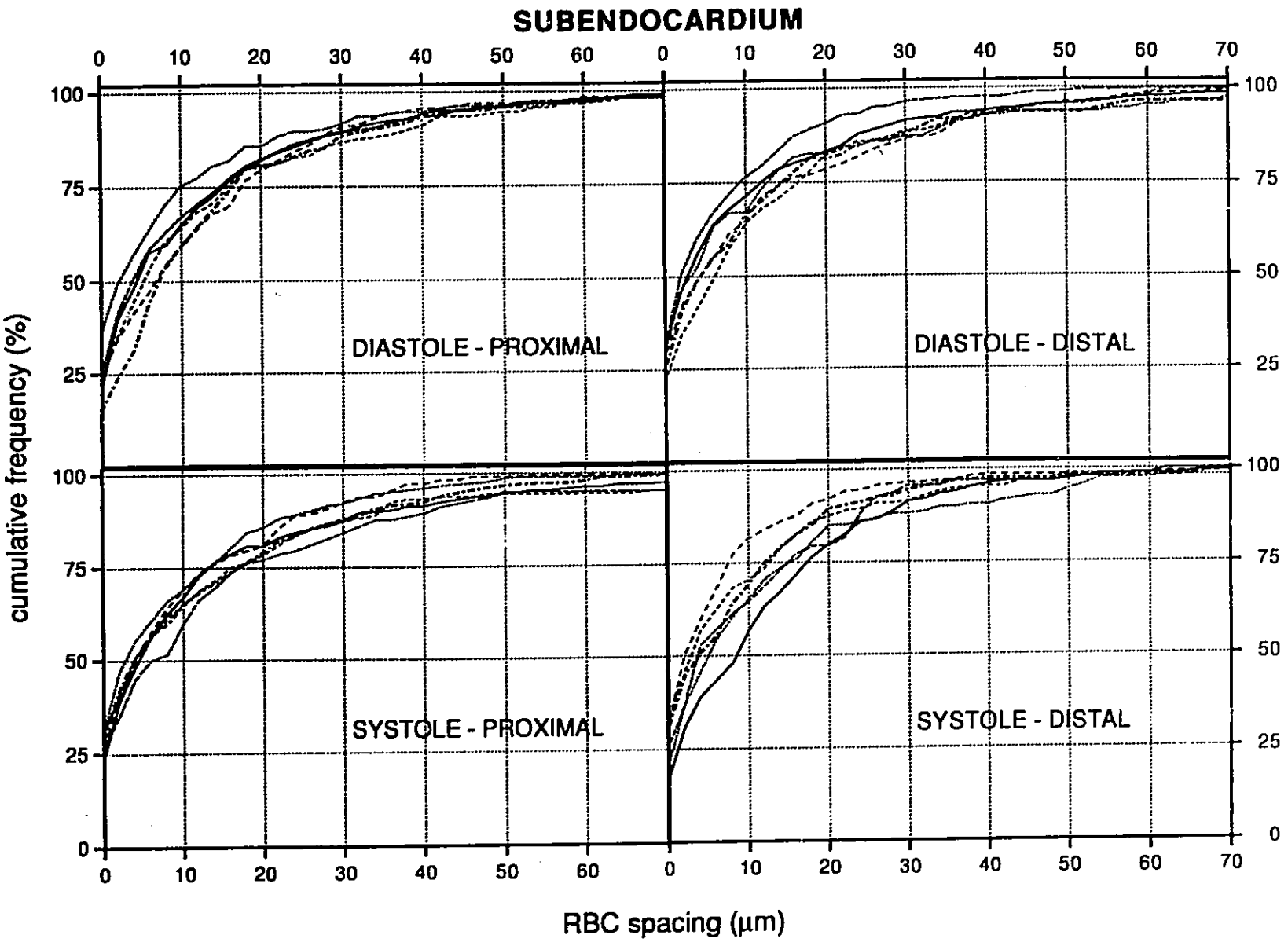
SUBENDOCARDIUM
DIASTOLE - PROXIMAL
DIASTOLE - DISTAL
SYSTOLE - PROXIMAL
SYSTOLE - DISTAL
cumulative frequency (%)
RBC spacing (µm)
0
10
20
30
40
50
60
70
0
25
50
75
100

represents values from one heart. The figures illustrate the remarkable consistency between hearts, except in proximal capillaries of the midmyocardium of diastolic-arrested hearts, where the frequency of low spacing values for one heart was consistently greater than the others. We are not aware of any possible explanation for this particular discrepancy.

Cumulative frequency line graphs were also plotted for means, categorized by region and phase, and compared between capillary type (Fig. 15). In most cases, capillaries located in distal portions of the capillary bed had a greater frequency of low RBC spacing values. In other words, shorter distances between RBCs were found more often in distal capillary portions. This trend is more noticeable in the midmyocardium than subendocardium. In the subendocardium during systole, the frequency of occurrence of low spacing values (0-10μm) was similar in capillaries located in proximal and distal portions of the capillary bed.

In order to examine changes in red cell content of capillaries, a number of capillary segments were sampled, and the number of RBCs contained within them was counted (Fig. 16, Table 3). As discussed in Chapter 3, these data were only collected in the midmyocardium, due to the greater amount of tissue available. There was a greater percentage of capillaries unperfused in proximal portions of the capillary bed compared to distal portions, in both diastole ($P=0.0488$) and systole ($P=0.0167$). The number of unperfused segments was slightly decreased in systole compared to diastole, however, significance was not reached. It seems that during the transition

Figure 15. Cumulative frequency (%) of RBC spacing values in capillaries of the subendo- (ENDO) and midmyocardium (MID) of rat hearts arrested in diastole (n=6) or systole (n=6), as a function of capillary type ("proximal" or "distal" portions of capillary bed). Each line represents the mean value for proximal or distal capillaries in that particular category. Lines are plotted with SEMs at 10μm intervals.

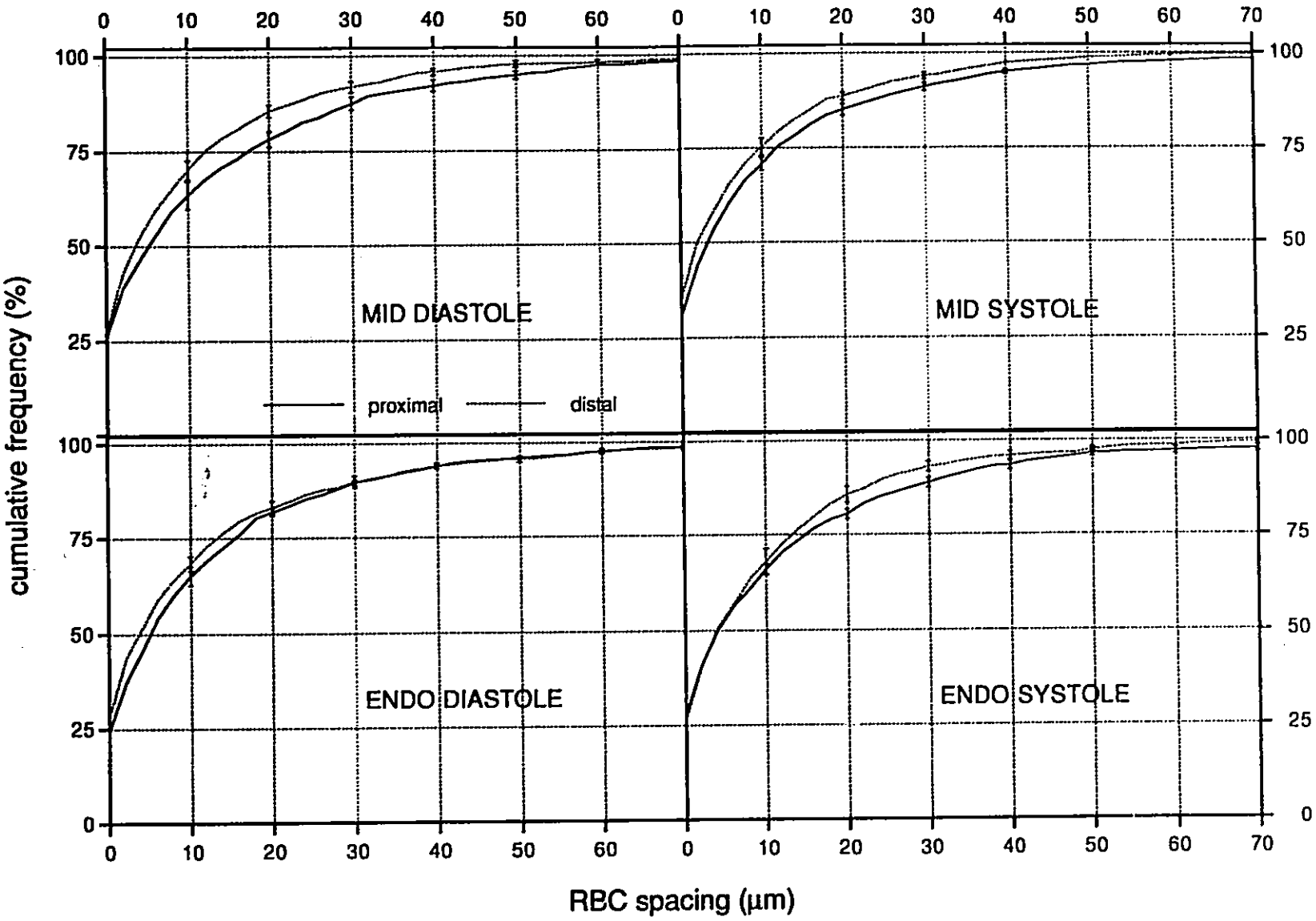
cumulative frequency (%)
RBC spacing (μm)
MID DIASTOLE
MID SYSTOLE
ENDO DIASTOLE
ENDO SYSTOLE
proximal
distal
0
10
20
30
40
50
60
70
0
25
50
75
100

Figure 16. Frequency (%) of occurrence of 0, 1, and >1 RBC in capillary segments in the midmyocardium of rat hearts arrested in diastole (n=6) or systole (n=6), as a function of capillary type. A capillary segment is defined as the capillary portion between 2 branch points. Results are presented as mean ± SEM. Mean values are inset at base of bars. There is a greater percentage of unperfused capillary segments in proximal portions of the capillary bed compared to distal portions, in both diastole (P=0.0488) and systole (P=0.0167).

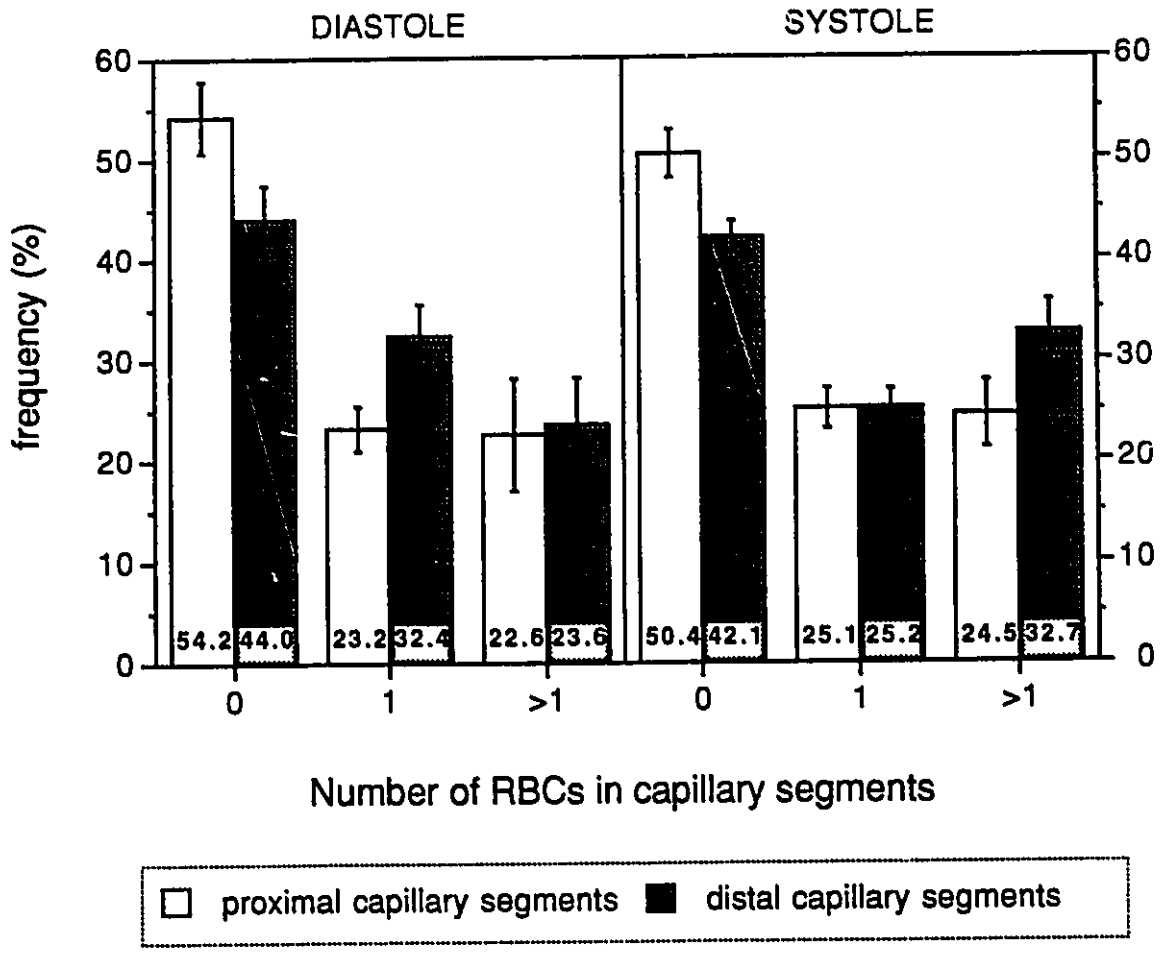
DIASTOLE
SYSTOLE
frequency (%)
60
50
40
30
20
10
0
54.2
44.0
23.2
32.4
22.6
23.6
50.4
42.1
25.1
25.2
24.5
32.7
0
1
>1
0
1
>1
Number of RBCs in capillary segments
proximal capillary segments
distal capillary segments

from diastole to systole, a redistribution of RBCs occurred in distal segments, from segments with one RBC to segments with more than one RBC. Thus, a similar number of unperfused segments exist, but more segments contain at least 2 cells in systole compared to diastole.

From capillaries with at least two RBCs present, the distribution of spacing patterns could also be analyzed. The frequency of occurrence of RBC spacing values equal to 0μm (representing "touching" RBCs, determined using a 63X objective on the microscope), greater than 20μm, and greater than 40μm were determined. There were no significant effects of region or capillary type on the frequency of touching RBCs (Fig. 17). There was, however, a significant main effect of cardiac phase, with a greater frequency of touching RBCs in systole compared to diastole (mean values irrespective of cardiac region or capillary type: SYS=12.4%, DIAS=10.6%, P=0.0029).

The main effect of capillary type on spacing values greater than 20μm (Fig. 18) was significant (P=0.0004). There was a greater frequency of values above 20μm in capillaries located in proximal portions of the capillary bed than in distal portions. Although there was a trend toward a greater frequency of spacing values above 20μm in diastole compared to systole, significance was not reached (P=0.0662). As can be seen from Figure 18, there appears to be a greater frequency of spacing values above 20μm in DIAS-MID than SYS-MID as well as in DIAS-ENDO than SYS-ENDO. However, this interaction of phase and region (irrespective of capillary type) on spacing values greater than 20μm was only marginally significant (phase*region,

Figure 17. Frequency (%) of occurrence of "touching" RBCs (spacing values of 0μm) in the subendo- (ENDO) and midmyocardium (MID) of rat hearts arrested in diastole (n=6) or systole (n=6), as a function of capillary type. Results are presented as mean ± SEM. Mean values are inset at base of bars. The main effect of cardiac phase is significant, with a greater frequency of spacing values equal to 0μm occurring in systole (P=0.0029).

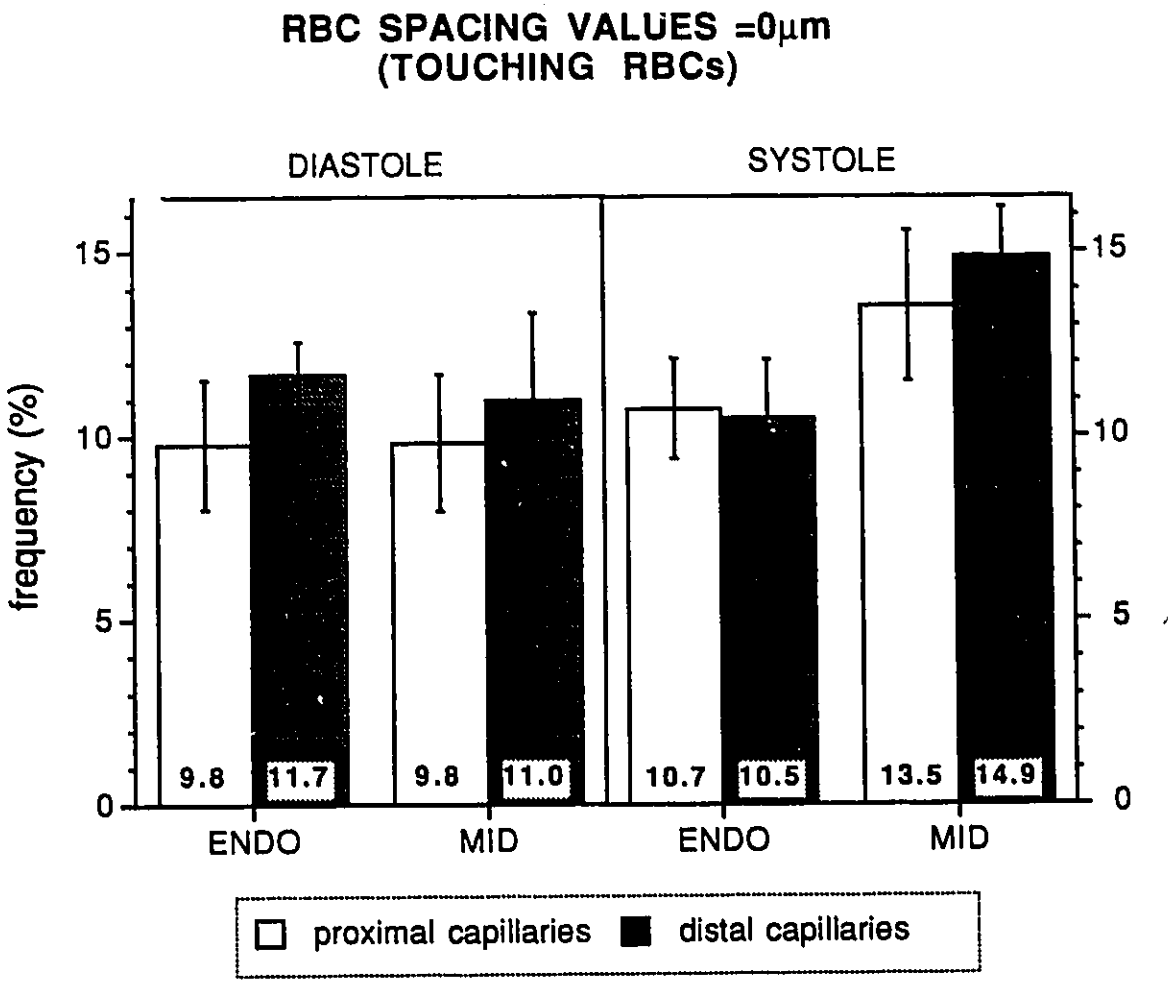
RBC SPACING VALUES =0μm
(TOUCHING RBCs)
DIASTOLE
SYSTOLE
frequency (%)
15
10
5
0
9.8
11.7
9.8
11.0
10.7
10.5
13.5
14.9
ENDO
MID
ENDO
MID
proximal capillaries
distal capillaries

Figure 18. Frequency (%) of occurrence of RBC spacing values ≥20μm in the subendo- (ENDO) and midmyocardium (MID) of rat hearts arrested in diastole (n=6) or systole (n=6), as a function of capillary type. Results are presented as mean ± SEM. Mean values are inset at base of bars. The main effect of capillary type is significant, with a greater frequency of spacing values above 20μm occurring in proximal capillaries (P=0.0004).

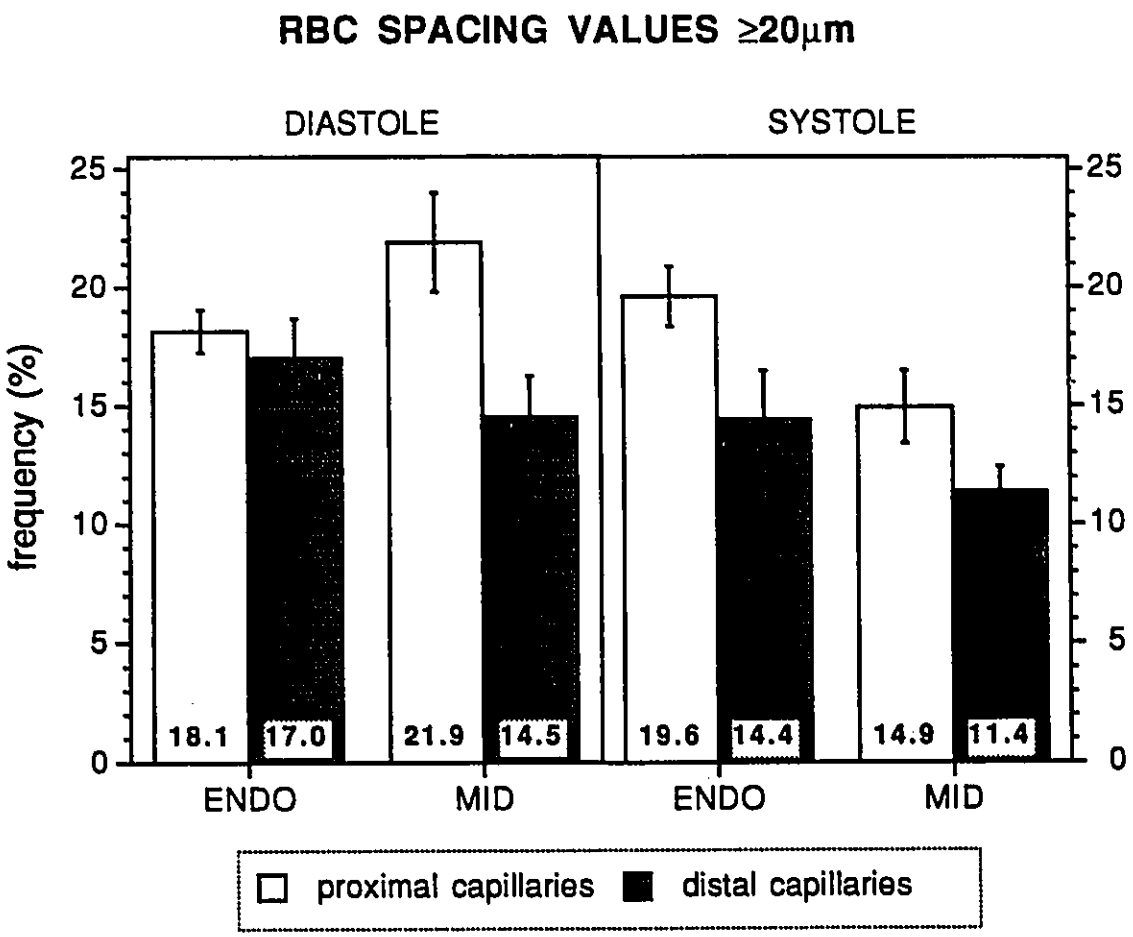
RBC SPACING VALUES ≥20μm
DIASTOLE
SYSTOLE
frequency (%)
25
20
15
10
5
0
18.1
17.0
21.9
14.5
19.6
14.4
14.9
11.4
ENDO
MID
ENDO
MID
proximal capillaries
distal capillaries

P=0.0517) Finally, phase and region appeared to influence the effect of capillary type. For example, in diastole, the differences between proximal and distal values seem to be greater in the MID than ENDO. However, these trends were not statistically significant (phase*region*capillary type, P=0.0866).

As a measure of extreme values for the distances between RBCs, we categorized values greater than 40μm (Fig. 19). The main effect of capillary type was once again significant, with a greater frequency of RBC spacing values above 40μm in proximal portions of the capillary bed (P=0.0028). There were no other statistically significant comparisons.

Figure 19. Frequency (%) of occurrence of RBC spacing values ≥40μm in the subendo- (ENDO) and midmyocardium (MID) of rat hearts arrested in diastole (n=6) or systole (n=6), as a function of capillary type. Results are presented as mean ± SEM. Mean values are inset at base of bars. The main effect of capillary type is significant, with a greater frequency of spacing values above 40μm occurring in proximal capillaries (P=0.0028).

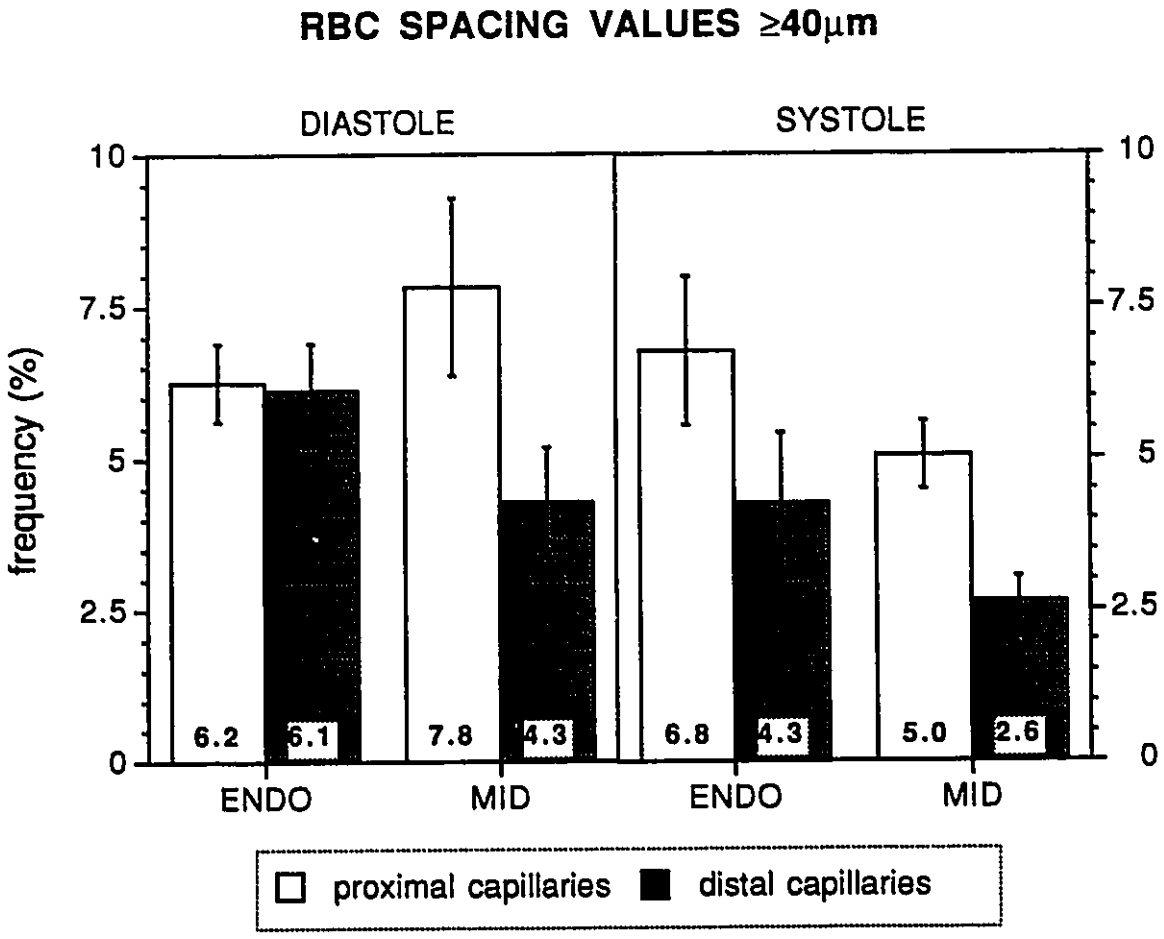
RBC SPACING VALUES ≥40µm
DIASTOLE
SYSTOLE
frequency (%)
10
7.5
5
2.5
0
6.2
6.1
7.8
4.3
6.8
4.3
5.0
2.6
ENDO
MID
ENDO
MID
proximal capillaries
distal capillaries

CHAPTER 5 DISCUSSION

5.1 Introduction

In the Introduction to this thesis, we discussed the importance of capillary Hct and related RBC spacing to oxygen supply to tissue, which was based primarily on theoretical studies. The present discussion concentrates on explanations of our findings as well as comparisons to results from other studies. General parameters are discussed first, followed by a more specific examination of phase, region and capillary type differences in these parameters. The final section of this chapter deals with the implications of our findings, as well as the contribution of this study to the understanding of oxygen transport to tissue.

5.2 Sarcomere lengths

The phase of the cardiac cycle was confirmed by myocyte sarcomere lengths determined in the midmyocardium (MID). In order to minimize any possible bias in measured sarcomere lengths due to possible differences between the base and apex of the left ventricle, multiple measurements were made at approximately the same level in the left ventricle (middle one-third). In addition, measurements were confined to the same region (midmyocardium).

The mean midmyocardial sarcomere lengths determined in this study for diastole (2.03μm) and systole (1.76μm) are in very close agreement with previous

studies. In 1967, Sonnenblick and coworkers determined average sarcomere lengths in the dog midmyocardium during diastole and systole to be 2.07 and 1.81μm, respectively. They also found that *in vivo*, average sarcomere lengths could increase to 2.25μm during dilated diastole (infusion-induced volume overload) and decrease to 1.60μm during potentiated systole (postextrasystolic potentiation), suggesting a reserve available with respect to sarcomere length. The maximal average sarcomere length in chronically dilated dog hearts (diastole) was found to be 2.27μm, suggesting that sarcomere lengths in the left ventricle are resistant to overstretch (Ross et al., 1971). A recent report from our lab (Batra and Rakusan, 1992) found mean sarcomere lengths in the rat midmyocardium to be 2.05 and 1.81μm during diastole and systole, respectively.

Although our values are in agreement with these previous studies, a wide range of sarcomere lengths have been reported within the myocardium. Poole and Mathieu-Costello (1990) reported mean sarcomere lengths to range from 2.09 to 2.23μm in the subepicardium (EPI) and 2.04 to 2.17μm in the subendocardium (ENDO) of diastolic-arrested rat hearts. Poole and coworkers (1992) determined mean sarcomere lengths to range from 1.35 to 2.06μm in the EPI and 1.44 to 1.93μm in the ENDO of systolic-arrested rat hearts. In both of these previous studies, there were no significant regional differences in mean sarcomere lengths.

The pharmacological induction of cardiac arrest used in this study may have attained some nonphysiological contraction of the myocardium. However, the values

obtained in this study are probably within the limits of attainable sarcomere lengths in rat myocardium. Furthermore, extreme values are useful, as two distinct populations are created for subsequent comparisons of the parameters of interest.

5.3 Parameters used in this study

In this section, the individual parameters measured in this study are discussed. The regional, phase and capillary type differences will be discussed in subsequent sections.

5.3.1 Capillary hematocrit

In this thesis, capillary hematocrit refers to the lineal fraction of capillary length occupied by red blood cells. In capillaries, where RBCs travel in single file, this length measurement should accurately reflect capillary Hct *in vivo*. The values for capillary Hct obtained in this study range from 6.9 to 19.9% (overall mean of 12.2%). These values are lower than those reported in the heart by other investigators (see Table 5). A major reason for these discrepancies lies in the method used to determine hematocrit. In our study, only capillaries with RBCs in single file were measured, and the resulting value represents capillary Hct. However, studies utilizing radioactive nucleotides for hematocrit determination in the heart result in values representing a tissue hematocrit, since vessels larger than capillaries (e.g. arterioles, venules) are included in the Hct value. The inclusion of these larger vessels may

Table 5. Hematocrit values* from published studies.

Species	Tissue	Hct (%)	Method	Notes	Author(s)
rat	cremaster	18	FITC labelled RBCs		Fisher et al. 1992
		17.8	*in vivo* microscopy		House & Lipowsky 1987
hamster		10.4			Klitzman & Duling 1979
		6.3		40 mmHg PO_2	
		18.5		8 mmHg PO_2 + contraction	
		21.5		35 days old	Sarelius et al. 1981
		24.2		57 days old	
		14.6		132 days old	
		12.2			Desjardins & Duling 1990
rabbit	tenuissimus	14			Ley et al. 1988
dog	heart (LV)	30	radiolabelled RBCs and plasma	tissue Hct	Eliasen et al. 1982
rat		30.8		tissue Hct	Rakusan 1971b
		25.3		tissue Hct, aortic constrict.	
		30.9		tissue Hct	Rakusan & Rajhathy 1972
		16.5		tissue Hct, anemia	
		43.9		tissue Hct, polycythemia	
		32		tissue Hct, EPI	Vicaut & Levy 1990
		22		tissue Hct, ENDO	
		33.1		tissue Hct, EPI	Baskurt et al. 1995
		23.2		tissue Hct, ENDO	
		55	FITC-labelled γ-globulin injection for vascular system visualization	EPI	Vetterlein et al. 1989
		46		ENDO	
		56		EPI, hypoxia	
		51		ENDO, hypoxia	

* values represent capillary Hct unless specified otherwise. LV, left ventricle; EPI, subepicardium; ENDO, subendocardium

therefore elevate the Hct value. In studies using radioisotopes, labelled RBCs (e.g. ^{51}Cr, ^{99m}Tc) and plasma tracers (e.g. ^{125}I-Albumin) are injected intravenously. Tissue Hct can then be calculated by relating radioactivity to plasma and RBC volumes in tissue samples.

Based on this methodology, Rakusan (1971b) determined tissue Hct in the terminal vascular bed (<100μm) of the rat left ventricle to be 30.8%. Vicaut and Levy (1990) reported tissue Hct values in the rat left ventricle of 22% in the ENDO and 32% in the EPI. Baskurt and coworkers (1995) found similar results in the rat left ventricle; 23.2% in the ENDO and 33.1% in the EPI. Eliasen and coworkers (1982) determined tissue Hct in the left ventricle of the dog to be 30%. Vetterlein and coworkers (1989) used FITC-labelled γ-globulins injected intravenously to make the vascular system visible and measured Hct in rat coronary capillaries. Hematocrit was calculated as the percentage of capillary length occupied by RBCs. In their study, capillary Hct was 46% in the ENDO and 55% in the EPI.

Since the reported values for Hct (Table 5) represent mean values, the variability of the data in space and time is neglected. Temporal and spatial heterogeneities have been reported in skeletal muscle capillaries for RBC velocity (Tyml et al., 1981; Tyml, 1986, 1987; Ellis et al., 1990, 1994), RBC flux (Ellis et al., 1990, 1994), and RBC perfusion (Tyml, 1987). These heterogeneities can contribute to variability in the mean values of Hct reported in Table 5.

It has long been known that capillary Hct in some tissues is lower than large vessel Hct. For example, capillary Hct in skeletal muscle has been found to range from approximately one-half to one-fifth of large vessel Hct at rest (e.g. Klitzman and Duling, 1979; Sarelius and Duling, 1982; Pries et al., 1986; House and Lipowsky, 1987). The reduction has not been reported to be as large in cardiac tissue as skeletal muscle, ranging from 50 to 80% of large vessel Hct (Rakusan, 1971b; Rakusan and Rajhathy, 1972; Eliasen et al., 1982; Vicaut and Levy, 1990). However, in cardiac tissue, these estimates are based on tissue Hct values, not capillary Hct values. In order to assess the effect of large vessel (venous) Hct on capillary Hct, our values for capillary Hct were normalized to large vessel Hct (capillary Hct / large vessel Hct). Our mean normalized Hct was 0.38, considerably lower than values reported in the literature (see Table 6). This is probably due to the fact that our hematocrit value represents capillary Hct, not tissue Hct which would be higher, thereby elevating the ratio. The variability in our normalized Hct values (expressed as coefficient of variation) did not decrease compared to capillary hematocrit variability, suggesting the independence of capillary Hct on large vessel Hct. In other words, the capillary Hct is maintained, despite differences in large vessel Hct, including inter-animal variability in large vessel Hct. This could be a safety mechanism so that capillary Hct is preserved to maintain tissue oxygenation in the event of fluctuations in large vessel Hct.

Table 6. Normalized hematocrit values from published studies.

Species	Tissue	Normalized Hct	Method	Notes	Author(s)
rat	cremaster	.48	*in vivo* microscopy		House and Lipowsky 1987
hamster		.39		35 days old	Sarelius et al. 1981
		.40		57 days old	
		.26		132 days old	
	cheek pouch	.20 - .50	fluorescent labelled RBCs		Sarelius and Duling 1982
rabbit	tenuissimus	.56	*in vivo* microscopy		Ley et al. 1988
dog	heart (LV)	.75	radiolabelled RBCs and plasma	tissue Hct	Eliasen et al. 1982
rat		.64		tissue Hct	Rakusan 1971b
		.52		tissue Hct, aortic constriction	
		.72		tissue Hct	Rakusan and Rajhathy 1972
		.70		tissue Hct, anemia	
		.83		tissue Hct, EPI	Vicaut and Levy 1990
		.55		tissue Hct, ENDO	

Values represent normalized capillary Hct unless specified otherwise.

This is also affirmed by Sarelius (1989) who studied the microcirculation in the cremaster muscle of golden hamsters after an acute reduction in systemic Hct. The results of her study suggest that tissue O_2 delivery from capillaries cannot be accurately predicted from changes in systemic O_2 transport capacity. Various parameters were examined (capillary RBC content, RBC velocity, and RBC flux). Two hemodiluted groups were studied: 30% and 50% of normal systemic Hct. If changes in capillary Hct were directly proportional to changes in systemic Hct, the various parameters studied should be different in the two hemodiluted groups. However, no distinguishable differences in the parameters measured were found, despite the significant difference in systemic Hct. The mechanisms by which capillary Hct is maintained despite systemic alterations are not fully understood.

There have been various attempts to explain the reduction in capillary Hct compared to large vessel values. The mechanisms can be classified as those acting outside the capillary and those acting inside. The Hct within the capillary may be reduced due to exclusion of cells from the entrance into the capillary. This may occur as a result of: (i) size limitations due to capillary diameter (e.g. depending on capillary diameter and RBC deformability, RBCs may not be able to enter the capillary), (ii) plasma skimming, which refers to a radial inhomogeneity of cell distribution in the feeding tube, and (iii) RBC screening, which refers to flow phenomena at a bifurcation, which causes cells to escape from flow regions feeding the capillary (Gaehtgens, 1980). Red cell exclusion has been shown to be dependent on capillary

flow rate, capillary diameter, as well as RBC aggregation (Gaehtgens, 1980). For example, the exclusion of red cells from capillaries increases as capillary diameter decreases from 11.0 to 3.3μm. Above 11μm, cell exclusion effects are negligible. In addition, it has been proposed that at a bifurcation, the daughter vessel with the higher flow receives an elevated Hct compared to the parent vessel, and those branches with lower flow receive a lower Hct (Yen and Fung, 1978).

Capillary Hct may also be reduced relative to the Hct of blood feeding the capillary by a mechanism occurring exclusively within the capillary tube. This is referred to as the "Fahraeus effect" (Fahraeus, 1928). To understand this effect, two terms need to be defined: the tube hematocrit (H_t) and discharge hematocrit (H_d). Tube Hct refers to the hematocrit of blood existing within a capillary at a given time. For example, if one could remove a vessel undisturbed and then empty its contents into a beaker, the Hct of blood in the beaker would be the tube Hct. This is the Hct commonly referred to as capillary Hct. In experimental studies, H_t is estimated from the number of RBCs, the mean volume of each cell, as well as capillary radius and length. The discharge hematocrit refers to the Hct of blood exiting the capillary. For example, if one collected blood flowing out of a capillary in a beaker, the Hct of the blood in the beaker would be the discharge Hct.

The original work of Fahraeus, as well as many subsequent studies of the Fahraeus effect, used glass tubes to examine the relationship of H_t to H_d *in vitro*. Essentially, the Fahraeus effect has been used to explain the reduction of H_t relative

to H_d in narrow tubes. The Fahraeus effect is a consequence of the difference in velocities of RBCs and plasma flowing through a tube. Red blood cells tend to travel near the centre of a tube where the velocity is higher than at the tube periphery (Cokelet, 1976; Duling and Desjardins, 1987). Thus, if the velocity of RBCs is greater than plasma, there will be a reduction in the number of RBCs existing within the capillary lumen at a given time and H_t will be reduced compared to H_d. If plasma and RBC velocity were identical, H_t would be equal to H_d, and the Fahraeus effect would not be acting.

Barbee and Cokelet (1971) examined the Fahraeus effect in glass tubes ranging between 29 and 221μm in diameter, which is greater than the range of capillaries. As tube diameter increased, the Fahraeus effect decreased (H_t/H_d increased). Cokelet (1976) determined H_t and H_d in glass tubes ranging from 8.1 to 23μm in diameter. The ratio of H_t/H_d decreased as tube diameter decreased from 23μm to approximately 15μm. Conversely, H_t/H_d increased with further decreases in tube diameter. Thus, as tube diameter decreases below 15μm, the Fahraeus effect decreases.

In 1979, Albrecht and coworkers examined the Fahraeus effect in glass tubes with diameters ranging from 3.3 to 11.0μm, through which RBC suspensions were perfused. As tube diameter decreased from 11.0 to 3.3μm, the Fahraeus effect decreased (H_t/H_d increased). Tube hematocrit was reduced to 0.67 of H_d in tubes of 11μm diameters, whereas, H_t was reduced to only 0.94 of H_d in tubes of 3.3μm diameter. In 1980, Gaehtgens also studied the flow of blood through glass capillaries

ranging from 3.3 to 12μm in diameter. Again, the Fahraeus effect became negligible as tube diameter approached 3.3μm. The reason for the reversal of the Fahraeus effect in smaller vessels (<15μm), may be due to the transition from multi-file flow to single-file flow (Gaehtgens, 1980). In single-file flow situations, a greater proportion of the tube cross section is occupied by the cell, thus reducing or eliminating the difference in cell velocity and medium velocity. Combining the results of the above studies, the Fahraeus effect was found to be maximal in tubes of 15-20μm diameter, which is at the level of arterioles. It decreased in larger as well as smaller tubes.

The Fahraeus effect depends on both the velocity profile and the radial distribution of RBCs across the tube. As mentioned earlier, RBCs travel preferentially in the centre of narrow glass tubes (Cokelet, 1976). The width of the cell-free layer adjacent to the cells (between RBC and capillary wall) depends on flow rate and tube diameter. Average plasma layer thickness was calculated to be approximately 0.2μm in glass tubes of 3.3μm diameter, and 0.5μm in tubes of 4.4μm diameter (Albrecht et al., 1979). In summary, the cell free layer, and consequently the Fahraeus effect, are relatively small at tube diameters representative of most of the nutritive capillary vessels (4-6μm; Gaehtgens, 1980). This strengthens the validity of our results, since if a significant plasma layer did exist, our measurements of lineal capillary Hct would not accurately reflect capillary Hct.

Studies in glass tubes have shown that the Fahraeus effect alone can only account for a reduction in the ratio of H_t/H_d from 1 to approximately 0.7 (Albrecht et al., 1979; Barbee and Cokelet, 1971; Cokelet, 1976; Gaehtgens, 1980). Since measured capillary Hct falls well below this value, other causative factors must exist. The Fahraeus effect may be exaggerated *in vivo* due to the physical structure of the capillary wall. For example, the distribution volume of plasma may exceed the distribution volume of RBCs due to a stationary plasma layer or plasma retardation (Klitzman and Duling, 1979; Desjardins and Duling, 1987). Surface irregularities in the microvessel wall create areas in the capillary accessible to plasma but not RBCs. In addition, if the plasma layer near the capillary wall is retarded (e.g. by interaction with the endothelial cell surface), mean plasma velocity would decrease and consequently, so would tube Hct. Desjardins and Duling (1990) examined the effect of the endothelial cell glycocalyx in regulating capillary Hct. The endothelial surface contains charged proteoglycans which may interact with plasma proteins. They hypothesized that capillary Hct may depend in some way on interactions between the luminal glycocalyx and plasma macromolecules which would reduce plasma velocity. Following microperfusion of capillaries with heparinase, an enzyme which removes heparan sulfate and heparin constituents of the glycocalyx, the reduction in capillary Hct was diminished. Thus, the matrix may reduce plasma motion and regulate microvessel volume through changes in composition, which occur in the order of seconds, thereby regulating capillary Hct.

5.3.2 Red blood cell spacing

In this study, red blood cell spacing represents the edge-to-edge distance between adjacent RBCs within an individual capillary. Mean RBC spacing values in the coronary capillary bed in individual hearts ranged from 6.6 to 18.8μm (overall mean 11.3μm). As mentioned in the Introduction, there has only been one study which specifically determined red cell spacing in the coronary microvascular bed of the rat (Honig et al., 1989). In their study, two populations of data were established: RBC spacing values less than 5μm and greater than 5μm. If the data for these two groups are pooled, the mean spacing value obtained is 9.6μm, only slightly lower than our value. However, their data are based on a very small number of capillaries obtained in one heart.

Data on RBC spacing in skeletal muscle capillaries have been collected *in vivo*, and the values in the literature are variable. In the rat cremaster, RBC spacing was reported to be 22.3μm and decreased to 11.4μm in response to chronic hypoxia (Fisher et al., 1992). In the cremaster muscle of hamsters, spacing was reported to be 7.7μm and 15.3μm in 35 and 132 day old animals respectively (Sarelius et al., 1981). In our study, the RBC spacing values in rat heart tend to be lower than skeletal muscle, presumably due to the greater metabolic demands of the heart.

Many *in vivo* studies in skeletal muscle capillaries report a lineal density value, representing the number of RBCs per capillary length. These values can be converted to RBC spacing values using the following equation:

$$\text{RBC spacing} = \frac{L - n\,d}{n - 1}$$

where L refers to the capillary length (μm), n refers to the number of RBCs and d refers to the RBC diameter (μm). Reported values of Hct can also be used to derive RBC spacing values, by substituting the following relationship into the equation above:

$$\text{Hct} = \frac{n\,d}{L}$$

Table 7 illustrates a variety of RBC spacing values derived using the above equations in both skeletal and cardiac muscle. However, these derivations are only estimations, and are dependent upon using a mean RBC diameter (species-dependent) for the calculation, neglecting possible alterations in RBC shape due to changes in vessel size. It should be noted that species differences in RBC diameter can contribute to large differences in RBC spacing values (e.g. frog RBC diameter is 3 times that of rat). The limitation of calculating RBC spacing values from lineal density and Hct values is that RBCs are assumed to be evenly spaced. Herein lies the need for realistic determination of RBC spacing values, from which heterogeneity of RBC spacing can be extrapolated.

To examine RBC spacing heterogeneity, the RBC spacing data obtained in this study were presented as cumulative frequency distributions (recall Figures 13, 14 and 15). Figures 13 and 14 illustrate the distribution of RBC spacing values in the midmyo- and subendocardium, respectively. Three important points are noteworthy.

Table 7. Red blood cell spacing values derived from published studies.

Species	Tissue	Derived RBC spacing (μm)	Derivation based on	Notes	Author(s)
frog	sartorius	30	lineal density		Ellis et al. 1990
		70	*in vivo*		Tyml et al. 1981
hamster	cremaster	3.9 - 6.1	lineal density		Sweeney and Sarelius 1990
		4.8			Sarelius 1989
		14.1		hemodiluted 49%	
		7.5		rest, 39 days old	Sarelius 1986
		5.5		rest, 62 days old	
		4.1		hyperemia, 39 days old	
		1.7		hyperemia, 62 days old	
		51	Hct (10.4%)		Klitzman and Duling 1979
		21	Hct (21.5%)		Sarelius et al. 1981
		8	*in vivo* observations	35 days old	
		15.3		132 days old	
rat	gracilis	11	lineal density		Ellis et al. 1990
	cremaster	22.3	*in vivo* observations		Fisher et al. 1992
		11.4		chronic hypoxia	
	heart	16	Hct (30.8%)	tissue Hct	Rakusan 1971b
		10	RBC spacing		Honig et al. 1989

First, the distributions illustrate the consistency between individual hearts. As mentioned earlier, there is an exception within proximal capillary portions in the midmyocardium of one diastolic-arrested heart. However, we cannot explain this discrepancy. Second, irrespective of cardiac phase, region, or capillary type, the distributions illustrate higher frequencies of lower RBC spacing values. For example, approximately 75% of the RBC spacing values are lower than 10μm. Third, these distributions are useful in that they allow the reader to draw their own conclusions regarding the data. For example, it was from these distributions that we categorized RBC spacing values as equal to 0μm, ≥20μm or ≥40μm (recall Figures 17-19). In order to determine a category representing extremely large spacing values, we used these distributions to see that approximately 10% of the data were above 40μm, thereby making it an extreme category. Similarly, such distributions can be incorporated into mathematical models, since they represent true experimental data, rather than theoretical.

5.3.3 Relationship between RBC spacing and capillary Hct

In our study, capillary Hct and RBC spacing are not directly related by an inverse proportion, despite the fact that RBCs are travelling in single file. The capillary Hct parameter incorporates data from capillaries perfused with RBCs as well as those capillaries with no RBCs (unperfused). Red blood cell spacing values are only determined from capillaries with at least two RBCs. If the distances between

erythrocytes were calculated from capillary Hct using a relationship equation, the resultant values would presume that RBCs are evenly distributed throughout all capillaries, and neglect the contribution of unperfused capillaries. A simple example of this relationship is illustrated in Figure 20, where two different RBC spacing patterns give rise to the same capillary Hct. Thus, Hct and RBC spacing, although related, give two different pictures which are important in understanding O_2 supply to tissue.

5.4 Cardiac cycle

Many differences exist in the heart during the cardiac cycle (e.g. systole and diastole). For example, canine left ventricular wall thickness increases 28% and ventricular blood volume decreases 61% from diastole to systole (Ross et al., 1967). Despite significant increases in wall thickness, fiber angles are not appreciably altered during the transition from diastole to systole (there is a slight increase in all fiber angles, which is constant throughout the wall) (Streeter et al., 1969). Pressure-flow relations also vary during the cardiac cycle. In most vascular beds, the pressure-flow relations are easily measured (R=P/F, where R represents resistance, P represents pressure and F represents flow). However, in the coronary microvascular bed, the situation is more difficult to assess. The cyclically contracting and dilating heart results in differences in tissue pressures which will also result in phasic changes of resistances in the vessels.

Figure 20. Schematic representation of capillaries with different red cell distributions. Black ovals represent red blood cells. Capillary hematocrit is defined as the aggregate RBC length divided by the total capillary length. Red blood cell spacing is defined as the average distance between RBCs (only capillaries with at least two RBCs will contribute to this parameter). The figure illustrates that similar capillary hematocrit conditions can be associated with different RBC spacing patterns. See section 5.3.3 for explanation.

capillary Hct = $\frac{\Sigma \text{ RBC length}}{\Sigma \text{ capillary length}}$

mean RBC spacing = $\frac{\Sigma \text{ RBC spacing}}{\text{total \# of spaces}}$

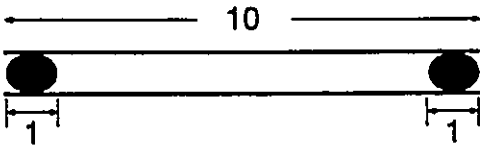

$\frac{2}{10}$

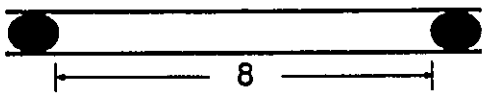

$\frac{2}{10}$ $\frac{6}{30} = 0.20$ $\frac{3 \times 8}{3} = 8$

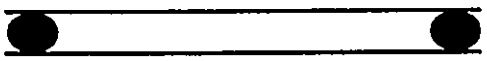

$\frac{2}{10}$

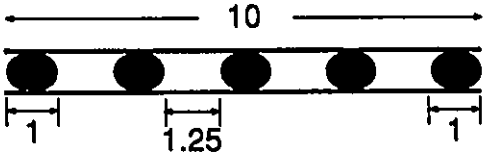

$\frac{5}{10}$

$\frac{1}{10}$ $\frac{6}{30} = 0.20$ $\frac{4 \times 1.25}{4} = 1.25$

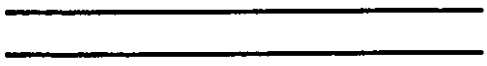

$\frac{0}{10}$

Blood flow through systemic arteries increases during systole and decreases during diastole. However, the reverse is true in coronary arteries, due to the compression of intramyocardial vessels during cardiac contraction. Intramyocardial pressure increases as the left ventricle contracts during systole, resulting in an increase in intravascular pressure. This occurs since vascular diameter and transmural vascular pressure do not change until blood moves out of the vessels. The intramyocardial tissue pressure counteracts aortic pressure and reduces the forward flow. If the intravascular pressure is greater than aortic pressure, which is often the case in the deeper layers of the left ventricle (Kirk and Honig, 1964a), a systolic-induced backflow may occur, pushing blood back toward the aorta. The development of intravascular pressure also causes an emptying of coronary vessels at the venous end, where there is no opposition. Thus, systole causes a reduction in coronary arterial inflow and an increase in coronary venous outflow. By examining the distribution of intramyocardial pressures during systole, researchers have shown that a transmural distribution of intramyocardial pressure exists during systole, and there would be little or no perfusion of the deep layers (subendocardium) but there would be perfusion of the more superficial layers (subepicardium) of the heart (Kirk and Honig, 1964a, 1964b). How this affects capillaries is debatable. The effects of cardiac contraction on blood flow have also been examined by Goto and coworkers (1991). In their study, ENDO flow was greater than EPI flow during diastole, whereas the reverse was true during systole. In addition, ENDO flow in systole was lower than during

diastole.

Given the pressure and flow alterations which occur during the cardiac cycle, it is important to establish whether geometrical conditions of the microcirculation adapt to maximize O_2 supply to tissue during various stages of the cardiac cycle. A recent study from our laboratory examined microvascular geometry in the rat myocardium during the cardiac cycle (Batra and Rakusan, 1992). The capillary domain, the area of tissue supplied by a single capillary, increased in systolic-arrested hearts. Thus, a greater area of tissue needed to be supplied by a single capillary in systole. This increase was greater in proximal portions of the capillary bed compared to distal portions. In addition, the heterogeneity of capillary spacing decreased in systolic-arrested hearts. The greater uniformity presumably improves geometrical conditions in the face of reduced flow. Finally, the branching angle of capillaries increased in systolic-arrested hearts, rather than increased tortuosity of vessels which would be expected from sarcomere shortening. Presumably, during systole, the geometrical alterations in capillary spacing and branching maintain O_2 supply in the heart during the transition from diastole, despite increases in domain sizes.

It would have been intuitively appealing for the distance between RBCs to decrease during systole, reducing the capillary barrier and thus counteracting the negative effects of increased domain sizes. In fact, we did see a trend toward decreased spacing in systole (irrespective of region and capillary type). However, this difference did not reach significance ($P=0.0725$). Interestingly, there was also an

increase in the number of cells "touching" in systolic hearts (P=0.0029). This difference seems to be most apparent in the midmyocardium, since the mean values are similar in diastole and systole for the subendocardium (see Figure 17). Thus, combined with a trend toward lower mean values for RBC spacing, the increased number of touching cells would act to decrease the capillary barrier, and thus improve conditions for the O_2 transfer.

One could expect that the compression and emptying of vessels during systole would result in a decreased Hct. However, there might be a differential effect of this compression on plasma and RBCs. For example, if only plasma would escape, Hct would increase. Goto et al. (1991) studied the effect of myocardial contraction on vessel diameters in rabbit hearts. Contraction did not alter the capillary diameter in the subepicardium, as capillary diameter was similar in diastole and systole. However, capillary diameter did decrease in the subendocardium due to contraction. Thus, one might expect differences in capillary Hct and RBC spacing in the subendocardium, especially during systole. Surprisingly, the results from our study suggest that Hct and RBC spacing are preserved during the cardiac cycle, despite the changes in extravascular pressure.

5.5 Regional differences

The myocardial wall is characterized by gradual changes in fiber angle, from EPI to ENDO. Along with this transmural structural alteration, differences exist

between the inner and outer layers of the left ventricle which suggest that the subendocardium is vulnerable to ischemia (for a recent review of regional heterogeneities, see Zimmer, 1994). As mentioned earlier, transmural differences in extravascular pressure exist, exaggerated during systole (Kirk and Honig, 1964a).

In addition, oxygen consumption of the subendocardium is greater than the subepicardium. Spotnitz et al. (1966) determined that a greater amount of work was performed, and hence O_2 consumed, in the ENDO than EPI. In their study, sarcomere lengths during diastole were greater in the ENDO than EPI, and during systole, there was a greater degree of sarcomere shortening in the subendocardium. Together, these results indicate a greater amount of work in the ENDO, and thus O_2 consumption. Winbury and coworkers (1971) determined that O_2 consumption in the ENDO is 1.7 times greater than EPI. Respiratory activity of mitochondria is also greater in the ENDO than EPI (Camici et al., 1984), further supporting the concept of increased O_2 consumption.

Weiss and Sinha (1978) determined O_2 saturation in small arteries to be equivalent transmurally, whereas O_2 saturation in small veins declined from subepicardium to subendocardium (EPI>MID>ENDO). Therefore, the ENDO had a significantly greater arterial-venous O_2 saturation difference than both the MID or EPI, and hence greater O_2 extraction (Weiss and Sinha, 1978; Weiss et al., 1978). No regional differences were found for blood flow (Weiss et al., 1978). Oxygen consumption was determined as the product of blood flow and O_2 extraction. The

ENDO O_2 consumption was 27% higher than EPI (MID was in between and not significantly different from either). Since blood flow was relatively constant, these differences in O_2 consumption are due to differences in O_2 extraction. Thus, the left ventricle uses energy unevenly during contraction, with the ENDO region using a larger share. Not only is O_2 consumption greater, but average tissue PO_2 decreases transmurally from outer to inner layers of the left ventricle (Kirk and Honig, 1964b). In addition, Kirk and Honig (1964b) reported regional blood flow differences, with flow being 25% lower in deeper regions.

Based on the regional differences in wall stress, metabolic requirements, and tissue PO_2, regional differences in capillary Hct and red cell spacing would be expected. Furthermore, these differences would be expected to be exacerbated by systole. However, in our study, there were no significant regional differences between the subendocardium and midmyocardium in either of these parameters. In addition, there was no effect of cardiac cycle on regional differences, as might have been expected.

There have been conflicting results in the literature regarding transmural Hct gradients in the left ventricle. The only study specifically looking at capillary Hct showed no regional differences between the ENDO and EPI in the left ventricle of rat heart (Vetterlein et al., 1989). In their study, the percentage of RBC-free capillary length was determined. The vascular system was visualized by FITC-labelled γ-globulin injections and RBCs were contrast-enhanced by light scattering. Although

the Hct was lower in the ENDO (i.e. greater cell-free portion), the difference was not significant. Radioactive nucleotides have been used in other studies to investigate regional differences in tissue Hct, as explained in section 5.3.1. Vicaut and Levy (1990) reported a significant transmural gradient in tissue Hct from EPI to ENDO in both systolic- and diastolic-arrested rat hearts. Baskurt and coworkers (1995) also established a clear linear decline in myocardial tissue Hct in rats from 33.1% in the EPI to 23.2% in the ENDO. Contrary to these findings, Eliasen and coworkers (1982) concluded that no regional differences existed in tissue Hct between the EPI and ENDO in dog heart. These controversies in the literature may be due to both the methods used and species differences. The study by Vicaut and Levy (1990) was most similar to ours, since rat hearts were frozen *in situ* immediately following pharmacologically induced cardiac-arrest. The major difference between their study and ours, possibly contributing to the different findings, is that capillary Hct was measured in our study, whereas tissue Hct was measured in theirs. Perhaps there is a Hct gradient in larger vessels (reflected in tissue Hct values), which are more prominent in outer layers of the heart. However, this gradient may not necessarily imply a capillary Hct gradient.

Our study did not include the subepicardium, and dealt with the inner (ENDO) and middle (MID) layers only. It is possible that ENDO-EPI differences might have been found and that MID-ENDO differences are not as noticeable. However, the MID region represents a greater portion of the left ventricle by volume. In addition,

sampling of the EPI is difficult due to its small size and the presence of larger branches of coronary arterioles and venules which are located toward the surface of the heart.

5.6 Capillary type differences

As mentioned in the Introduction, an original contribution from our laboratory was the ability to distinguish coronary capillaries at two locations within the capillary bed. This allows investigators to ask questions about O_2 supply at different portions of the capillary bed, where PO_2 conditions are different. Using dual staining of capillary walls, capillaries which stained blue were classified as proximal, and those which stained red were classified as distal. It is assumed that PO_2 in distal portions of the capillary bed is lower than proximal portions as a result of O_2 being extracted by the tissue in proximal portions of the capillary bed. However, the relationship between capillary PO_2 levels and tissue PO_2 levels was only recently elucidated. In 1995, Vetterlein and coworkers combined the AP/DPP IV staining of capillary walls with the ability to detect cellular hypoxia in the tissue via NADH fluorescence. The aim of their study was to determine if hypoxia developed lengthwise along perfused capillaries, under low flow conditions. Indeed, tissue located near proximal portions of the capillary bed had lower incidence of hypoxia compared to those regions distal to arterioles.

Given the geometrical alterations between proximal and distal portions of the capillary bed, it is not surprising that capillary type differences also exist for capillary Hct and red cell spacing. Recall, in distal capillaries, capillary domain size decreases, vessel diameter increases and heterogeneity of capillary spacing decreases (Batra et al., 1991, 1992). The effect of capillary type in this study is clear: capillary Hct increases in distal capillaries, and the distances between red cells decrease. These are two separate findings, because changes in RBC spacing do not necessarily imply changes in capillary Hct, and vice versa (recall Fig. 20). Presumably, capillary Hct increases distally in order to increase the O_2 carrying capacity of the blood in a region of the capillary bed where PO_2 would be lower. In addition, red cell spacing decreases, resulting in a decrease in the capillary barrier, or extraction pressure for O_2 release.

A teleological explanation alone, however, is not sufficient. Although conflicting, there are several possible explanations for Hct and RBC spacing alterations. It is conceivable that some of these exert their effects to a different degree along the length of the capillary network. For example, the slight increase in capillary diameter from 5.9μm in proximal portions to 6.3μm in distal portions of the coronary capillary bed (Batra et al., 1992) may cause RBCs to move closer together, decreasing RBC spacing values. Since plasma and RBC volume are conserved, this would result from a possible redistribution of plasma from between cells to the cell free layer adjacent to the capillary wall.

Second, fluid loss across the capillary endothelium is a process which may affect capillary Hct. As fluid exits the capillary, Hct increases. Filtration is known to exceed reabsorption in most tissues, with the excess fluid drained via the lymphatics. Accordingly, Hct would be greatest midway in the capillary network, where filtration is complete and reabsorption has not yet begun. Once reabsorption begins, capillary Hct would decrease again to values similar, but slightly higher than those in proximal capillary portions of the capillary bed (due to incomplete reabsorption). Hence, although fluid loss may be a factor in elevating capillary Hct, the effect would be small.

Third, it has been shown that heparinase treatment diminishes the reduction in capillary Hct from large vessel Hct, due to the removal of endothelial cell surface molecules (Desjardins and Duling, 1990). Recall, endothelial cell surface molecules may interact with and decrease plasma velocity, thereby reducing capillary Hct. Perhaps there is naturally a differential distribution of macromolecules on the endothelial cell surface. If so, there may be a differential effect of plasma retardation along the length of the capillary resulting in higher Hct values in distal portions of the capillary bed. In fact, there is a differential distribution of Alkaline Phosphatase and Dipeptidyl Peptidase IV in capillary walls. This may be the case for other macromolecules as well.

Fourth, RBC aggregation and/or deformability affect the passage of RBCs through the vasculature. RBC aggregation *in vivo* is not fully understood. Changes

in aggregation have been implicated in changes in blood viscosity, RBC velocity and ultimately tissue oxygenation. For example, aggregation of RBCs has been shown to decrease arteriolar RBC velocity (Vicaut et al., 1994). It is conceivable that RBC aggregation might exert different effects at different levels of the microvascular network. For example, aggregation of RBCs may be greater in distal portions of the capillary bed, possibly reducing RBC velocity and elevating capillary Hct. Changes in RBC size, shape, and resulting deformability may also affect the ability of an erythrocyte to pass through capillaries and consequently influence O_2 transfer to tissue (Betticher et al., 1995; Langenfeld et al., 1994). It is unclear, however, how alterations in deformability would occur differentially along the capillary bed. The size of a RBC may increase as it traverses the path from arteriole to venule (i.e. venular Hct is greater than arteriolar Hct). This may result in a decrease in RBC velocity in distal portions of the capillary bed, increasing capillary Hct. However, quantitative conclusions cannot be made, since data regarding cell size changes along the arterio-venous pathway is not available.

5.7 Implications for O_2 transport to tissue

Distal portions of the microvascular bed have lower PO_2 values than proximal portions. The preeminent finding in this study, and not surprisingly so, was the marked differences in capillary Hct and red cell spacing at two different locations within the coronary capillary bed. The increase in capillary Hct as well as the shorter

distances between RBCs in distal portions of the capillary bed create more favourable geometrical conditions for O_2 transport. Presumably, the increased Hct provides a greater [Hb] and O_2 content at distal portions of the capillary bed. In addition, shorter distances between RBCs reduce the intracapillary resistance to O_2 transport, by reducing the capillary barrier. Conversely, the capillary barrier would be higher closer to arterioles, preventing O_2 waste from proximal capillary portions containing blood with higher PO_2.

Oxygen supply to tissue cannot be explained by one or two variables alone - the picture is far more complex. The dynamic interplay among capillary geometrical conditions ultimately results in certain circumstances for O_2 transport. For example, capillary domains are known to decrease in distal portions of the coronary capillary bed compared to proximal regions (Batra et al., 1991). This reduces the area of tissue supplied by an individual capillary. The increased Hct, decreased RBC spacing and decreased domain area may act together, perhaps synergistically, to provide optimal conditions for O_2 supply. This may not always be the case, however. For instance, capillary domain size has been shown to increase in systole, in both proximal and distal portions of the capillary bed. This occurs, in part, as a result of the physical contraction of the heart, affecting myocyte dimensions. In this study, the trend toward decreased spacing in systole may be acting to reduce the capillary barrier so that O_2 delivery to this larger region of tissue is enhanced.

As eluded to many times in this thesis, the mean values presented for many determinants of O_2 supply are only valuable if interpreted correctly. Quite often, the more important feature is the heterogeneity of data rather than the mean. Turek and Rakusan (1981) have clearly shown the dependence of tissue oxygenation on the heterogeneity of capillary spacing, rather than the mean intercapillary distance. The same may be true for RBC spacing and capillary Hct. It is well known that heterogeneity of capillary Hct exists *in vivo*, within and among capillaries. Although recent modelling studies have been examining the particulate nature of blood, heterogeneities have not been accounted for. The reasons are two-fold: (i) the increased computational requirements associated with heterogeneous spacing patterns, and more importantly (ii) the lack of realistic input data. It was the objective of this study to provide such realistic input data. In fact, data obtained and presented in this thesis will subsequently be used in future theoretical models by our collaborators in The Netherlands (Dr. L. Hoofd, Dr. Z. Turek, C. Bos).

CHAPTER 6 SUMMARY AND CONCLUSIONS

6.1 Summary

An adequate supply of oxygen is required for proper tissue function. This is especially true in the heart, an organ which relies almost entirely on oxidative metabolism. Due to the technical difficulties in directly measuring PO_2 in the heart, investigators rely on mathematical modelling to estimate tissue PO_2 under various physiological and pathophysiological conditions.

Theoretical studies have demonstrated that RBC spacing is an important determinant of O_2 supply to tissue. Federspiel and Sarelius (1984) have shown that as the distance between red blood cells increases, a constant flux of oxygen can no longer be maintained at the capillary wall. In 1986, Federspiel and Popel determined that O_2 conductance out of a capillary is an inverse function of the distance between RBCs. Other investigators (Hoofd et al., 1994; Bos et al. 1995) have quantified the resistance to O_2 transport out of the capillary (the capillary barrier, CB) as a PO_2 drop across the capillary wall (extraction pressure, EP). The EP has been found to increase as the distance between red cells increases.

Despite the importance of RBC spacing and related capillary Hct to O_2 supply, no realistic values have been obtained in the coronary capillary bed. To our knowledge, only two experimental studies exist which address capillary hematocrit and red cell spacing in coronary capillaries. However, these studies do not include

an extensive sampling design. The reason for the lack of this information is probably the lack of methodology to collect such data. With this in mind, the first part of this study involved the development of two novel experimental procedures for staining and freezing cardiac tissue. Rapid freezing was achieved *in situ* by using precooled copper clamps, specifically designed to match the shape of rat hearts. We are confident that transmural freezing of the heart is rapid, maintaining realistic geometric conditions of the red cells within capillaries. The staining procedure involved the modification and adaptation of a previously developed method which distinguished capillaries located in proximal and distal portions of the capillary bed (Batra et al., 1989). We developed a triple stain which, based on staining colours, allowed simultaneous visualization of two locations in the capillary bed as well as the RBCs within them. Therefore, we were able to collect realistic data for capillary Hct and RBC spacing at two distinct locations in the capillary bed, in two regions of the rat left ventricle arrested in systole or diastole.

Several morphometric parameters were defined: capillary hematocrit, normalized capillary Hct, RBC spacing and red cell content. The preeminent findings in this study were the differences in capillary hematocrit, normalized hematocrit and RBC spacing at two different locations in the capillary bed (summarized in Table 8). Essentially, distal portions of the capillary bed had a greater hematocrit and shorter mean distances between RBCs than proximal portions. In addition, there were trends towards increased frequencies of low RBC spacing values in distal portions of the

Table 8. Summary of major results.

	Capillary type	Region of heart	Cardiac phase
Capillary hematocrit (Hct)	distal > proximal *	endo ↔ mid	diastole ↔ systole
Normalized capillary Hct	distal > proximal *	endo ↔ mid	diastole ↔ systole
Red blood cell spacing	distal < proximal *	endo ↔ mid	diastole ↔ systole

endo, subendocardium; mid, midmyocardium; distal, distal portion of capillary bed; proximal, proximal portion of capillary bed; ↔, no significant effect; * statistically significant main effect (split plot ANOVA, $P \leq 0.05$).

capillary bed. Furthermore, there was a significant increase in the frequency of spacing values ≥20μm and ≥40μm in proximal portions of the capillary bed. Conditions for O_2 transport are not as favourable in distal portions of the capillary bed compared to proximal portions since the O_2 content is lower, due to O_2 extraction in earlier portions of the capillary bed. Presumably, the changes in capillary hematocrit and RBC spacing in distal portions of the capillary bed are adaptations to this lower PO_2. For example, an increase in capillary Hct in distal portions of the capillary bed increases O_2 content in the blood at this location. The decrease in red cell spacing decreases the resistance to O_2 transport out of the capillary (capillary barrier) in distal portions of the capillary bed. Conversely, the capillary barrier would be greater in proximal portions, possibly preventing O_2 waste in earlier portions of the capillary bed.

Despite the fact that pressure-flow conditions, O_2 metabolism and capillary geometry vary in the myocardium, no significant regional or phase differences were found in our measured parameters. Perhaps the lack of significant differences is in fact significant! This suggests that the geometrical conditions for O_2 supply at the level of the RBC are adequate under normal physiological conditions in both regions of the heart during diastole and systole.

Within the last two decades, the concept of oxygen delivery to tissue has changed dramatically. The dominant PO_2 gradients from red cell interior to tissue interior are now thought to occur within the capillary, not within the tissue as the

Krogh model assumed. The data obtained in this study can now be used as input data in future mathematical models which will incorporate realistic red cell spacing values.

6.2 Conclusions

The main conclusions from this study are as follows:

1. It is possible to: (i) rapidly freeze rat hearts *in situ*, and (ii) subsequently stain the tissue to simultaneously visualize red blood cells within capillaries at two locations within the capillary bed (proximal and distal portions of the capillary bed).

2. Capillary hematocrit was greater in distal portions of the capillary bed than in proximal portions.

3. Red blood cell spacing values were lower in distal portions of the capillary bed than in proximal portions.

4. Capillary hematocrit and red blood cell spacing values were not affected by either phase of the cardiac cycle or region of the left ventricle.

5. There were no interactions between phase of the cardiac cycle and region of the left ventricle which affected either capillary hematocrit or red blood cell spacing values.

REFERENCES

Albrecht, K.H., Gaehtgens, P., Pries, A. and Heuser, M. (1979). The Fahraeus effect in narrow capillaries (i.d. 3.3 to 11.0μm). *Microvasc.Res.* **18**, 33-47.

Aroesty, J. and Gross, J.F. (1970). Convection and diffusion in the microcirculation. *Microvasc.Res.* **2**, 247-267.

Barbee, J.H. and Cokelet, G.R. (1971). The Fahraeus effect. *Microvasc.Res.* **3**, 6-16.

Baskurt, O.K., Edremitlioglu, M. and Temiz, A. (1995). Effect of erythrocyte deformability on myocardial hematocrit gradient. *Am.J.Physiol.* **268**, H260-H264.

Batra, S., Koyama, T., Gao, M., Horimoto, M. and Rakusan, K. (1992). Microvascular geometry of the rat heart arteriolar and venular capillary regions. *Jap.Heart J.* **33(6)**, 817-828.

Batra, S., Kuo, C. and Rakusan, K. (1989). Spatial distribution of coronary capillaries: A-V segment staggering. *Adv.Exp.Med.Biol.* **248**, 241-247.

Batra, S. and Rakusan, K. (1990). Morphometric analysis of capillary nets in rat myocardium. *Adv.Exp.Med.Biol.* **277**, 377-385.

Batra, S. and Rakusan, K. (1992). Capillary length, tortuosity, and spacing in rat myocardium during cardiac cycle. *Am.J.Physiol.* **263**, H1369-H1376.

Batra, S., Rakusan, K. and Campbell, S.E. (1991). Geometry of capillary networks in hypertrophied rat heart. *Microvasc.Res.* **41**, 29-40.

Betticher, D.C., Reinhart, W.H. and Geiser, J. (1995). Effect of RBC shape and deformability on pulmonary O_2 diffusing capacity and resistance to flow in rabbit lungs. *J.Appl.Physiol.* **78(3)**, 778-783.

Bos, C , Hoofd, L. and Oostendorp, T. (in press). The effect of capillary blood flow on the oxygen release into rat heart tissue: Model calculations with point-like sources representing the erythrocytes. *Adv.Exp.Med.Biol.*

Bos, C., Hoofd, L. and Oostendorp, T. (1995). Mathematical model of erythrocytes as point-like sources. *Math.Biosci.* **125 (2)**, 165-189.

Bos, C., Hoofd, L. and Turek, Z. (1994). Local plasma convection can be important for oxygen release in tissue capillaries. *Adv.Exp.Med.Biol.* **361**, 1-6.

Camici, P., Ursini, F., Galiazzo, F., Bellitto, L., Pelosi, G., Marzilli, M., L'Abbate, A., and Barsacchi, R. (1984). Different respiratory activities of mitochondria isolated from the subendocardium and subepicardium of the canine heart. *Basic Res.Cardiol.* **79**, 454-460.

Clark, A. and Clark, P.A.A. (1983). Capture of spatially homogeneous chemical reactions in tissue by freezing. *Biophys.J.* **42**, 25-30.

Clark, A. and Clark, P.A.A. (1986). The end points of the oxygen path: transport resistance in red cells and mitochondria. *Adv.Exp.Med.Biol.* **200**, 43-47.

Clark, A., Federspiel, W.J., Clark, P.A.A. and Cokelet, G.R. (1985). Oxygen delivery from red cells. *Biophys.J.* **47**, 171-181.

Cokelet, G.R. (1976). Macroscopic rheology and tube flow of human blood. In: *Microcirculation*, edited by Grayson, J. and Zingg, W. New York: Plenum, pp. 9-31.

Desjardins, C. and Duling, B.R. (1987). Microvessel hematocrit: measurement and implications for capillary oxygen transport. *Am.J.Physiol.* **252**, H494-H503.

Desjardins, C. and Duling, B.R. (1990). Heparinase treatment suggests a role for the endothelial cell glycocalyx in regulation of capillary hematocrit. *Am.J.Physiol.* **258**, H647-H654.

Duling, B.R. and Desjardins, C. (1987). Capillary hematocrit - what does it mean? *NIPS* **2**, 66-69.

Dupont Company. (1979). *Instruction manual: staining procedures for plastic embedded tissue*, Newtown,Connecticut: pp. 28.

Eliasen, P., Amtorp, O., Tøndevold, E. and Haunsø, S. (1982). Regional blood flow, microvascular blood content and tissue haematocrit in canine myocardium. *Cardiovasc.Res.* **16**, 593-598.

Ellis, C.G., Wrigley, S.M. and Groom, A.C. (1994). Heterogeneity of red blood cell perfusion in capillary networks supplied by a single arteriole in resting skeletal muscle. *Circ.Res.* **75**, 357-368.

Ellis, C.G., Wrigley, S.M., Potter, R.F. and Groom, A.C. (1990). Temporal distributions of red cell supply rate to individual capillaries of resting skeletal muscle, in frog and rat. *Int.J.Microcirc.: Clin.Exp.* **9**, 67-84.

Fahraeus, R. (1928). Die Strömungsverhältnisse und die Verteilung der Blutzellen im Gefäßystem. *Klin.Wochenschr.* **7**, 100-106 in: Albrecht, K.H., Gaehtgens, P., Pries, A. and Heuser, M. (1979). The Fahraeus effect in narrow capillaries (i.d. 3.3 to 11.0μm). *Microvasc.Res.* **18**, 33-47.

Federspiel, W.J. and Popel, A.S. (1986). A theoretical analysis of the effect of the particulate nature of blood on oxygen release in capillaries. *Microvasc.Res.* **32**, 164-189.

Federspiel, W.J. and Sarelius, I.H. (1984). An examination of the contribution of red cell spacing to the uniformity of oxygen flux at the capillary wall. *Microvasc.Res.* **27**, 273-285.

Fisher, A.J., Schrader, N.W. and Klitzman, B. (1992). Effects of chronic hypoxia on capillary flow and hematocrit in rat skeletal muscle. *Am.J.Physiol.* **262**, H1877-H1883.

Fletcher, J.E. (1978). Mathematical modeling of the microcirculation. *Math.Biosci.* **38**, 159-202.

Fletcher, J.E. (1980). On facilitated oxygen diffusion in muscle tissue. *Biophys.J.* **29**, 437-458.

Gaehtgens, P. (1980). Flow of blood through narrow capillaries: rheological mechanisms determining capillary hematocrit and apparent viscosity. *Biorheology* **17**, 183-189.

Garvey, W., Fathi, A., Bigelow, F., Carpenter, B. and Jimenez, C. (1987). A combined elastic, fibrin, and collagen stain. *Stain Technol.* **62**, 365-368.

Gayeski, T.E.J. and Honig, C.R. (1986). Shallow intracellular O_2 gradients and absence of perimitochondrial O_2 "wells" in heavily working red muscle. *Adv.Exp.Med.Biol.* **200**, 487-494.

Goto, M., Flynn, A.E., Doucette, J.W., Jansen, C.M.A., Stork, M.M., Coggins, D.L., Muehrcke, D.D., Husseini, W.K. and Hoffman, J.E. (1991). Cardiac contraction affects deep myocardial vessels predominantly. *Am.J.Physiol.* **261**, H1417-H1429.

Groebe, K. and Thews, G. (1989). Effects of red cell spacing and red cell movement upon oxygen release under conditions of maximally working skeletal muscle. *Adv.Exp.Med.Biol.* **248**, 175-185.

Hellums, J.D. (1977). The resistance to oxygen transport in the capillaries relative to that in the surrounding tissue. *Microvasc.Res.* **13**, 131-136.

Heron, M.I. and Rakusan, K. (1994). Geometry of coronary capillaries in hyperthyroid and hypothyroid rat heart. *Am.J.Physiol.* **267**, H1024-H1031.

Homer, L.D., Weatherby, P.K. and Kiesow, L.A. (1981). Oxygen gradients between red blood cells in the microcirculation. *Microvasc.Res.* **22**, 308-323.

Honig, C.R., Feldstein, M.L. and Frierson, J.L. (1977). Capillary lengths, anastomoses, and estimated capillary transit times in skeletal muscle. *Am.J.Physiol.* **233(1)**, H122-H129.

Honig, C.R., Frierson, J.L. and Gayeski, E.J.T. (1989). Anatomical determinants of O_2 flux density at coronary capillaries. *Am.J.Physiol.* **256**, H375-H382.

Honig, C.R. and Gayeski, T.E.J. (1989). Precapillary O_2 loss and arteriovenous O_2 diffusion shunt are below limit of detection in myocardium. *Adv.Exp.Med.Biol.* **248**, 591-599.

Hoofd, L., Bos, C. and Turek, Z. (1994). Modelling erythrocytes as point-like O_2 sources in a Kroghian cylinder model. *Adv.Exp.Med.Biol.* **345**, 893-900.

Hoofd, L., Olders, J. and Turek, Z. (1990). Oxygen pressures calculated in a tissue volume with parallel capillaries. *Adv.Exp.Med.Biol.* **277**, 21-29.

Hoppeler, H., Mathieu, O., Krauer, R., Claassen, H., Armstrong, R.B. and Weibel, E.R. (1981). Design of the mammalian respiratory system VI. Distribution of mitochondria and capillaries in various muscles. *Resp.Physiol.* **44**, 87-111.

House, S.D. and Lipowsky, H.H. (1987). Microvascular hematocrit and red cell flux in rat cremaster muscle. *Am.J.Physiol.* **252**, H211-H222.

Judd, R.M. and Levy, B.I. (1991). Effects of barium-induced cardiac contraction on large- and small-vessel intramyocardial blood volume. *Circ.Res.* **68**, 217-225.

Kirk, E.S. and Honig, C.R. (1964a). An experimental and theoretical analysis of myocardial tissue pressure. *Am.J.Physiol.* **207(2)**, 361-367.

Kirk, E.S. and Honig, C.R. (1964b). Nonuniform distribution of blood flow and gradients of oxygen tension within the heart. *Am.J.Physiol.* **207 (3)**, 661-668.

Klitzman, B. and Duling, B.R. (1979). Microvascular hematocrit and red cell flow in resting and contracting striated muscle. *Am.J.Physiol.* **237(4)**, H481-H490.

Kreuzer, F. (1982). Oxygen supply to tissues: the Krogh model and its assumptions. *Experientia* **38**, 1415-1426.

Krogh, A. (1919). The number and distribution of capillaries in muscles with calculations of the oxygen pressure head necessary for supplying the tissue. *J.Physiol.* **52**, 409-415, in: Rakusan, K. *Oxygen in the Heart Muscle*, Springfield, Illinois:Charles Thomas, 1971a. pp. 1-100.

Langenfeld, J.E., Machiedo, G.W., Lyons, M., Rush, Jr.B.F., Dikdan, G. and Lysz, T.W. (1994). Correlation between red blood cell deformability and changes in hemodynamic function. *Surgery* **116(5)**, 859-867.

Ley, K., Lindbom, L. and Arfors, K.E. (1988). Haematocrit distribution in rabbit tenuissimus muscle. *Acta Physiol.Scand.* **132**, 373-383.

Lojda, Z. (1979). Studies on dipepti.'yl(amino)peptidase IV (glycyl-proline naphthylamidase). *Histochemistry* **59**, '53-166.

Mainwood, G.W. and Rakusan, K. (1982). A model for intracellular energy transport. *Can.J.Physiol.Pharmacol.* **60(1)**, 98-102.

Poole, D.C., Batra, S., Mathieu-Costello, O. and Rakusan, K. (1992). Capillary geometrical changes with fiber shortening in rat myocardium. *Circ.Res.* **70**, 697-706.

Poole, D.C. and Mathieu-Costello, O. (1990). Analysis of capillary geometry in rat subepicardium and subendocardium. *Am.J.Physiol.* **259**, H204-H210.

Popel, A.S. (1989). Theory of oxygen transport to tissue. *Crit.Rev.Biomed.Eng.* **17 (3)**, 257-321.

Pries, A.R., Ley, K. and Gaehtgens, P. (1986). Generalization of the Fahraeus principle for microvessel networks. *Am.J.Physiol.* **251**, H1324-H1332.

Rakusan, K. (1971a). *Oxygen in the Heart Muscle*, Springfield, Illinois:Charles Thomas, pp. 1-100.

Rakusan, K. (1971b). Vascular capacity and hematocrit in experimental cardiomegaly due to aortic constriction in rats. *Can.J.Physiol.Pharmacol.* **49(9)**, 819-823.

Rakusan, K., Batra, S., Veprek, P. and Turek, Z. (1993). Capillary density, distribution, and length parameters related to oxygen supply in myocardial hypertrophy and atrophy. In: *Idiopathic dilated Cardiomyopathy. Cellular and molecular mechanisms, clinical consequences*, edited by Figulla, H.R., Kandolf, R. and McManus, B. New York: Springer-Verlag, pp. 155-164.

Rakusan, K., Hoofd, L. and Turek, Z. (1985). The effect of cell size and capillary spacing on myocardial oxygen supply. *Adv.Exp.Med.Biol.* **180**, 463-475.

Rakusan, K. and Rajhathy, J. (1972). Distribution of cardiac output and organ blood content in anemic and polycythemic rats. *Can.J.Physiol.Pharmacol.* **50(7)**, 703-710.

Rakusan, K. and Tomanek, R.J. (1986). Distribution of mitochondria in normal and hypertrophic myocytes from the rat heart. *J.Mol.Cell.Cardiol.* **18**, 299-305.

Rakusan, K. and Turek, Z. (1985). The effect of heterogeneity of capillary spacing and O_2. *Adv.Exp.Med.Biol.* **191**, 257-262.

Ross, Jr.J., Sonnenblick, E.H., Covell, J.W., Kaiser, G.A. and Spiro, D. (1967). The architecture of the heart in systole and diastole. *Circ.Res.* **21(4)**, 409-421.

Ross, Jr.J., Sonnenblick, E.H., Taylor, R.R., Spotnitz, H.M. and Covell, J.W. (1971). Diastolic geometry and sarcomere lengths in the chronically dilated canine left ventricle. *Circ.Res.* **28**, 49-61.

Sarelius, I.H. (1986). Cell flow path influences transit time through striated muscle capillaries. *Am.J.Physiol.* **250**, H899-H907.

Sarelius, I.H. (1989). Microcirculation in striated muscle after acute reduction in systemic hematocrit. *Resp.Physiol.* **78**, 7-17.

Sarelius, I.H., Damon, D.N. and Duling, B.R. (1981). Microvascular adaptations during maturation of striated muscle. *Am.J.Physiol.* **241**, H317-H324.

Sarelius, I.H. and Duling, B.R. (1982). Direct measurement of microvessel hematocrit, red cell flux, velocity and transit time. *Am.J.Physiol.* **243**, H1018-H1026.

Sheehan, D.C. and Hrapchak, B.B. (1980). Mallory's aniline blue collagen stain. In: *Theory and practice of histotechnology*, Detroit: Battelle Press, pp. 191.

Sonnenblick, E.H., Ross, J., Covell, J.W., Spotnitz, H.M. and Spiro, D. (1967). The ultrastructure of the heart in systole and diastole. *Circ.Res.* **21**, 423-431.

Spotnitz, H.M., Sonnenblick, E.H. and Spiro, D. (1966). Relation of ultrastructure to function in the intact heart: sarcomere structure relative to pressure volume curves of intact left ventricles of dog and cat. *Circ.Res.* **18**, 49-66.

Streeter, D.D., Spotnitz, H.M., Patel, D.P., Ross, J. and Sonnenblick, E.H. (1969). Fiber orientation in the canine left ventricle during diastole and systole. *Circ.Res.* **24**, 339-347.

Sweeney, T.E. and Sarelius, I.H. (1990). Spatial heterogeneity in striated muscle arteriolar tone, cell flow and capillarity. *Am.J.Physiol.* **259**, H124-H136.

Tsai, A.G. and Intaglietta, M. (1989). Local tissue oxygenation during constant red blood cell flux: a discrete source analysis of velocity and hematocrit changes. *Microvasc.Res.* **37**, 308-322.

Tsai, A.G. and Intaglietta, M. (1992). Local tissue oxygenation by statistically distributed sources. *Microvasc.Res.* **44**, 200-213.

Turek, Z., Hoofd, L. and Rakusan, K. (1986). Myocardial capillaries and tissue oxygenation. *Can.J.Cardiol.* **2(2)**, 98-103.

Turek, Z., Olders, J., Hoofd, L., Egginton, S., Kreuzer, F. and Rakusan, K. (1989). PO_2 histograms in various models of tissue oxygenation in skeletal muscle. *Adv.Exp.Med.Biol.* **248**, 227-237.

Turek, Z. and Rakusan, K. (1981). Lognormal distribution of intercapillary distance in normal and hypertrophic rat heart as estimated by the method of concentric circles: its effect on tissue oxygenation. *Pflügers Arch.* **391**, 17-21.

Turek, Z., Rakusan, K., Olders, J., Hoofd, L. and Kreuzer, F. (1991). Computed myocardial PO_2 histograms: effects of various geometrical and functional conditions. *J.Appl.Physiol.* **70(4)**, 1845-1853.

Tyml, K. (1986). Capillary recruitment and heterogeneity of microvascular flow in skeletal muscle before and after contraction. *Microvasc.Res.* **32**, 84-99.

Tyml, K. (1987). Red cell perfusion in skeletal muscle at rest and after mild and severe contractions. *Am.J.Physiol.* **252**, H485-H493.

Tyml, K., Ellis, C.G., Safranyos, R.G., Fraser, S. and Groom, A.C. (1981). Temporal and spatial distributions of red cell velocity in capillaries of resting skeletal muscle, including estimates of red cell transit times. *Microvasc.Res.* **22**, 14-31.

Vetterlein, F., Hemeling, H., Sammler, J., Pethö, A. and Schmidt, G. (1989). Hypoxia-induced acute changes in capillary and fiber density and capillary red cell distribution in the rat heart. *Circ.Res.* **64**, 742-752.

Vetterlein, F., Menzel, F., Kreuzer, H. and Schmidt, G. (1991). Acute changes in microvascular blood flow distribution in the myocardium of the rat during partial occlusion of the right coronary artery; effects of dihydroergotamine. *Int.J.Microcirc.* **10**, 289-302.

Vetterlein, F., Prange, M., Lubrich, D., Pedina, J., Neckel, M. and Schmidt, G. (1995). Capillary perfusion pattern and microvascular geometry in heterogeneous hypoxic areas of hypoperfused rat myocardium. *Am.J.Physiol.* **268**, H2183-H2194.

Vicaut, E., Hou, X., Decuypère, L., Taccoen, A. and Duvelleroy, M. (1994). Red blood cell aggregation and microcirculation in rat cremaster muscle. *Int.J.Microcirc.* **14**, 14-21.

Vicaut, E. and Levy, B.I. (1990). Transmural hematocrit gradient in left ventricular myocardia of rats. *Am.J.Physiol.* **259**, H403-H408.

Weiss, H.R., Neubauer, J.A, Lipp, J.A. and Sinha, A.K. (1978). Quantitative determination of regional oxygen consumption in the dog heart. *Circ.Res.* **42(3)**, 394-401.

Weiss, H.R. and Sinha, A.K. (1978). Regional oxygen saturation of small arteries and veins in the canine myocardium. *Circ.Res.* **42(1)**, 119-126.

White, J.C. (1950). Investigations on some cellular stain reactions. *Proc.Biochem.Soc.Biochem.J.* **46**, 24-25.

Winbury, M.M., Howe, B.B. and Weiss, H.R. (1971). Effect of nitroglycerin and dipyridamole on epicardial and endocardial oxygen tension - further evidence for redistribution of myocardial blood flow. *J.Pharmacol.Exp.Ther.* **176 (1)**, 184-199.

Yen, R.T. and Fung, Y.C. (1978). Effect of velocity distribution on red cell distribution in capillary blood vessels. *Am.J.Physiol.* **235(2)**, H251-H257.

Zimmer, H.G. (1994). Some aspects of cardiac heterogeneity. *Basic Res.Cardiol.* **89**, 101-117.

APPENDIX 1 TRIPLE STAINING PROCEDURE

Staining method and incubating media for the demonstration of RBCs, as well as enzyme activity in the endothelium of capillaries distal and proximal to their feeding arterioles. The dual staining of capillary walls is modified from Batra et al. (1989).

Staining Procedure

1. Frozen tissue sections (16μm) are cut directly into a fixative bath (1:1 chloroform:acetone; vol/vol, 45mL/45mL) which had been precooled in dry ice to approximately -22°C.

2. Leave sections in fixative bath at room temperature (21°C) for 15min.

3. Pick up sections onto slides (e.g. place slide into bath).

4. Place slides in Papanicolaou Orange G-6 for 40min. at room temperature.

5. Rinse slides in distilled water (2 rinses).

6. Incubate slides in Dipeptidyl Peptidase IV (DPP IV)-sensitive medium for 110min. at room temperature (see next page for medium recipe).

7. Rinse slides in distilled water (2 rinses).

8. Incubate slides in Alkaline Phosphatase (AP)-sensitive medium for 25min. at room temperature (see next page for medium recipe).

9. Rinse slides in distilled water (2 rinses).

10. Postfix slides in 4% Formalin for 15min.

11. Rinse slides in distilled water (3 rinses).

12. Coverslip slides using glycerol gelatin.

Incubating Media

DPP IV:

1.	14 mg	Glycy-l-prolin-4-methoxy-ß-Naphthylamide
2.	0.5 mL	N,N-dimethylformamide
3.	14 mg	Fast blue B salt
4.	10 mL	Acetate buffer pH 5.4- 5.6

AP:

1.	10 mg	Naphthol AS-MX phosphate
2.	0.5 ml	N,N-dimethylformamide
3.	10 ml	tri-HCl buffer pH 9.2
4.	20 mg	Variamine Blue Salt RT

Mix as follows: { [1 + 2] + [3 + 4] }.

All chemicals are from SIGMA.

Buffers:

Acetate Buffer:

Stock solutions

A: 0.2M solution of acetic acid (1.155mL in 100mL H_2O)

B: 0.2M solution of sodium acetate ($C_2H_3O_2Na{\cdot}3H_2O$, 0.68g in 25mL H_2O)

2.4mL of A + 22.6mL of B, diluted to 50mL with H_2O

Tris(hydroxymethyl)aminomethane (Tris) Buffer:

0.303g in 25mL H_2O (adjust to pH of 9.2 with HCl)

APPENDIX 2 FREEZING AND EXCISION OF RAT HEART

The following diagram illustrates the exposed heart. A loose loop was made with a silk ligature around the large vessels exiting at the base of the heart. The ligature was used to slightly elevate the heart during freezing, making it more accessible to the precooled clamps. The clamps were introduced into the chest cavity immediately following cardiac-arrest, and fully encased the heart *in situ*. One of the two specifically designed copper blocks (which comprise the freezing clamps) is also illustrated below.